WASM: Minerals, Energy and Chemical Engineering

Distributed Acoustic Sensing for Seismic Imaging and Reservoir Monitoring Applied to CO_2 Geosequestration

Julia dos Santos Maia Correa

This thesis is presented for the Degree of

Doctor of Philosophy

of

Curtin University

December 2018

AUTHOR'S DECLARATION

To the best of my knowledge and belief this thesis contains no material previously published by any other person except where due acknowledgment has been made.

This thesis contains no material which has been accepted for the award of any other degree or diploma in any university.

Signature: Julia de Santa Ana Cruz.
……

Date: 15/May/2019

“I am among those who think that science has great beauty.” - Marie Curie

ABSTRACT

Seismic monitoring constitutes an essential step during the development of a CO_2 geosequestration project, as it assures the injected fluid is safely stored in subsurface. However, seismic monitoring surveys are highly expensive as an extensive amount of equipment needs to be deployed. Additionally, the required access to large areas during the survey lead to high environmental and social impact.

In this context, I test the applicability of using Distributed Acoustic Sensing (DAS) to come up with a cost-effective technology for permanent and continuous seismic monitoring in CO_2 geosequestration projects. DAS uses standard fibre-optic cables to form a series of distributed seismic receivers. Fibre-optic cables are relatively inexpensive, offer long durability and can operate in extreme conditions. Moreover, DAS is able to acquire seismic data instantaneously along the whole length of the cable at fine spatial sampling intervals.

For this research, two different land-based sites were used to conduct a series of experiments with the objective of exploring properties of DAS as a seismic sensor. In the first site, I utilise a 900 m deep test well located in the National Geosequestration Laboratory (NGL) in Perth, Western Australia. The experiments aim to compare DAS and conventional seismic sensors, geophones and hydrophones, at both zero-offset and offset VSP geometries. I use fibre-optic cables both cemented behind the casing and inside the borehole coupled to the fluid.

The main focus of this thesis is, however, set at the second site - the CO2CRC Otway project. The Otway project is located approximately 240 km away from Melbourne, Australia. Stage 1 of the project was the first Australian demonstration of CO_2 geosequestration. Lately, the project site was transformed into an in-situ laboratory to develop and test various technologies relevant to carbon capture and sequestration. The site has two wells instrumented with fibre-optic cables (one well has the fibre on production tubing; the other well behind the casing). The wells contain a set of straight single-mode fibres, though, one of the cemented cables has a combination of conventional single-mode and special high-sensitive DAS fibres. An additional 40 km of fibre optic cable is deployed in eleven receiver line trenches along

with 908 buried geophones to test the applicability of DAS for surface seismic applications. This massive DAS receiver array was used to acquire a series of zero-offset and offset VSP surveys, time-lapse 3D VSP and surface 3D surveys, during Stage 2C of the project. This stage is focused on advances in the seismic monitoring of small-scale supercritical CO_2 injection into a saline aquifer at 1500 m depth. In this thesis I analyse both surface and VSP DAS data to develop DAS signal processing techniques and study different cable designs and ways of deployment.

CO2CRC Otway project is heading towards its third stage. This stage would focus on continuous downhole monitoring techniques. Seismic monitoring will be conducted using a combination of multi-well 4D VSPs and continuous time-lapse offset VSPs acquired using surface orbital vibrators (SOVs). As a precursor for this stage, two SOVs were permanently deployed on site. Analysis of the data acquired using cemented fibre optic cables and the permanent seismic sources is also a part of this thesis.

Through the analysis of these multiple datasets I demonstrate that DAS is the receiver of choice in many monitoring applications which would benefit from permanent receiver installation. DAS can outperform conventional geophones as a seismic sensor, particularly when used to conduct monitoring of the subsurface. The DAS VSP acquired with cemented cable successfully imaged the reservoir and provided a result comparable to the geophone data. The use of engineered fibre provides improved sensitivity since it increases light backscatter, and a shorter fibre-optic cable can also further improve the DAS results by allowing a high pulse repetition rate during acquisition. However, the nature of the measurement is different from that of a conventional sensor and must be taken into account, from survey design to data processing and interpretation.

Keywords: fibre-optics sensing, distributed acoustic sensing, CO_2 geosequestration, and reservoir monitoring

ACKNOWLEDGEMENTS

Firstly, I would like to acknowledge CO2CRC for providing financial support towards this PhD program. Funding for CO2CRC Otway Project is provided through its industry members and research partners, the Australian Government under the CCS Flagships Programme, the Victorian State Government and the Global CCS Institute. I acknowledge financial assistance provided through Australian National Low Emissions Coal Research and Development (ANLEC R&D) supported by the Australian Coal Association Low Emissions Technology Limited and the Australian Government through the Clean Energy Initiative for the development of the Otway Project.

I sincerely thank my supervisor, Prof. Dr. Roman Pevzner, whose support guided me through the completion of this PhD research. I am grateful for all the interesting scientific discussions we shared. I thank him for all the long hours, sometimes his personal hours, spent revising material I wrote. I also appreciate his wisdom of knowing when to put pressure, and when to give calming affirmations that “it is going to be okay” - even after my pc stopped working just a few weeks before submitting the thesis.

I also thank the support and help from my co-supervisor, Prof. Dr. Andrej Bona, who never hesitated to help me whenever I needed, promptly revising papers I wrote and readily giving advice on research. I appreciate all the occasions he came to my desk and very kindly asked about my research.

Additionally, I sincerely thank Dr. Tim Dean for all the help, advice and guidance throughout this research. I also thank Dr. Konstantin Tertyshnikov, who always promptly offered his help and who has been involved in every field campaign. I thank Prof. Dr. Boris Gurevich for all his support through reading papers and giving advice. I thank immensely Dr. Jon Cocker for reading and correcting this thesis. Additionally, I am thankful to (in alphabetical order) Anton Egorov, Dr. Stanislav Glubokovskikh, Murray Hehir, Dr. Muhammed Hossain, Dominic Howman, Dmitry Popik, Sofya Popik, Nichole Sik, Dr. Milovan Urosevic, Dr. Sinem Yavuz and Sasha Ziramov.

Furthermore, I am grateful for our research collaborations with the Lawrence Berkeley National Laboratory. This research was only possible through our fruitful partnership with LBNL. With this partnership, we were able to build the fibre-optics network at the Otway Project, as well as installing the SOV sources. I particularly thank Barry Freifeld, who has always been so helpful and prompt when I asked for feedback on papers. I also thank Michelle Robertson, Thomas Daley, and Todd Wodd, who have been involved in field trips to Otway, as well as involved in the design of the fibre-optics network and SOV sources.

I am grateful to Silixa Ltd for providing the equipment used in this research, as well as for the support and advice on well instrumentation and DAS data acquisition. I particularly thank Mahmoud Farhadiroushan, Tom Parker and Andy Clarke for their contribution.

I cannot thank enough the support from my beloved parents, Sheila and Reinaldo Correa, and brother, Rodrigo Correa, who have always supported me throughout my life. I especially express my heart-felt gratitude for my parents for always investing in our education. I thank you for being such loving and kind parents, always giving the best you could for us. To my brother, I thank you for always giving me inspiration and being the person I look up to. Lastly, I sincerely thank Iestyn Williams for his love and support throughout the duration of this PhD.

All of you were, through smaller or significant actions, important to me for succeeding in this PhD research. To you all, I am immensely grateful.

TABLE OF CONTENTS

LIST OF FIGURES

LIST OF TABLES

GLOSSARY

3-C – Three component

CCS – Carbon capture and storage

DAS – Distributed acoustic sensor

FO – Fibre optic

IU – Interrogator unit

Multi-mode optical fibre – A type of optical fibre with core diameter of typically $50\mu m$ to $62.5\mu m$, and cladding diameter of $125\mu m$. The large core diameter allows for multiple modes of light to propagate

NGL – National Geosequestration Laboratory

OVSP – Offset vertical seismic profiling

PRF – Pulse repetition frequency

P-S wave – Converted wave from a downgoing P-wave to an upgoing S-wave

P-wave – Primary compressional/longitudinal acoustic wave

S/N – Signal to noise ratio

Single-mode optical fibre – A type of optical fibre with a small core diameter (typically $9\mu m$) in comparison with the cladding diameter ($125\mu m$). This allows only one mode of light to propagate, decreasing the light reflections as it travels along the fibre. As a result, such fibre types provide less attenuation of the light

S-wave – Secondary transverse acoustic wave

VSP – Vertical seismic profiling

CHAPTER 1 INTRODUCTION

1.1 Overview

In this thesis, I focus on demonstrating the successful use of Distributed Acoustic Sensing (DAS) for land-based seismic imaging and reservoir monitoring. Multiple surface and downhole seismic surveys were acquired using DAS and conventional geophone data between March 2015 and March 2018 at two Carbon Capture and Storage (CCS) sites in Australia: (1) the CO2CRC Otway Project and (2) the National Geosequestration Laboratory (NGL) research facility. Comparisons of datasets from these sites will clearly demonstrate the ability of DAS to provide a cost-effective low-impact alternative to conventional seismic surveys, and that intelligent choice of DAS technology, DAS settings, seismic source effort, and fibre optic (FO) cable type, geometry and installation are critical to project success.

CCS is a procedure to capture carbon dioxide and permanently store it in geological formations. While the world's energy matrix shifts from primarily fossil fuel sources, CCS is seen as an effective solution to mitigate greenhouse gas emissions in the short to mid-term. A power plant equipped with a CCS system could reduce its total CO_2 emissions by 80-90%, compared to a power plant without CCS (IPCC, 2005). The captured CO_2 is usually stored in depleted gas reservoirs or in saline aquifers. To make sure the injected gas is safely stored in the subsurface, several monitoring techniques are required, including time-lapse seismic (IPCC, 2005). Time-lapse or 4D seismic is a key procedure in the context of CCS projects as it provides assurance monitoring and conformance monitoring. This means that we can determine that no leakage of the injected CO_2 has occurred. Additionally, 4D provides monitoring of the behaviour of the injected gas, as well as assurance that the development of gas plume proceeds as predicted.

In principle, 4D seismic is the process of acquiring repeated surveys over time to monitor reservoir changes (Lumley, 2001). For this, each repeat survey needs to replicate as close as possible the same acquisition parameters and conditions so that the observed changes are related specifically to changes in the reservoir. However, conventional time-lapse surveys involve the use of large amounts of seismic

equipment (e.g. thousands of geophone channels, vibrator trucks). Also, such surveys need large personnel crews to deploy and retrieve the equipment. As a result, conventional time-lapse seismic surveys are usually very costly compared to other geophysical or remote sensing techniques. Due to its high cost, time-lapse surveys are acquired with a gap of, sometimes, years. This results in sparse temporal resolution, which reduces the effectiveness of the time-lapse analysis.

Due to the regular deployment and retrieving of equipment, such surveys are highly invasive on the land and environment. Also, as such surveys are highly complex, usually conventional surface seismic acquisition takes a long time to be completed (months) and a long time for the data processing to achieve interpretable results (from months to a year). Limited land access is also a common issue during a conventional time-lapse survey. As mentioned before, time-lapse seismic relies on repeating the same acquisition parameters. However, certain acquisition conditions might not be repeatable (e.g. traffic noise levels, time-varying near surface conditions, blocked access to certain area on the survey plan). These inconsistencies contribute to high levels of time-lapse noise. In the context of CCS, land access is especially problematic as CCS projects are usually located in populated areas, close to power plants. Furthermore, non-commercial CCS projects might have limited resources, which means finding a cost-effective seismic monitoring technique is particularly desirable.

DAS can mitigate some of the issues related to conventional time-lapse seismic. DAS is a fibre-optic sensing technique that uses standard fibre-optic cables to create an array of virtual seismic receivers. DAS senses strain along a continuous fibre, caused by impinging seismic waves (Parker and Shatalin, 2014). DAS offers many advantages for seismic acquisition and monitoring, compared to conventional receivers. DAS can be installed permanently in wells and on the surface, solving issues associated with regular deployment and retrieving of seismic receivers. With this, land impact and acquisition footprint are reduced. Additionally, fibre cables present long equipment durability. With the permanent installation of fibres, DAS can acquire on-demand seismic acquisition at small spatial sampling (> 0.25 m, in some interrogators). As a result, time-lapse surveys can be acquired more frequently, which increases temporal resolution.

As a consequence of the above, DAS can help to reduce some of the issues related with the logistics of conventional seismic monitoring acquisition, while reducing the costs of surveys. DAS applied to seismic imaging and monitoring represents a promising technology, particularly in the context of CO_2 monitoring (Bacci et al., 2017; Cox et al., 2012; Daley et al., 2013; Freifeld et al., 2016; Harris et al., 2017).

In the Oil & Gas industry, time-lapse surveys offshore are common practice. Permanent reservoir monitoring has been implemented in oil fields, such as in Grane (Berraki et al., 2017), in Valhal (Van Gestel et al., 2008), and in BC-10 (Galarraga et al., 2015). Peace River heavy oil field is a good example of an implementation of permanent monitoring in onshore environment (La Follett et al., 2015). Moreover, DAS has been demonstrated for use in seismic monitoring of hydrocarbon production (Al Adawi et al., 2013; Hance et al., 2016; Hornman et al., 2015; Mateeva et al., 2014; Mestayer et al 2011). DAS has also been applied in a variety of application, such as earthquake detection (Biondi et al, 2017; Lindsey, et al., 2017; Martin et al., 2017; Pevzner et al., 2018), ambient noise interferometry (Dou et al., 2017; Pevzner et al., 2018), and microseismic detection (Bakku et al., 2014a; Webster et al., 2013).

As previously mentioned, this thesis is focused on using DAS for seismic acquisition and monitoring in the context of CCS. More precisely, I focus on showing the use of DAS at the CO2CRC Otway project site. The Otway project is Australia's first demonstration of deep geological storage of carbon dioxide. The project is managed by CO2CRC, a non-for-profit research institution aimed at the demonstration of various technologies applied to CCS. At Otway, we want to develop a cost-effective monitoring technique to image the development of an injection of CO_2 into a saline aquifer. At this present moment, the Otway project is currently finalizing its Stage 2C and initiating Stage 3 of the project. A detailed description of the Otway project can be found in Chapter 3.

During Stage 1 of the Otway project, we monitored the injection of a CO_2 gas mixture into a depleted gas reservoir using conventional onshore time-lapse techniques. For this, 4D seismic surveys were acquired using an array of geophones deployed on the surface. 4D VSP was acquired at the same time using conventional three-component geophone tools. At this stage, the conventional monitoring techniques were able to detect the injection (Gurevich et al., 2014), however, high

levels of time-lapse noise were present on the data due to the surface deployment of the geophones.

As a result, in the next stage of the project, Stage 2, a permanent seismic array was deployed on site (Freifeld et al., 2016). The permanent array consisted of 908 buried geophones. The geophones were buried in attempt to reduce time-lapse noise. Additionally, approximately 40 km of fibre optic cables were installed, along with the surface geophones and along the injector well (on tubing). 4D surface seismic and 4D VSP with geophones were the main monitoring tool (Pevzner et al., 2017). The repeatability of the time-lapse seismic increased significantly with the buried array (Shulakova et al., 2015). Also, the acquisition efficiency was improved as the survey duration was reduced to a few days. However, certain issues with acquisition remained, such as land access and invasiveness.

A main focus for the Stage 3 of the project was to reduce the acquisition footprint, reduce costs, and automate acquisition (Jenkins et al., 2017). For this, the monitoring will be achieved using multi-well VSP with permanently installed DAS in wells, and an array of permanent sources installed on the surface.

The use of DAS technology in Otway has the objective of developing a cost-effective monitoring strategy to image the CO_2 injection. In this thesis, I analyse a series of DAS datasets acquired during Stage 2C and Stage 3 of the Otway Project. These datasets include 3D surface seismic, 3D VSP with on tubing fibre deployment, 3D VSP with cemented fibre, as well as a series of offset VSPs acquired with conventional vibrator sources and permanent surface sources. I discuss the evolution of the use of DAS at the Otway Project. I analyse the different DAS datasets and discuss the lessons learnt from our experiments at Otway. Also, I analyse the imaging capabilities of DAS associated with different acquisition configuration and settings. In this thesis, I focus on the technical discussion of DAS acquisition and processing, as well as on the comparison of DAS sensors with conventional seismic sensors. The interpretation of the seismic data is outside of the scope of this work.

1.2 Research motivation and aim

Distributed acoustic sensing can dramatically decrease the cost of land based seismic imaging and reservoir monitoring, not only in CO_2 sequestration projects, but

also in Oil & Gas production projects. The main goal of this research project is to develop a cost-effective and reliable seismic monitoring technique based on DAS, applied to CCS. In order to achieve this, this thesis has the following objectives:

- Development of optimal DAS processing flows and algorithms;

- Evaluate overall performance of DAS and data quality. Compare DAS data with conventional seismic receivers (geophone and hydrophone);

- Compare various DAS cable designs, including standard fibres, helically wound fibres, and engineered/enhanced sensitivity fibres;

- Compare various cable deployment methods, including surface deployment, well deployment on tubing, cemented fibres, and fibre cables deployed loosely in the well;

- Analyse DAS imaging capabilities using difference types of seismic sources (vibrator trucks, surface orbital vibrator);

- Analyse the capabilities of using primarily DAS for monitoring at the Otway Project.

1.3 Thesis structure

This thesis is structured into nine chapters. The two first chapters are background chapters. The main work related to this research is presented in the next five chapters. Each chapter analyses a different type of DAS dataset. This thesis is organized in chronological order, meaning that the chapters are organized from the first set of data I analysed to the last set of data. The last chapter of this thesis is dedicated to research conclusions.

Chapter 2 and Chapter 3 describe the background needed for the development of this thesis. Chapter 2 describes the seismic method and elasticity theory. Also, in this chapter the reader will find the theory and principles of the DAS measurements, as well as a description of the physical measurements of the DAS receivers in comparison with geophone and hydrophone measurements.

Chapter 3 discusses different carbon capture and storage projects around the world and how seismic monitoring is used in their context. I describe the two project sites I use in this thesis: Otway Project and NGL research facility. For the Otway Project, I describe the history of the project and the development of its different stages. This chapter finishes with a short description of the NGL research facility.

Chapter 4 presents a series of field trials that took place at the NGL research facility. The field trials consist of a series of offset VSPs using DAS, conventional 3-component geophones, and hydrophones; with the objective of comparing the different datasets and analysing the advantages associated with each receiver. In this chapter, I aim to illustrate the main differences of the datasets and how to choose a seismic receiver depending on the survey objective.

In the next chapters, I analyse the different datasets acquired at the Otway Project site. Chapter 5 shows the results of 3D surface seismic acquired with DAS as part of the Stage 2C. The datasets presented in this chapter consist of the first experiments acquired with DAS using the permanent receiver array. The data showed in this chapter is possibly the first ever 3D surface seismic acquired with DAS, to the author's knowledge. Here, I analyse the data quality of surface seismic datasets acquired with DAS and the lessons learnt. The experience with the processing of the surface DAS taught us how to handle and manage the large volume of DAS datasets. Also, by analysing these datasets, we learnt to consider DAS angle sensitivity in survey planning. I also conclude that the high levels of noise on the surface DAS contribute to poor repeatability. The data acquired with a helically wound cable is also shown in this chapter. The lessons we learnt here were applied on the acquisition of the next surveys at Otway.

Chapter 6 shows the data acquired with DAS deployed on the tubing of the injector well, also as part of the Stage 2C of project. The 3D VSP with DAS on tubing was acquired simultaneously with the surface DAS survey. In this chapter, I discuss the performance of the 3D VSP with DAS on tubing and its imaging capabilities. I analyse the signal-to-noise ratio of the 3D DAS VSP. I conclude this chapter by demonstrating how the extremely long fibre contributed to the low signal-to-noise ratio on the data and how the data quality can be improved.

In the next chapters, I move to the data acquired during Stage 3 of the project. The lessons learnt from our experiments from the Stage 2C largely led the planning and acquisition of the DAS data as part of an initial assessment for the Stage 3. Although the data acquired during Stage 2C presented low signal-to-noise ratio, we saw the potential of using DAS for imaging during the next stage. As a result, a new well was drilled and a set of cemented fibres cables was installed. This well will be used for the monitoring program during Stage 3.

Chapter 7 shows the first Offset DAS VSP acquired on site using the cemented fibre installed in the new well. In this chapter, I look at the performance of DAS VSP across different offsets, up to 2 km far from the well, in relation to the target depth of 1500m. Here, I compare the VSP acquired with DAS using different fibre design (standard fibre and enhanced sensitivity fibre) and acquired with conventional 3-component geophones. Also, a series of field trials of DAS VSP were acquired with permanently installed surface orbital vibrators. The surface vibrators are part of the monitoring program for Stage 3. The results from these experiments showed that DAS VSP coupled with surface orbital vibrators can be used to image the injection interval.

After the successful field trials with the cemented DAS for offset VSP, we use the cemented fibre to acquire a 3D VSP. Chapter 8 analyses the result of the 3D VSP acquired with the cemented DAS and analyse its imaging capabilities. In this chapter, I also compare the quality of the 3D VSP with on tubing deployed fibre (acquired during the Stage 2C) and the 3D VSP with the cemented fibre.

In the last chapter, Chapter 9, the results presented in this thesis are summarized. In this chapter, I discuss the conclusions of this research, as well as the lessons learnt and future outlook regarding the use of DAS for seismic imaging and monitoring at the Otway Project and with a more global perspective.

1.4 Thesis contributions

This thesis contributes to the broader knowledge of the DAS method. I discuss processing techniques targeted at managing the large data volume produced by DAS. Also, I show the acquisition of DAS with different fibre deployment, different fibre designs, as well as discuss ways to improve data quality with DAS aimed at seismic imaging and seismic monitoring.

This research is part of a research/collaboration group from Curtin University composed of professors, research assistants, and PhD students. The research group works on various subjects, in particular for the application of technologies for CO_2 sequestration, for application at the CO2CRC Otway Project. This thesis specifically contains a result of collaborations of various researchers from different areas within the group. Appendix A shows the papers related to this PhD research and the contributions from each co-author. My specific role in this collaboration includes the following:

- I participated in almost every survey acquisition as field crew at various positions, from vibroseis spotter to senior observer;
- I processed all datasets in this thesis, using commercially available seismic processing software (SeisSpace, RadExPro, Vista);
- I contributed to development of the Curtin in-house MATLAB codes used for DAS data processing building on the existing codes and collaborating with the group;
- I have written most of the text for the extended abstracts presented in conferences, as well as papers published in journals related to the findings presented in this thesis where I am listed as a first author and contributed to other publications led by other researchers and research students;
- I partially contributed to the development process of the monitoring program for the Stage 3 of the Otway Project from the results produced throughout this research project.

Overall, the research presented here contributes to the following:

- Processing algorithms and processing flows specific for DAS data were developed;
- Observed angle sensitivity on DAS, seen primarily on surface deployment, and how the acquisition planning can affect the quality of the acquired DAS data
- Analysed 3D VSP acquired with on tubing fibre deployment and cemented fibre. Both deployments methods are compared;
- 3D VSP with DAS effectively images the CO_2 injection interval at Otway;

- Offset VSPs with DAS and permanently installed surface vibrators can image the injection interval, offering an alternative on-demand and automated cost-effective method to monitor the injection;
- Different seismic receivers were compared. Discussed the advantages of using each receiver depending on the survey objectives.

CHAPTER 2 BACKGROUND

2.1 Seismic imaging and monitoring

2.1.1 Seismic reflection method

In this section, I explain the principles of seismic reflection method and explore two deployment methods for seismic reflection: surface seismic and vertical seismic profile (VSP). I focus on these two methods as they are used for the acquisition of the datasets presented in this thesis.

Seismic is the most popular geophysical method in terms of industry expenditure due to its high accuracy and high resolution (Telford et al., 1990). The basic concept of seismic imaging is based on the measurement of the travel time of an elastic wave from the source to the seismic sensor in order to accurately reconstruct images of the earth in space. The acoustic wave is usually generated in active surveys from an artificial source of energy. In the case of passive surveys, no active source is used and the background acoustic energy itself is recorded and analysed. To record the acoustic energy, seismic sensors are planted on the ground or deployed in-sea. Geophone sensors are commonly used on land, and hydrophone sensors used in water. The time travel information recorded by the seismic sensors together with the velocity (obtained through, for example, sonic logging or semblance analysis) can then determine the depth of a given reflector layer.

One of the first known active seismic experiments dates from the 1848 and 1851 when Mallet calculated the seismic velocity of acoustic waves from an “artificial earthquake” (black powder as the seismic source) by recording the travel time with a seismoscope. The source energy was generated by burying a charge of gun powder. Theoretical work in the field of seismology was further developed by Schmidt in 1888, where he predicted that the velocity of seismic waves would increase with depth. Further work within the scope of theory of reflected and refracted waves was published by Knott in 1899, prior to Wiechert and Zoeppritz in 1907. Since then, the method gained increasing popularity as the technology grew, enabling major applications in

geological engineering and in the oil and gas industry. A detailed history on refraction and reflection seismology can be found in Allen (1980) and Weatherby (1940).

In active seismic reflection methods, an artificial acoustic source, such as explosives, vibrator truck, or airgun, is used. The source position is known as "source point", "shot point", or "vibration point" (in case of a vibrator truck source). The geophones start recording from the moment the source is fired. The vibrator source is unique from the other usual sources in which it generates a sweeping signal in a range of frequencies. Alternatively, the geophone can record continuously; the sweep would then be "harvested" from the data by matching the trigger time stamp with the geophone recording. The vibrator truck is built to be a mobile and more environmental friendly alternative to the explosive source. The recorded seismic from a vibrator truck needs to be cross-correlated with the recorded seismic to generate a zero phase Klauder wavelet; the sweep signal is characterized by strong amplitudes throughout seismic frequencies (Chapman et al., 1981).

The seismic method relies on the elastic (or visco-elastic) propagation of waves through the rocks. These deformations change the size and shape of an elastic body. Once these forces are removed, the body returns to its original shape. The relations between applied forces and deformation can be expressed in terms of stress and strain (e.g. Sheriff and Geldart, 1995; Telford et al., 1990).

To understand the elastic properties, one can define stress as the force F per unit of area A, $\frac{F}{A}$. If the force is perpendicular to the area, the stress is called *normal stress*. If the force applied to the unit area is tangential, the stress is called a *shear stress*. If the applied stress is neither perpendicular nor parallel to the area, the stress can be expressed in terms of components of normal and shearing stresses, and comprises a tensorial measurement quantity.

By assigning a Cartesian coordinate system to an uniform body of dimensions *dx dy dz*, the normal stress applied to the sides perpendicular to the x-axis can be denoted as σ_{xx}, and the shearing stresses as σ_{yx} and σ_{zx}, where the first subscript denotes the direction of the force parallel to the axis and the second subscript denotes the surface perpendicular to the axis (Figure 2.1). Having said this, we can denote the

stresses on a surface perpendicular to the y-axis as σ_{xy}, σ_{yy}, and σ_{zy}, and the stresses on a surface perpendicular to the z-axis as as σ_{xz}, σ_{yz}, and σ_{zz}.

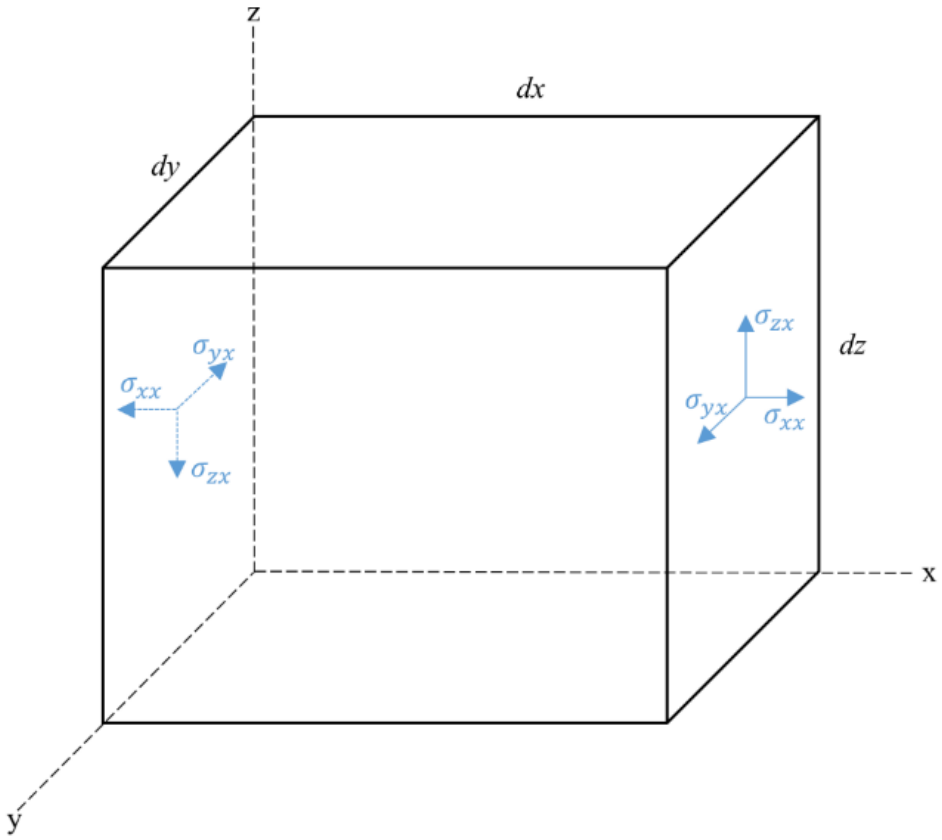

Figure 2.1 Stresses acting on both surfaces perpendicular to x-axis.

Strain is the fractional change in dimension and shape caused by stresses applied to an elastic body (Figure 2.2). In another words, strain is a measure of the deformation of a body relative to its prior or reference shape. Therefore, the strain ε of a body of length L, which change in length is ΔL, can be calculated as $\varepsilon = \frac{\Delta L}{L}$.

We can compute the strain along the x-axis of a body of length Δx, after a displacement of $u(x)$. For this, let us observe the vertices A and B of the body at its initial shape, which become vertices A' and B' after the displacement. When a stress is applied to the body, vertex A undergoes a displacement of $u(x)$, while vertex B undergoes a displacement of $u(x + \Delta x)$. Through a Taylor series expansion, the displacement $u(x + \Delta x)$ of vertex B can be represented in linear approximation as $u(x) + \frac{\partial u}{\partial x}\Delta x$. Therefore, the strain experienced by the body along the x-axis is

$$\varepsilon_x = \frac{\Delta L}{L} = \frac{L_{final} - L_{initial}}{L_{initial}} = \frac{(\Delta x + u(x) + \frac{\partial u}{\partial x}\Delta x - u(x)) - (\Delta x)}{\Delta x}$$

$$\varepsilon_x = \frac{\partial u}{\partial x} \qquad (1)$$

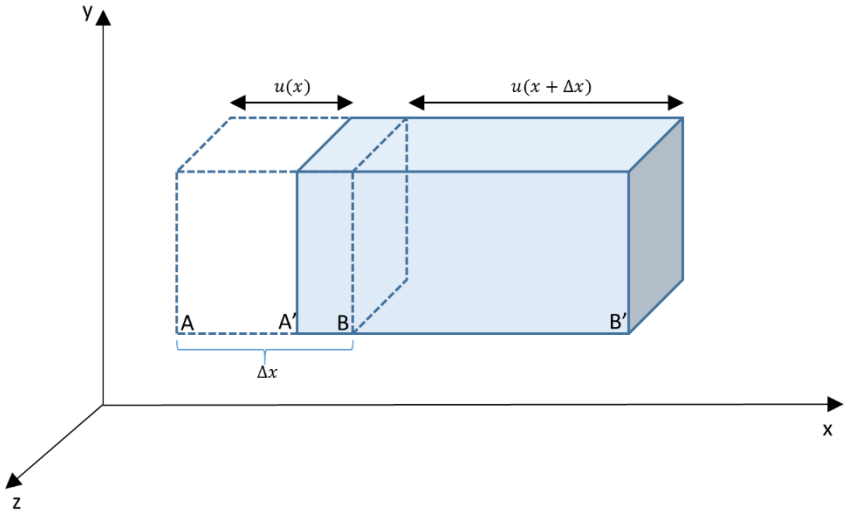

Figure 2.2 Strain tensor along the x-axis.

By doing the same process in respect to *y*-axis for displacement *v*, and in the to *z*-axis for displacement *w*, we can describe the strains as

$$\varepsilon_x = \frac{\partial u}{\partial x} \qquad \varepsilon_y = \frac{\partial v}{\partial y} \qquad \varepsilon_z = \frac{\partial w}{\partial z}.$$

Now, we can see that strain is a dimensionless measurement. Hooke's law states that, for an elastic behaviour, the stress applied to a body is proportional to the strain. This law is the basis of elasticity theory. Normal strain is defined for deformation that occurs as a result of a parallel stress. The normal strain is denoted as ε_{xx}, ε_{yy}, and ε_{zz}.

Apart from the normal strain, shear strain can also occur. Shear strain occurs when the displacement is relative to a different direction other than the displacement direction. In addition to the strain, the body can suffer simple rotation about the axes. The details regarding shear strain and rotation are outside the scope of this thesis. For further explanation on elasticity theory, the reader can refer to Sheriff and Geldart (1995), Telford et al. (1990), and Atkin and Fox (1980).

Two types of waves can propagate in an infinite homogenous isotropic medium: P-wave and S-wave. The P-wave, also known as primary wave or compressional wave, corresponds to changes in the dilatation (change in volume per unit volume) of a body. The particle motion within a P-wave is parallel to the wave propagation. The S-waves, also known as secondary or shear waves, move particles perpendicularly to the propagation of the wave. The P-waves and S-waves are called body waves because they propagate through the interior of the earth (Sheriff and Geldart, 1995).

Surface waves propagate in the vicinity of the surface. The surface waves can be classified as *Rayleigh waves*, *Stoneley waves*, *Love waves*, or *tube waves*. The Rayleigh waves are regularly seen in land exploration seismology and are often a matter of concern during seismic processing. In the seismic data, Rayleigh waves are identified as noise, also commonly called as *ground roll*. They propagate along a free surface of a solid. In the case of rock-air interface, the elastic constants and density of the air are so much lower than a rock that this interface can be considered a free surface. Rayleigh waves present longitudinal and transverse particle motion. The Stoneley waves and Love waves are also known as surface waves, though, less commonly seen on seismic data. Stoneley waves propagate in the boundary of a solid-solid. Love waves are horizontally polarized surface waves; they are common for causing horizontal shift on the earth during an earthquake. Tube waves are also classified as surface waves, though, commonly seen only on VSP data. They travel along the surface between the well casing and the well fluid. They are generated by a disturbance at the well head, such as a Rayleigh wave, that passes by the top of the borehole and perturbs the fluid in the well.

2.1.2 Surface seismic

In the surface seismic method, the sources and receivers are located on the surface of the earth (Figure 2.3). As mentioned before, for land surveys, explosives and vibroseis sources are commonly used. Geophones are the usual seismic receivers that acquire the backscattered energy generated by the source signal. In marine surveys, airguns are used as sources together with hydrophone streamers as receivers.

Surface seismic surveys can be either 2D or 3D. One of the main benefits of 3D surveys in relation to 2D is that it can image off-plane reflectors. However, 3D seismic acquisitions are considerably more expensive due to the large amount of equipment, and personnel, needed for the acquisition. The reader can refer to textbooks, such as Telford et al. (1990), for more information on surface seismic acquisition.

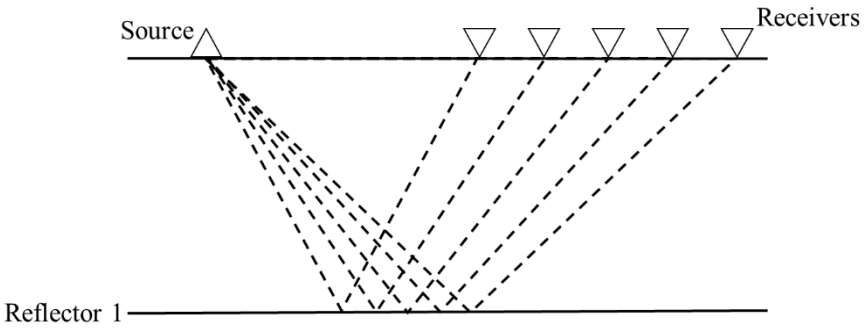

Figure 2.3 Surface seismic configuration.

2.1.3 Vertical seismic profiling

In a VSP configuration, the seismic receivers are located inside a borehole, and sources are either on the surface or also inside the borehole (Galperin, 1985; Hardage, 2000). VSP datasets differ from surface seismic in many ways, as they contain both upgoing and downgoing wavefield. The illumination pattern is also different in comparison with the surface seismic, given that the position of the receivers results in recording a wavefront with distinct wave path. VSP records present lower noise levels as the seismic receivers are usually positioned in a low noise environment (i.e. well).

VSP surveys can be categorised as zero-offset, near-offset, far-offset, and walk-away, which reference the position of the source (Figure 2.4). In the zero-offset and near-offset configurations, the source is located on the surface in vertical or near vertical alignment with the well. This type of configuration is usually used so the well information can be tied to the surface seismic information, or to obtain velocity information from the time-depth curve of first arrivals. In the offset VSP geometry, the sources are located far from the well. This type of configuration is useful for imaging the geology in more detail and away from the well. In a walk-away VSP,

multiple source points are acquired along different shot positions usually along a line passing through the well head. This will consequently increase the imaging range within a survey (Oristaglio, 1985).

However, in such configurations the VSP image is limited to a 2D seismic image around the borehole. Since the area of interest is always a volumetric body, 2D surveys cannot properly solve the target's distribution and properties. To overcome this, the VSP survey can be acquired using a distribution of shots in an area on the surface, which will generate a 3D VSP image (Zhang et al., 1996). This configuration is ideal for producing subsurface images with increased spatial resolution.

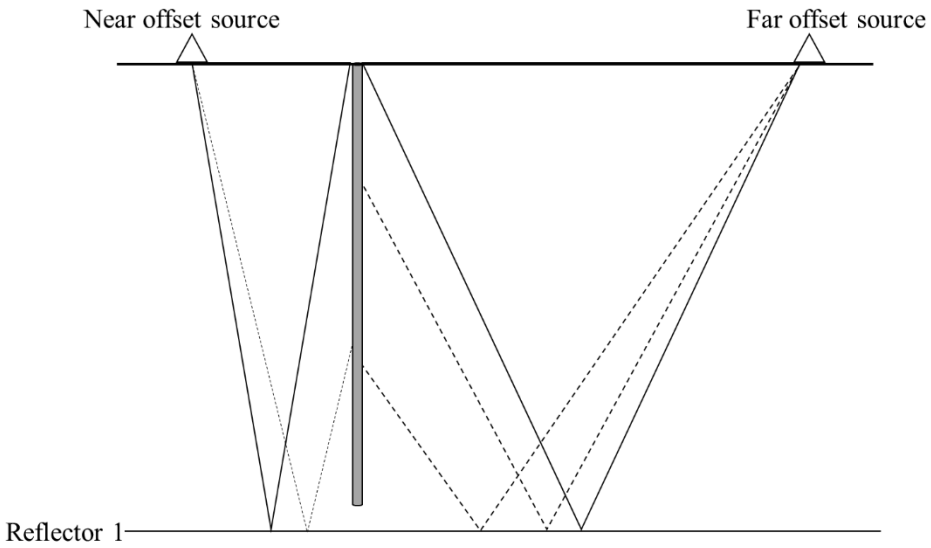

Figure 2.4 Illustration of two VSP configurations: near and far offset. Well trajectory is displayed in grey and the selected idealised raypaths demonstrate different illumination of the horizontal reflector.

2.1.4 Time-lapse seismic monitoring

Time-lapse seismic monitoring acquires several seismic surveys over a period of time with the objective of detecting changes in the physical properties of a reservoir or target interval. The aim of time-lapse seismic monitoring is to image and track the changes of a reservoir, and possibly predict the changes. When repeat surveys are 3D seismic surveys, the time-lapse imaging is also referred to 4D seismic.

Seismic monitoring applications began in 1980s with Nur et al (1984) who, through rock physics measurements, predicted that processes to enhance oil recovery, such as steam injections, should provide a difference in the seismic signal.

To acquire time-lapse seismic, each seismic survey is ideally acquired with repeated acquisition parameters (e.g. source type, source interval, receiver interval) and similar conditions (e.g. noise levels), so that the difference observed between surveys can be attributed to changes in the reservoir conditions (Lumley, 2001). However, repeating the same survey conditions over time is not trivial. Access to a certain area may be restricted for example, making it impossible to repeat the exact source/receiver locations. Additionally, noise levels may vary during the day, or even during the year, compromising the similarity of each survey in comparison to the reference survey. The level of similarity between surveys can be measured by calculating the repeatability, which quantifies the likeness between two traces (Kragh and Christie, 2002).

2.1.5 Permanent reservoir monitoring

Permanent reservoir monitoring (PRM) is the practice of constant surveillance of reservoir conditions, such as pressure and temperature. It helps to understand the dynamic behaviour and subtle changes in the reservoir, aiming to improve oil recovery and increase safety in operations. The full instrumentation of wells provides real-time monitoring of the conditions inside the borehole and its surrounding.

PRM involves a complex number of sensors and equipment working simultaneously. The largest permanently installed seismic array is in the Valhall oil field, in the North Sea, with recording capacity of more than 30 terabytes of data (Van Gestel et al., 2008). Other well-known permanent reservoir monitoring projects were implemented in Grane field (Berraki et al., 2017) and in BC-10 field (Galarraga et al., 2015).

Most PRM projects are located offshore. This happens because, when it comes to onshore permanent monitoring, the data is often affected by certain conditions that overcome the time-lapse signal. Such issues include seasonal or diurnal near-surface variations and poor signal to noise ratio. Also, surveys acquired with permanent installations onshore are expensive in comparison with acquisitions using retrievable

systems. Hornman et al. (2015) proposes alternatives to lower the costs of onshore permanent monitoring and shows that using fibre-optics as a seismic sensor can be a cost-effective alternative. Jervis et al. (2018) demonstrates land time-lapse monitoring at a complex desert environment for CO_2 enhanced oil recovery. The Schoonebeek field is also another example of onshore continuous seismic reservoir monitoring (Cotton et al., 2013).

Several of these permanent sensors used for permanent reservoir monitoring belong to the group of fibre-optic sensors. Fibre-optic sensors are especially suited for well installations due to their inherent long durability and robustness. In the next section, I discuss the principles of distributed fibre-optics sensing, which represents a specific group of fibre-optic sensors.

2.2 Fundamentals of distributed fibre-optic sensing

2.2.1 History of distributed fibre-optics sensors

The beginning of modern fibre-optic sensing starts with the appearance of low-loss optical fibres in the 1970's. Since then, a wide variety of fibre-optic sensors were published in the literature, fuelled by mostly military interest. One of the first commercialized fibre-optic sensors was the fibre-optic gyroscope. Also in the 70's, the first developments in optical time-domain reflectometry (OTDR) were published. The OTDR technology would serve as a base for the development of distributed optical sensing later on. After major investment by the telecommunication industry in the 1990's, fibre-optics experienced widespread adoption. With this, the price of a single-mode fibre decreased from $10 as sold in the 70's, to approximately $0.10 per metre (Udd and Spillman Jr, 2011).

After successful field trials in the early 90's, oil and gas companies started investing significantly in fibre optics sensing systems for in-well monitoring. The first downhole installation of a fibre-optic system happened in 1993; the installation was aimed at pressure and temperature sensing (Johannessen et at., 2012). One of the first seismic applications of fibre-optic sensing was published by Bostick (2000), when fibre point sensors recorded the response to seismic excitations in a well. Since mid-2000's, the seismic industry has seen an increased investment in the use of distributed sensing, as opposed to fibre point sensors.

A specific kind of distributed sensor, however, has caught the attention of the seismic industry during the last couple of decades. Distributed Acoustic Sensing (DAS) has seen rapid development for seismic applications, particularly propelled by investments from the oil and gas industry.

DAS is particularly interesting for seismic because it enables the acquisition of seismic data along a single continuous fibre-optic cable, sampled at small spatial intervals. This means that DAS can facilitate techniques not possible with conventional seismic acquisition. For example, DAS can acquire seismic using "virtual" distributed receivers spaced at distances as small as 25 cm. This is nearly impossible for conventional seismic acquisition as it would be extremely costly due to the amount of receivers - and time – needed for such deployment and retrieval. Additionally, the fibre cable can be installed permanently on the ground or in wells for continuous on-demand seismic monitoring. Using fibres for permanent monitoring eliminates the risk of electronic equipment failure associated with conventional sensors. As the fibre-optic cable is also relatively robust, maintenance of the cable is minimal during the lifetime of a well. For the oil and gas industry, these advantages result in significant savings in the long-term.

When it comes to VSP acquisition, DAS is especially suited as the method presents increased sensitivity for incident waves that are polarized along the cable. The first field tests of DAS showed the successful application of the technology for the acquisition of VSP surveys (Mestayer et al. 2011; Miller et al. 2012).

In the following section, I will explain the principles of the DAS method and the main aspects and characteristics associated with the measurement. For an in-depth overview of fibre-optic sensing and DAS, the reader can find more details in Hartog (2017).

2.2.2 Optical time-domain reflectometry

Optical time-domain reflectometry (OTDR) is a well-stablished technique to detect imperfections and determine their location within the optical-fibre. OTDR systems were first demonstrated in 1970's (Barnoski and Jensen, 1976; Personick, 1977). Today, they are widely used in the optical communication industry to assure the integrity of optical fibres. When applied to sensing applications, the principles of

OTDR systems are used in order to detect variations in the loss or scattering coefficient of a continuous fibre (Kersey, 2011).

When a light pulse is sent through an optical fibre, the power of the light decays along its way due to numerous attenuation processes. If the fibre is homogeneous and in a uniform environment, the decay in the intensity of the backscattered light is exponential in relation to time due to the intrinsic loss in the fibre (Kersey, 2011). If a defect is present in the fibre, the intensity of the backscattered light will change. By monitoring the variations of the backscattered light, the OTDR can determine the position of the defect, given that the refractive index of the fibre and the travel-time of the backscattered light are known.

The power of the backscattered light P_s detected at time delay t can be written as

$$P_s(t) = (1-k)kP_0Dr(z)exp\{-\int_0^z 2\alpha_i(z)dz\}, \quad (2)$$

where P_0 is the peak power of input pulse, z is the distance in the fibre equal to $ct/2n$, $\alpha_i(z)$ is the attenuation coefficient in nepers (1 neper = 4.34 dB in power) per unit length, n is the refractive index of the fibre core, c is the velocity of the light, k is the input fibre coupler power splitting ratio, $r(z)$ is the effective backscatter reflection coefficient per unit length, and D is the length of the light pulse in the fibre. If a localized loss is present in the fibre, the slope of the logarithm of the power of the backscattered light will change.

Most of the emitted light is attenuated by Rayleigh scattering. Rayleigh scattering is an elastic mechanism and is one of the main mechanisms governing the decay of the light. Rayleigh scattering happens when the light reflects on random microscopic variations of refraction index inside the fibre core. Due to Rayleigh backscattering, approximately 0.1% to 1% of the total emitted light to the optical fibre is returned.

For measurements based on Rayleigh backscatter, the measurement is analysed with respect to loss $\alpha(z)$ or scattering $r(z)$ mechanisms. The backscatter coefficient is mostly dependent on the temperature. This mechanism is weak in solid-core fibres,

though, it is visible when using fluid-core based fibres (Hartog, 1983). The strain information along the fibre can be analysed by measuring the loss coefficient.

However, other types of scattering also occur when light travels through a fibre. Apart from Rayleigh scattering, scattering effects can also be classified as Raman scattering and Brillouin scattering. Each scattering effect is sensitive to a particular range of physical conditions (e.g. changes in temperature, pressure, strain). In order to obtain a certain measurement, a system is built based on a specific scattering effect that will be sensitive to the desired measurement.

Raman scattering is a less predominant attenuation mechanism. It is an inelastic process when a small portion of the photons are scattered from molecular vibrations, which changes the frequency of the photons. Therefore, in Raman scattering, the backscattered photons have a different frequency than the incident photons. As Raman scattering is sensitive to the excitations of molecules, Raman-based measurements usually are aimed at detecting changes in temperature.

Brillouin scattering is also an inelastic process somewhat similar to Raman scattering as it is caused by the vibrational properties of matter. In Brillouin scattering, however, the light interacts with phonons (acoustic vibration). This results in a shift in frequency at much smaller scales than Raman scattering. This property makes Brillouin-based systems more versatile than Raman-based systems as it can sense strain and temperature changes in glass, and measurements can be made over long distances.

2.2.3 Distributed acoustic sensing

This thesis shows applications on the use of DAS method for seismic, therefore, I focus on the theory of this particular sensing method.

DAS, sometimes referred to as Distributed Vibration Sensing (DVS), is a fibre-optics sensing technique that creates virtual distributed sensors using OTDR principles to detect small changes in the elongation of the fibre. Rayleigh scattering, unlike Raman or Brillouin scattering, is based on random static scatterers that are “frozen” in the fibre during the manufacturing process. DAS systems are based on coherent OTDR (COTDR) techniques, meaning a narrow-band pulse that is emitted produces coherent

backscatter. The phase relationship within the scattering signal is stable, although random (Hartog et al., 2013).

DAS acquisition utilizes an Interrogator Unit (IU) attached to one end of the fibre. The IU sends a series of laser pulses and then it monitors the backscatter light. The light travels through the glass with an approximate velocity of $2x10^8$ m/s, meaning that it occupies a 10m section of the cable for a 50ns long pulse. Knowing the elapsed time for the light to return to the IU, it is possible to identify where the backscatter took place.

DAS relies on distributed sensors, as opposed to point sensors. Point sensors measure a certain property or behaviour that occurs at that particular location. A distributed fibre sensor uses the fibre cable itself to sense a certain property, and its response is a combination of the responses along a section of the fibre. To understand what DAS measures, we have to understand the principles involved in its acquisition. As DAS is a relatively new method derived from fibre-optics sensing, most geophysicists are not familiar with its principles.

There are many practical approaches to build a DAS system. These approaches can be separated basically into amplitude-based systems and phase-based systems. Most commercial DAS systems for seismic purposes are based on differential phase-measuring.

Amplitude-based coherent OTDR measures the intensity of the backscattered signal from each point of the fibre (Figure 2.5). This type of systems are very sensitive to disturbances in the fibre, such as strain and temperature (Shatalin et al., 1998). They suffer from high nonlinearity. This type of systems determine accurately the position of a disturbance, however, they are limited in determining the correct amplitude, frequency, and phase of a signal. An example of application of such systems is in intrusion detection.

Phase-based systems compare the phase of the backscattered signal between two sections of the fibre. When strain is applied to a specific finite area of the fibre, the elongation of the fibre will cause a delay of the backscattered signal. As a result of the random scatterers in the fibre, the phase of the backscattered pulse itself is also random. The phase of the backscattered light is determined by the summation of the

phase of different scatterers within the area of the fibre occupied by the laser pulse. When a change in strain occurs, not only the phase in that section of the fibre will change, but also the phase of the backscattered signal from all subsequent sections of the fibre will alter. The relation between the strain and phase change is linear (Juškaitis et al., 1994). Comparing the phase change of the backscattered signal between two sections of the fibre is the main principle in phase-based systems.

There are different ways to compare the phase change in a DAS system. Some systems use a single pulse, other systems use a dual-pulse. Certain systems process the backscattered light in the optical domain, some transfer to electrical signal and then process it.

One approach is launching a single pulse (narrow frequency) and comparing the phase difference between two sections of the fibre before it is sensed by the optical detectors (Figure 2.6). In this approach, the phase needs to be recovered (different systems use different methods of interferometric recovery approach to detect the phase). The usual approach, though, splits the backscattered signal when it returns to the launching end, and sends each into separate paths of different lengths. Then the signal is recombined and sent to a coupler. The phase can be recovered by monitoring outputs from the coupler (Posey et al., 2000). Farhadiroushan et al. (2010) demonstrated a single pulse interrogator with similar approach, though, using a Michelson interferometer.

In the approach developed by Hartog and Kader (2012), a single pulse is also used, though, the signal is converted to the electrical domain and then digitally processed. This system is known as the heterodyne distributed vibration sensing (DVS) system (Figure 2.7). An advantage of doing the phase differentiation in the digital domain is that certain acquisition parameters, such as spatial resolution (i.e. gauge length) can be altered in the processing, as opposed to selected during the acquisition.

Some DAS systems use a dual-pulse technique (Dakin and Lamb 1990) (Figure 2.8). In this type of system, two pulses are emitted with different frequencies with separation equal to the gauge length (explained later in this section). As the pulses have different frequencies, when recording the backscattered signal, the two pulses

can be easily separated (through usual techniques applied in telecommunication industry).

There are different techniques which can be used to calculate the difference in phase of the backscattered signal. For commercial DAS systems, the exact method in each system is unknown due to proprietary information. Among various operating parameters of a DAS system, perhaps the most important are the *pulse length*, the *gauge length*, and the *pulse repetition frequency (PRF)*. These three parameters mostly control the signal to noise ratio and resolution of the measured signal.

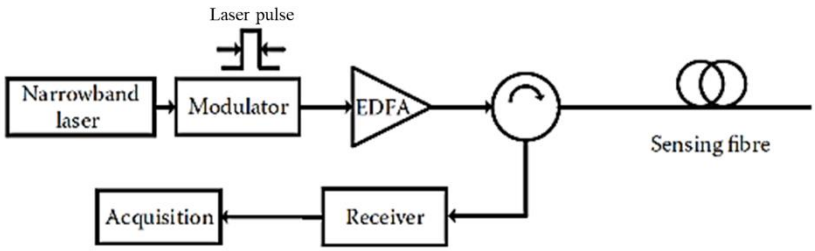

Figure 2.5 Amplitude-based coherent OTDR (reproduced from Hartog, 2017, and from Shatalin, 1998). EDFA stands for erbium-doped fibre amplifier.

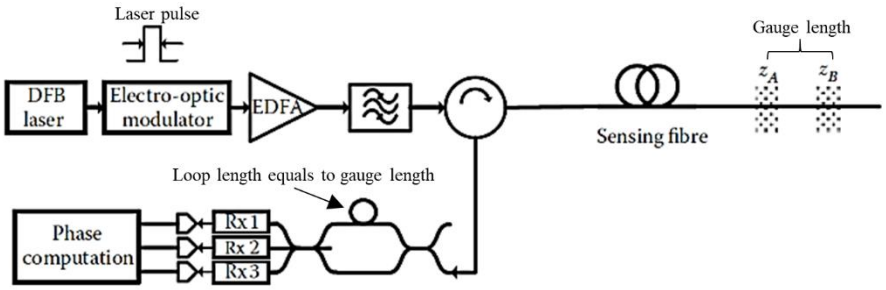

Figure 2.6 Single pulse DAS system based on interferometric phase demodulation (reproduced from Hartog, 2017, and from Posey et al., 2000). DFB stands for distributed fibre feedback.

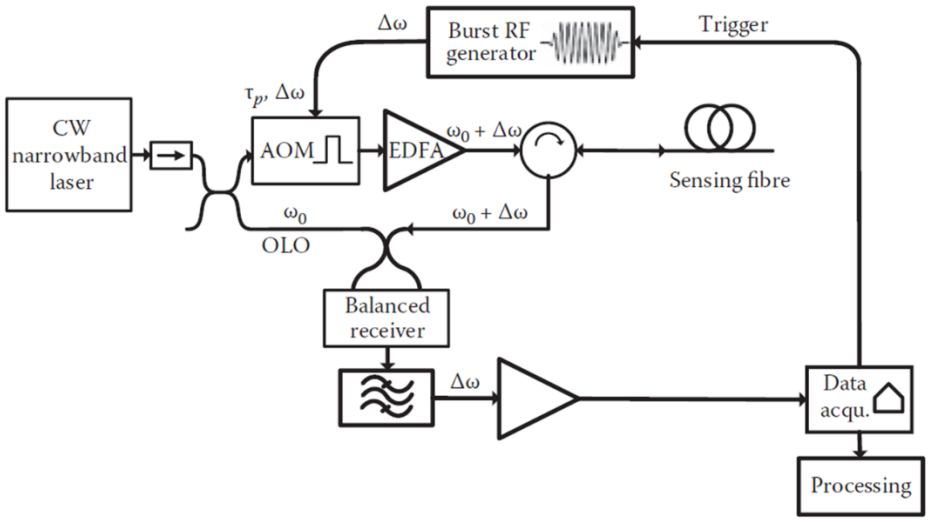

Figure 2.7 Heterodyne DVS system (reproduced from Hartog, 2017). OLO stands for optical local oscillator, and AOM stands for acousto-optic modulator. τ_p is the pulse length, and ω is the frequency.

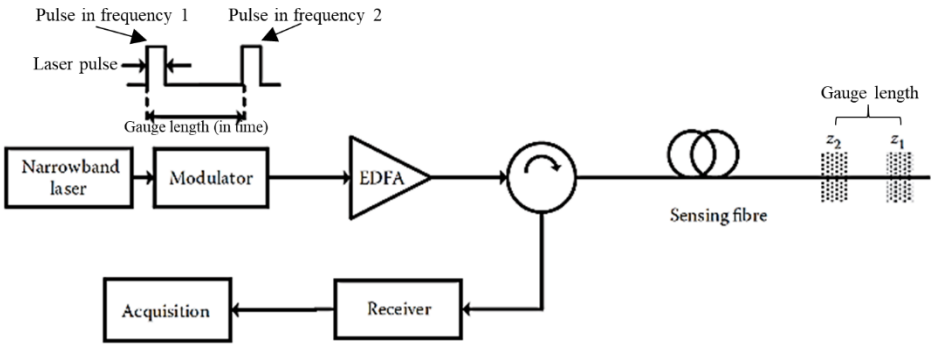

Figure 2.8 Dual-pulse DAS system (reproduced from Hartog, 2017, and from Dakin and Lamb, 1990).

The pulse length is the duration of the emitted light. So if an emitted pulse light had total duration of 50 ns, this means that the pulse is occupying a 10 m section along the fibre. The gauge length (Figure 2.9) is the physical distance between two points in the fibre used to compute the difference in phase of the backscattered light. The gauge length has an attenuation effect on the seismic wave. It acts in practice similar to a Gaussian filter (Dean et al., 2016a). Some DAS systems have a fixed gauge length (e.g. 10 m gauge length used in experiments described later in the thesis), and some have variable gauge length which can be chosen in the DAS IU.

The gauge length parameter directly influences the signal to noise ratio and resolution of the data. The bigger the gauge length, the better the signal to noise ratio, however, large gauge lengths reduce the resolution. Also, as a note of caution, when the gauge length is reduced to smaller than the pulse length, this causes the relation between phase and strain to be non-linear. To choose an appropriate gauge length for acquisition, one needs to take into consideration the expected resolution to be achieved. Dean et al. (2016a) demonstrates how to determine the optimum gauge length for acquisition that does not degrade the resolution and provides a satisfactory signal to noise ratio.

An important aspect of DAS acquisition to consider is that the gauge length and pulse length together determine the spatial resolution. Though, the spatial resolution should not be confused with the spatial sampling, which, in some DAS systems, can be as low as 25 cm. Reducing the gauge length will naturally increase the resolution, with a trade-off in signal to noise ratio proportional to spatial resolution squared (Parker et al., 2014).

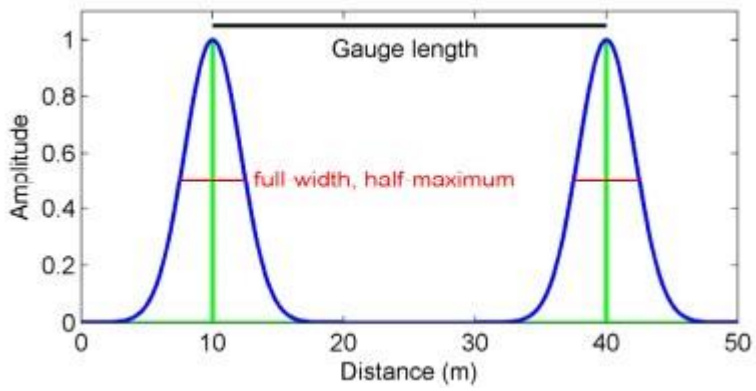

Figure 2.9 The relationship between gauge length and pulse width (reproduced from Dean et al., 2016).

The PRF controls how fast the light pulse is fired from the IU. In most systems, only one light pulse should be occupying the fibre at all times. Therefore, the length of the fibre controls the maximum usable PRF, since the emitted pulse must travel along the fibre length and return to the IU before the next pulse can be launched. The higher the PRF, the more accurate is the discrimination of phase. Discriminating more accurately the phase means that the final DAS data contains less phase noise, and thus, higher S/N. For the acquisition of DAS data, one should select the highest possible PRF for a given fibre length. The speed of light in the glass is approximately $2x10^8$ m/s, therefore, for a 10km fibre, the maximum PRF is approximately 10 kHz. This means that the laser is being pulsed at 10 kHz rate, and thus being sampled at 10 kHz.

To correctly sample the phase, the sampling rate of a DAS system is far higher than any usual seismic acquisition system, as sampling frequencies are usually above kHz scale in DAS systems. Frequencies are then down-sampled usually to 1 kHz to suit seismic applications. Frequencies as low as 8 mHz, and as high as 49.5 kHz, have been measured using DAS (Parker et al., 2014). This means that DAS applications extend beyond the usual seismic bandwidth.

2.2.4 DAS limitations

The main limitations seen on the DAS method are associated with its strong angular dependence and signal to noise ratio. Furthermore, the gauge length and pulse length add further limitation associated with the resolution of the data.

DAS data often have lower signal to noise ratio compared to geophone sensors data. DAS usually possesses high levels of random noise, or also referred to phase noise. Though, as phase noise is random, it can be easily attenuated by stacking, for example, repeating a shot acquired in the same location or increasing PRF. With this, the signal should increase as $\sqrt{N}$, where N is the number of repeated shots.

As technology develops, the quality of DAS data approaches that of conventional receivers. In recent experiments, DAS data showed superior quality than geophones due to its high spatial sampling and relatively low levels of noise (Correa et al., 2017a). The high spatial sampling is a major advantage offered by DAS as it is able to accurately sample reflections at small spatial intervals. Further developments into "enhanced" fibres that are specifically engineered to increase light backscatter will further increase the sensitivity of the fibre and signal to noise ratio (Farhadiroushan, 2018).

Due to the relatively rigid characteristics of the fibre, broadside incident waves are hardly detected. As DAS is measuring the change of fibre length in a gauge length, any orthogonal incident P waves will not be detected. In fact, incident P-waves on DAS data decay as cosine squared of the angle of incidence (Kuvshinov, 2016), as opposed to geophone data, which decays as cosine of the angle of incidence. Due to its unique directivity response, DAS is more suitable to VSP applications, as most of the desirable P-wave reflections are polarized along the fibre axis.

The gauge length and pulse length determine the resolution of the data. Usual gauge lengths vary from 2 to 40 m. Small gauge lengths will provide response similar to that of a point sensor, however at the cost of signal to noise ratio. The pulse length of the laser also results in resolution limitations. Though, the selected gauge length should be larger than the pulse length to ensure a monotonic response.

As the DAS signal is a result of a phase summation within a section of fibre, this summation at times results in destructive interference, which yields zero amplitude strain. As demonstrated in Dean et al. (2016), the gauge length in DAS systems causes a destructive interference effect in the seismic signal wavenumber. As wavenumber $k = f/V$, where f is frequency and V is seismic velocity, it is noticeable that the gauge length will also affect certain frequencies, depending on the apparent

seismic velocity. These notches happen when the measured wavelength of a seismic wave is equal to the gauge length.

"Fading" is another issue that affects DAS measurements. Fading happens when the resulting summation of the amplitudes from different scatterers within a gauge length approaches zero. This destructive interference effect happens occasionally.

Depth calibration (in case of VSP survey) is another limitation associated with the DAS method. DAS IU calculates the position of each trace in relation to the emitting end. The distance is calculated by analysing the travel time of the backscattered light. The time, however, varies depending on the reflective index of the fibre. The DAS IU is configured for a certain fibre cable length, and the location for each virtual sensor can be determined precisely within the fibre domain. However assigning a geographical location in *x, y, z* to the virtual sensors is not trivial. For example, a fibre cable deployed in a well might have a slack, which makes it difficult to assign depths based on the fibre length. For seismic applications, correct positioning is fundamental to determine correctly the location of a reflector in subsurface. At this stage, there is no standard method for depth calibration of DAS data that provides accurate and precise positioning.

2.2.5 DAS applications

Within the seismic industry, DAS has been mostly applied to VSP configuration. Though, DAS applications extend beyond the seismic industry, to include security, road management and gas pipes integrity surveillance. DAS presents itself as a unique sensor when compared to conventional seismic receivers as the method can vary PRF and gauge length parameters, with this, adapting itself to the objective of the survey.

For VSP acquisition, fibres cemented behind the casing usually provide the optimal signal to noise ratio (S/N) in comparison to other cable deployments (e.g., cable deployed on the tubing or inside the tubing). However, it might not be operationally practical to cement DAS cables even in new wells, as this can potentially increase the risk to the well integrity. In such cases, DAS can be deployed on the well tubing (Barberan et al., 2012; Didraga, 2015) or simply suspended inside the well.

Furthermore, recent developments offer wireline cables with built-in fibres for DAS (Hartog et al. 2014).

DAS has been used in a wide variety of applications within the seismic industry. Most seismic surveys with DAS are targeted at VSP configuration (3D VSP, walkaway VSP, or offset VSP surveys). Several publications demonstrate the acquisition of DAS data for VSP (e.g. Barberan et al., 2012; Correa et al., 2017b; Didraga 2015; Hartog et al., 2014; Miller et al., 2012; Willis et al. 2016).

Additionally, DAS can also be used for the acquisition of surface seismic. Correa et al. (2017c) demonstrated the first ever 3D surface seismic acquired with DAS to the author's knowledge, though, the acquired datasets showed strong angle sensitivity, which limited the imaging depth. Bakulin et al. (2017) demonstrates the application of DAS for near surface characterization by using a series of shallow holes instrumented with fibre-optics. Recent developments have presented the concept of "helically wound fibre" (HWC), where the fibres are spiralling around the core of the cable to increase sensitivity to broadside incident waves (Hornman, 2017). The HWC cable facilitates the application of DAS on surface seismic due to the increased angle sensitivity.

DAS has seen major development propelled by the Oil & Gas industry for applications aimed at permanent reservoir monitoring. Mateeva et al. (2014) and Mestayer et al. (2011) have demonstrated that DAS produces acceptable levels of repeatability between surveys, being a promising technology for continuous reservoir monitoring. DAS has also been applied successfully for 3D VSP in the Valhall oil field (Hance et al., 2016). Field trials with DAS VSP in Trinidad demonstrated similar results to ocean-bottom cable data (Zhan et al., 2015). Lopez et al. (2017) suggests the application of 4D DAS VSP in deep-water offshore Brazil, however, the technology is still to be implemented. Additionally, 3D VSP with DAS was acquired in a heavy oil field in South Oman (Al Adawi et al., 2013), where it was used with the objective of testing DAS for permanent reservoir monitoring. The acquired DAS data showed comparable results with the data acquired with conventional receiver.

In the context of CO_2 sequestration, use of DAS has also been demonstrated for seismic imaging and monitoring. Daley et al. (2013) showed promising results of

DAS VSP acquired at the Citronelle site, Otway site, and Ketzin site. Freifeld et al. (2016) showed DAS acquired on the surface using a HWC cable and a straight cable, and also acquired for VSP with a straight cable. Harris et al. (2017) showed the imaging of fluid injection using DAS at the Aquistore project site. Miller et al. (2016) demonstrated DAS acquired with multi-mode and single-mode fibre-optic cables also at Aquistore. Gotz et al. (2018) has demonstrated DAS for the acquisition of multi-well VSP at the Ketzin site. At the Quest CCS Project, a walk-away DAS VSP was acquired to monitor the injected CO_2 plume (Bacci et al., 2017).

Another application of DAS is earthquake detection. Martin et al. (2017) continuously recorded DAS on the surface fibre-optic cable, identifying a variety of events, including earthquakes. Biondi et al. (2017) concludes the suitability and efficiency of DAS for earthquake detection. Lindsey et al. (2017) concludes that DAS array could complement early earthquake warning systems. Pevzner et al. (2018) also shows the detection of earthquakes by DAS deployed in a well.

DAS can also be used for ambient noise interferometry. Dou et al. (2017) demonstrates the efficacy of using DAS for near surface seismic monitoring by recording infrastructure noise. Zeng et al. (2017) concludes that ambient noise recorded with DAS is a practical way to provide subsurface information.

An additional major application of DAS is for microseismic detection in the monitoring of hydraulic fracking. Webster et al. (2013) used DAS to detect microseismic events. Bakku et al. (2014b) showed that DAS is usable for time-lapse fracture monitoring. Cole et al. (2018) also estimated source parameters of microseismic events from DAS data.

2.3 Principles and physics of seismic sensors

Geophone and hydrophone receivers are widely used sensors in the seismic industry for the acquisition of land seismic and marine seismic. With the recent emergence of DAS as a new seismic sensor, there is a need to understand the basics of what is recorded by DAS, how the DAS sensor interacts with a plane wave, as well as recognizing the main differences between a DAS record and a geophone or hydrophone record.

In this section, I review the principles of the physical measurements of a geophone, hydrophone, and DAS. I also demonstrate mathematically how each receiver interacts with a monochromatic plane wave.

2.3.1 Geophones

Geophones are motion sensors that respond to the vibrations of the earth. The usual mechanism in geophone sensors consists of a magnet mounted on a spring inside a wire coil, which consequently generates an electric current due to the variations of the magnetic field caused by the magnet movement generated by the vibrations, as prescribed by Faraday/Lenz Law. For most of the frequency range of seismic waves, the geophone response is proportional to particle velocity, or the time derivative of particle displacement u in a particular direction, say z. For displacement u described by a monochromatic plane wave $\vec{A}e^{-i(\omega t-\vec{k}\vec{x})}$, one can describe the particle velocity as:

$$v_z = \frac{\partial u_z}{\partial t} = -i\omega A_z e^{-i(\omega t - k_z z)}, \qquad (3)$$

where z is the spatial coordinate, t is time, k_z is the z-component of the wave vector, ω is the angular frequency, and A_z is the magnitude of the displacement in the z direction.

The geophones can be viewed as forced harmonic oscillators, which are governed by the natural frequency (also referred as the resonance frequency) and the damping of the sensor. The natural frequency of the system depends on the rigidity of the spring and the mass of the attached to the spring. For ground motion with frequency below the natural frequency of the oscillator, the geophone outputs large uncontrolled vibrations that cannot be accurately recorded, resulting in a response that deviates from the ground displacement velocity. For this reason, damping is introduced to the geophone sensors in order to attenuate this effect (Lowrie, 1997).

2.3.2 Hydrophones

Hydrophone sensors are pressure responsive devices. They have piezoelectric transducers that emit an electric signal as a reaction to pressure, which allows them to

be used in fluid environments (Brown et al., 2002). The pressure sensed in a hydrophone can be expressed as

$$P = -\rho c^2 \left(\frac{\partial u_x}{\partial x} + \frac{\partial u_y}{\partial y} + \frac{\partial u_z}{\partial z}\right) \quad (4)$$

Considering harmonic waves propagating in a fluid medium only along the z-axis, one can express pressure P as

$$P = -\rho c^2 i k_z A_z e^{-i(\omega t - k_z z)} \quad (5)$$

where ρ is the density and c is the velocity of the wave.

The coupling of hydrophone sensors is done through the fluid. The sensors are simply deployed by suspension in the borehole fluid, with no need for clamping to the formation. As a result, the tool can be moved faster, which allows for greater coverage and spatial sampling when compared to clamped geophone acquisition. As the overall time of acquisition is significantly faster than the geophones, VSP surveys with hydrophones can be considerably cheaper.

The use of hydrophones for VSP surveys is a cheaper and faster alternative to geophones, as they can be easily deployed in large numbers. Additionally, hydrophones have the ability to record higher frequencies in the order of kHz, which makes them particularly ideal receivers when using high frequency sources, such as sparkers (Delvaux et al., 1987). Though, the sensitivity of the sensor can be reduced if the borehole is cased (Winbow, 1991), as in most wells used for hydrocarbon exploration. Though, in mineral exploration, wells drilled for the purpose of geological characterization can be left uncased.

Experiments carried out by Marzetta et al. (1988) demonstrated VSP data acquired by hydrophones were contaminated by high levels of background tube wave noise. Krohn and Chen (1992) also evaluated the use of hydrophones in boreholes, concluding that signal-to-noise ratio of hydrophone VSP data is inferior to geophone data, mostly due to the strong presence of tube wave noise. However, they also showed that, for frequencies above 300 Hz, hydrophone performance is similar to geophones. Therefore, the strong presence of tube wave noise is seen as a disadvantage towards the use of hydrophones for VSP surveys as it can compromise the quality of the

recorded signal (Krohn and Chen, 1992). Furthermore, Zimmerman and Chen (1993) demonstrated that hydrophones record higher frequencies than geophones.

2.3.3 DAS

DAS is a fibre-optic sensing technology that senses changes in the elongation of an optical-fibres. In principle, DAS works in a similar way as an OTDR system. DAS, however, can distinguish the amplitude, frequency, and phase response of the detected acoustic wavefield (Parker et al. 2014).

The DAS record is proportional to the strain on the fibre (or proportional to the strain rate, depending on the interrogator unit). As the name suggests, DAS is not a point measurement, as geophones and hydrophones, but a distributed one. That is, its response corresponds to the strain sensed over a continuous section of fibre; this section of fibre is determined by the gauge length.

In summary, DAS detects changes on the elongation of the fibre length along the gauge length (Parker et al. 2014). A relationship between strain and particle velocity (as acquired by the geophone sensor) can be demonstrated by calculating the derivative of the particle displacement $u = Ae^{-i(\omega t - \vec{k}\vec{z})}$ in space

$$\varepsilon_{zz} = \frac{\partial u_z}{\partial z} = ik_z u_z = \frac{ik_z}{-i\omega} v_z = \mp v_z / c \qquad (6)$$

which means that the strain recorded by DAS is proportional to the particle velocity v_z divided by the apparent seismic velocity c (phase velocity), with the sign determining the direction of propagation. k_z and v_z are the vector wavenumber and particle velocity projections to the vertical axis, respectively.

The projection of the vector wavenumber and particle velocity can be described as $k\cos\gamma$ and $v\cos\gamma$, where γ is the angle of incidence in respect to the normal. One can describe the strain response of a P-wave scalar potential of a plane wave along the z-axis as

$$\varepsilon_{zz} = ikA_0 \cos^2\gamma \, e^{-i(\omega t - k_z z)} . \quad (7)$$

Note a cosine squared term appears to describe the strain. This cosine squared term describes the directionality pattern of DAS data, as the amplitudes decay as cosine squared of the angles of incidence (Kuvshinov, 2016).

A fibre cable along the z-axis will also suffer deformation induced from the S_v component of an S-wave (except for a vertically incident S-wave). The S_v wave will provoke particle displacement along the vertical plane containing the fibre cable. The component S_h of an S-wave will not cause any strain in the fibre as the particle displacement of this component is along the horizontal plane. The strain response of a S_v can be described as

$$\varepsilon_{zz} = ikA_0 \sin\gamma \cos\gamma \, e^{-i(\omega t - k_z z)}. \quad (8)$$

The reader can refer to Bakku (2015) for more details. The strain response as acquired by the DAS systems, however, suffers alterations as a result of the applied pulse length and gauge length from the acquisition system. Both the pulse length and gauge length act as a filter on the amplitudes. Moreover, DAS response can be further described in terms of pulse length and gauge length (Bona et al., 2017; Correa et al. 2017a). For this, its response can be approximated to

$$\frac{d}{dt}\int_{-L/2}^{+L/2}\left(u\left(z-\frac{G}{2}+l,t\right)-u\left(z+\frac{G}{2}+l,t\right)\right)w(l)dl,$$

where G is the gauge length, L is the pulse length, and $w(l)$ is the laser pulse shape function. By substituting u with $\vec{A}e^{-i(\omega t-\vec{k}\vec{x})}$ and calculating the integral, DAS response can be described in terms of gauge length and pulse length as

$$A_z e^{-i(\omega t-k_z z)}\frac{\omega}{k_z}\left(e^{\frac{ik_z L}{2}}-e^{\frac{-ik_z L}{2}}\right)\left(e^{\frac{ik_z G}{2}}-e^{\frac{-ik_z G}{2}}\right).$$

This derivation is similar to with that described by Bakku (2015) and Dean et al. (2016).

In summary, DAS response is similar to hydrophones response as it does not distinguish direction of the recorded event, showing an upgoing and downgoing event with the same polarity. Furthermore, DAS is similar to the geophone sensors as it is

unidirectional and dependent on the angular response. Chapter 4 will provide a field comparison between the three types of receivers and discuss their main characteristics.

In the next chapter, I present a range of carbon sequestration projects that use seismic monitoring as the main method to detect changes in the reservoir. Some of these projects have chosen DAS technology as their main or secondary seismic sensor.

CHAPTER 3 CARBON CAPTURE AND STORAGE

3.1 Seismic monitoring in CCS projects

Carbon capture and storage (CCS) consists of capturing carbon dioxide and storing it into an underground geological reservoir. CCS is one of the many technologies available to mitigate rising atmospheric temperatures, presenting a short- to mid-term solution to lower carbon dioxide emissions into the atmosphere. It is seen as one of the most important technologies in the mitigation of CO_2 emissions as it can capture large volumes of carbon dioxide directly from power plants and industries, and store it underground for millions of years (IPCC, 2005).

CCS projects have been successfully applied in a wide variety of industries, ranging from oil refining, to steel and iron production, to fertiliser production (GCCSI, 2017). CCS projects can be associated with enhanced oil recovery (EOR) activities, or they can be exclusively for the storage of carbon dioxide. In the last case, the gas is usually injected in deep saline aquifers or in depleted gas reservoirs. There are presently 23 large-scale CCS projects all over the world in operation or under construction, and several smaller-scale CCS facilities (Figure 3.1). They capture together more than 40 million tonnes of carbon dioxide per annum, which equates to removing more than 8 million vehicles off the roads (GCCSI, 2018).

Time-lapse seismic monitoring is a crucial procedure in the life of a CCS project as it assures the safe storage of the injected gas in subsurface (eg. Freifeld et al., 2009). The purpose of seismic monitoring is mainly to provide assurance and compliance during the course of the program. It assures the injected gas is safely stored in the subsurface, while identifying possible areas of leakage. Furthermore, it images and tracks the movement of the gas inside the reservoir and ensures it assumes the predicted behaviour. To conduct seismic monitoring, several seismic surveys are routinely acquired to image the surrounding geology and to track the gas plume. Conventional 4D surface seismic or time-lapse VSP surveys are the common choice of seismic monitoring techniques as they provide good coverage and detailed stratigraphic information. However, such surveys are costly, especially in the context of CCS, where resources are usually more limited compared to the hydrocarbon

production projects. For this reason, there is a special need in CCS to develop cost-effective seismic monitoring techniques that can image the development of the injected gas plume with precision, while reducing operational costs.

Figure 3.1 Current commercial large-scale CCS facilities in operation or under construction (light blue circle), large-scale facilities completed (grey circle), small-scale facilities in operation (green circle), small-scale facilities completed (yellow circle), test centre (dark blue circle) (image extracted from GCCSI, 2018).

3.1.1 Large-scale CCS projects

CCS operations are classified as large-scale when injecting over 800 kt per annum of captured carbon dioxide from coal-based power plants, or when injecting over 400 kt per annum from other intensive industry activities, such as gas power plants, fertilisers, and chemicals industry (GCCSI, n. d.). Many large-scale CCS projects rely on time-lapse seismic for assurance and compliance monitoring of the injected gas.

The first CCS project in the world to inject and store carbon dioxide was the Sleipner CO_2 storage facility. The Sleipner project is located offshore Norway and it has injected over 17 million tonnes of CO_2 since its inception in 1996. The project uses mainly time-lapse seismic and gravimetric surveying to monitor the development of the CO_2, injected into a saline reservoir (Arts et al., 2004). In total, ten 3D seismic and four gravity surveys have been acquired (Fürre et al., 2017). Through the time-

lapse seismic surveys, the project has demonstrated the safe containment of CO_2 in the subsurface.

The Cranfield project is located in Mississippi, USA. It has stored over 5 million metric tons of CO_2 associated with EOR. The Cranfield project also uses seismic to monitor the injected plume. For this, a series of 4D seismic and time-lapse VSP surveys are acquired (Hovorka et al., 2013). Operations ceased in 2015, though, monitoring is still underway with no signs of leakage.

The Gorgon Carbon Dioxide project is aimed to be the World's largest sequestration project, and it is planned to inject a total of 120 million tonnes of CO_2 over its lifetime. The Gorgon project is located in northern Australia, and it is exclusively dedicated to the storage of carbon dioxide captured from a natural gas processing plant and stored in deep sandstone reservoirs. The project is still in development; 4D seismic is part of the reservoir monitoring plan of the project (Flett, et al. 2009).

The Petrobras Santos Basin Pre-Salt Oil Field CCS injects carbon dioxide for enhanced oil recovery. It is located offshore Brazil in ultra-deep waters, in the oil producing field of Lula. The commercial scale project started in 2013, injecting almost 1 million tonnes of CO_2 per year. The reservoir monitoring also includes 4D seismic. The CCS projects developed in Brazil are mostly applied to oil and gas production as more than 80% of the country's energy matrix is generated from hydropower, as opposed to coal, oil or gas power plants which have a high carbon footprint (Beck et al., 2011).

GoldenEye CCS project injects CO_2 captured from a gas-based power station, located in the UK. At least 10 million tonnes of CO_2 will be injected into a depleted gas reservoir over ten years. An interesting aspect of this project is that time-lapse VSP is a major component of the monitoring program, which also includes the acquisition of a multi-well DAS VSP (Dean and Tucker, 2017).

The Quest CCS project, located in Canada, is another large-scale facility dedicated for the storage of approximately 1 million tonnes of CO_2 per year. The seismic monitoring in the Quest project is based on 4D surface seismic and time-lapse VSP monitoring (Bourne et al., 2014). After a successful field trial acquiring a walk-

away line with DAS and geophone (Mateeva et al., 2014), DAS VSP was added to the monitoring program.

Illinois Industrial Carbon Capture and Storage program demonstrates the injection of 1 million tonnes of CO_2 per year into a sandstone formation (Gollakota and McDonald, 2014). The CO_2 is captured from an ethanol biofuel plant. The unique seismic monitoring strategy in the project includes the use of permanently installed DAS in wells and along surface lines, as well as permanently installed orbital vibrator sources (McDonald, 2018).

The South West Hub is a commercial scale CCS project still in the development phase located in Western Australia. The CO_2 will be captured from industrial facilities and power plants in the local region. The project is designed to have the capability to store 2.5 Mtpa during the base case. DAS can be used for the seismic monitoring program with the acquisition of VSP surveys, cross-well and passive seismic (Stalker and Whittaker 2017).

To summarize, large-scale CCS projects are mostly associated with oil and gas production or power plants. Large-scale projects tend to use conventional time-lapse techniques to image the reservoir. However, in more recent projects, such as the South West Hub and Illinois Industrial CCS, less conventional reservoir monitoring technologies (e.g. DAS, passive seismic, permanent vibrator sources) have started to be incorporated into the monitoring program as a way of developing cost-effective monitoring approaches.

3.1.2 Small-scale CCS projects

Small-scale CCS projects provide valuable information on the design and development of technologies that are later on implemented in large-scale projects. The objectives of these smaller-scale projects often involve testing and assessing the feasibility of a particular technology for CCS, and to gain operational experience. There are several small-scale CCS projects around the World currently in operation.

The Frio Brine Pilot was the first CCS project in the United States to demonstrate the storage of carbon dioxide into a dedicated geological formation, in this case, a saline aquifer. Before the Frio project, the CO_2 was injected into depleted

hydrocarbon reservoirs. To date, the Frio project has been completed successfully. The project used time-lapse VSP seismic monitoring as one of the techniques to image small amounts of CO_2 (Daley et al., 2008).

Ketzin Pilot Project is a CCS demonstration located in Germany. It was the first CCS project in Europe. It is one of the largest storage pilots in the world, injecting over 67 kt of CO_2. The Ketzin monitoring program involves time-lapse surface seismic and VSP. An important aspect of the monitoring is the use of permanently installed fibre-optic cable in the wells for DAS and DTS acquisitions (Martens et al., 2013; Gotz et al., 2018).

Citronelle CCS is an integrated project to capture and store CO_2, retrofitted to a coal-fired power plant. The project was concluded in 2015, having over 114 kt of CO_2 successfully injected and stored. The three year monitoring program involves the acquisition of on tubing DAS VSP (Daley et al., 2016).

Aquistore Carbon Capture project demonstrates the storage of CO_2 into a deep saline formation. This project uses 4D VSP to characterize the injection and storage. DAS is also a big part of the monitoring program, as only the DAS system is utilised for the acquisition of 4D VSP surveys. The 4D VSP with DAS is acquired using a fibre-optic cable cemented in the monitoring well. (Harris et al., 2017). However, issues related to the deployment of the fibre in the deeper portion of the well and the distance of the nearest offset resulted in a blind spot at the location of the plume.

The CO2CRC Otway pilot project is one of the largest CO_2 storage laboratories in the world. The project is recently concluding Stage 2, where 15 kt of CO_2/CH_4 gas mixture were injected into a saline reservoir and seismically monitored during three years (Pevzner et al., 2017). Previously, during Stage 1 of the project, over 60 kt of gas mixture were injected into a depleted gas reservoir, seismic monitoring was primarily utilised to conduct assurance monitoring (Gurevich et al., 2014). The project now is preparing to start Stage 3, which will focus on multi-well monitoring of an additional injection using DAS (Jenkins et al., 2017).

National Geosequestration Laboratory (NGL) is a test facility dedicated to research focused on the storage of CO_2. The NGL facility is located in Perth, Australia, and it is a partnership between various institutions, focused on research applied to the

South West Hub project (GCCSI, 2017). The facility enables studies on well monitoring and verification, and geophysical characterisation. It also provides a testing facility for DAS acquisition trials.

3.2 CO2CRC Otway Project

In this thesis, I analyse the data acquired from two different sites aimed for CCS research. The main study area for this thesis is the CO2CRC Otway project. Additionally, a second site, the NGL research facility, is also utilized for the acquisition of small-scale field tests of the DAS method.

CO2CRC Otway Project is Australia's first demonstration of the deep geological storage of carbon dioxide. The project provides technical information on the injection, storage and monitoring of carbon that will influence national policy and industry while providing assurance to the community. The project's site is located in the southeast of Australia, in the state of Victoria, approximately 240 km southwest from Melbourne and 10 km from the south coast (Figure 3.2). Since its inception in 2006, the Otway Project site became a research facility for carbon dioxide geosequestration research. The CO_2/CH_4 gas mixture is naturally occurring and produced by a nearby gas well (Butress-1), and transported through horizontal gas pipes for approximately 2 km, until reaching the injection well, where the gas is injected into dedicated geological formations.

The Otway Project site is located in the Otway Basin, on Australia's southern continental margin. The Otway basin was deposited as a result of the rifting between Australia and Antarctica, initiated during the Late Jurassic. The deposits during the Early Cretaceous rifting are characterised by fluvial and lacustrine sediments. Following the further development of the north-south rift during the Late Cretaceous, large deltas prograded southwards from the margin, resulting on depositions characterised by deltaic sediments.

A second rifting phase in the Late Cretaceous is initiated with the change in extension from north-south to northeast-southwest. This resulted in a distinct structural arrangement in the basin. In some areas of the basin, such as in the Shipwreck Trough, the occurrence of strike-slip motion developed structures with both extensional and compressional components. The Late Cretaceous deposits are

represented by the Sherbrook Group, which includes the Waarre Formation, the main exploration focus in the area, and Paaratte Formation (Partridge, 2001).

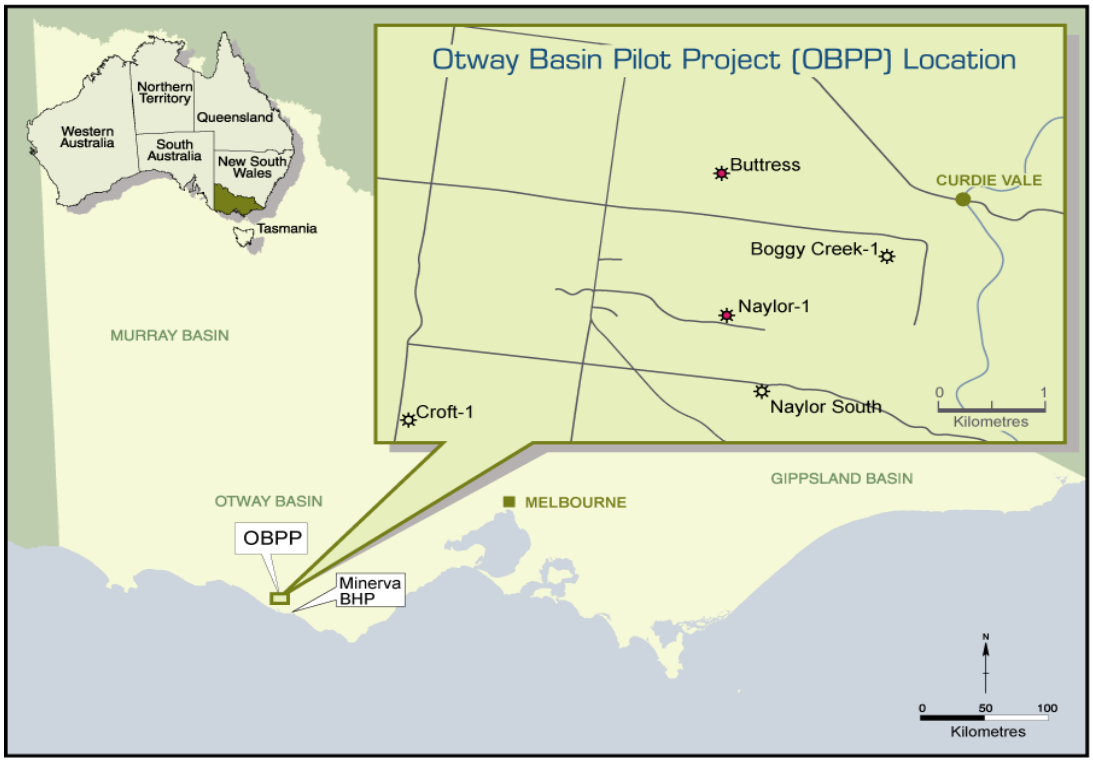

Figure 3.2 CO2CRC Otway Project location (CO2CRC, n.d.).

At the Otway Project, seismic monitoring is carried out to track the evolution of the injected CO_2 plume, aiming to provide assurance that the gas is safely stored in the subsurface and to validate our understanding of the behaviour of the CO_2. The planned seismic monitoring program consists of a series of 3D surface seismic, 3D VSP, and offset VSP to image the movement of the gas plume (Gurevich et al., 2014).

Other monitoring techniques are also used to detect possible leakage, such as direct sampling in the monitoring well, monitoring of ground water chemistry, and monitoring the composition of soil gas (Jenkins, 2014). To this date, the Otway project has concluded Stage 1, and it is currently finalising Stage 2C and initiating Stage 3.

Stage 1 of the project, completed in 2010, utilised conventional surface 4D seismic in conjunction with 4D VSP acquired with geophones in order to conduct primarily assurance monitoring of 65,000 t of supercritical CO_2/CH_4 gas mixture (80% CO_2, 20% CH_4) injection into a depleted Naylor gas field at 2 km depth in Waarre formation (Jenkins et al., 2012; Gurevich et al., 2014). The CO_2-rich gas is naturally

occurring and extracted from a gas well (Buttress-1) (Figure 3.3). The seismic monitoring program for Stage 1 included the acquisition of 3D surface seismic and 3D VSP surveys. The baseline survey was acquired in December 2007 through January 2008, and two monitoring surveys were acquired in 2009 and 2010 (Gurevich et al., 2014). During this stage, the gas produced in Buttress well was injected into CRC-1 well. Naylor-1 (the original producer) well was the monitor well for this stage.

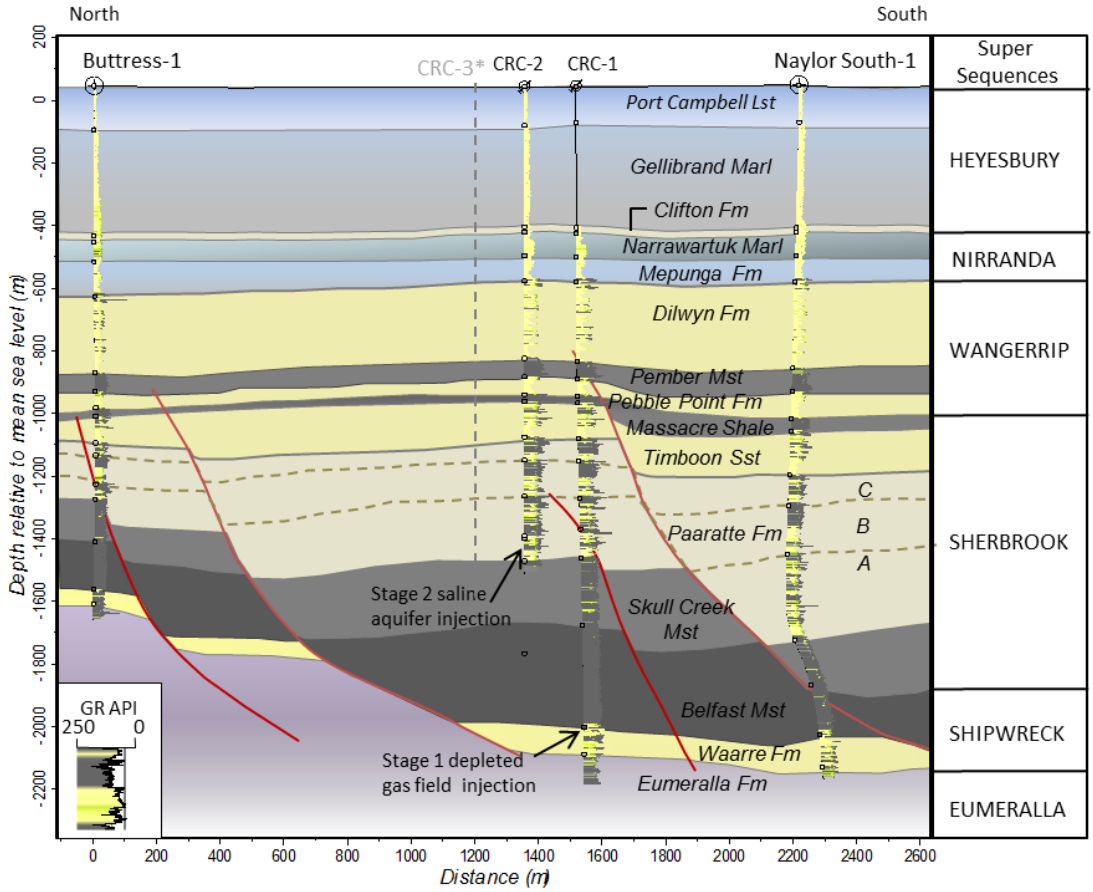

Figure 3.3 North-South cross-section with stratigraphy, wells, and faults (red) (CO2CRC, n.d.).

This thesis is focused on the results of Stage 2C of the Otway project. Stage 2C aims to monitor a 15 kt injection of the same CO_2/CH_4 gas mixture. During this stage, the gas was injected through CRC-2 well and into a saline aquifer, at approximately 1500 m depth (Figure 3.3).

The saline aquifer is located within the Paaratte Formation. Paaratte Formation was deposited as a result of shallow marine, deltaic sediments in the Sherbrook Group, building out into the Shipwreck Trough (Krassey et al., 2004). The formation comprises a combination of carbonaceous rocks (deposited at a later stage of the rifting when more open water conditions were established), interbedded with fine-grained sandstones, siltstone and mudstones.

To monitor the evolution of the injected gas plume during Stage 2C, a 3D seismic monitoring array was installed on-site in March 2015. The permanently installed array was buried underground as a way to decrease levels of noise while increasing time-lapse repeatability (Shulakova et al., 2015). Additionally, the permanent deployment of receivers was expected to decrease costs of acquisition. The buried seismic receivers were deployed along 11 receiver lines, with varying lengths from 2 km to 3 km long each line (Figure 3.4). The installed buried seismic array consists of 909 conventional 5 Hz geophones (Sercel SG-5) buried at 4 m depth at 15 m intervals, ~40 km of fibre-optic cables (Figure 3.5c), and two permanently installed orbital vibrators (Figure 3.5a).

The fibre-optic cable is deployed along the tubing in the injection well (CRC-2) and buried along the 11 surface lines (together with the buried geophone array) at 0.8 m (Pevzner et al., 2017). The fibre cables were deployed in two sections, where each section of cable was deployed continuously, forming ~20 km of cable length in each section. Three types of fibre-optic cables were installed. For the surface lines, a single-mode fibre wrapped in 11 degrees along the cable (in respect to the cable axis) was deployed on all lines in a loop (Figure 3.5b and d). A helically wound fibre wrapped at 30 degrees (Figure 3.5e) along the cable axis was deployed on over half of receiver line 5, along the north side. Also, a single-mode straight fibre cable was deployed attached to the tubing of CRC-2 well, in a loop along the well.

In addition to the permanent receiver array, two permanent surface orbital vibrators (SOV1 and SOV2) are installed on-site (Figure 3.5a) (Freifeld et al., 2016).

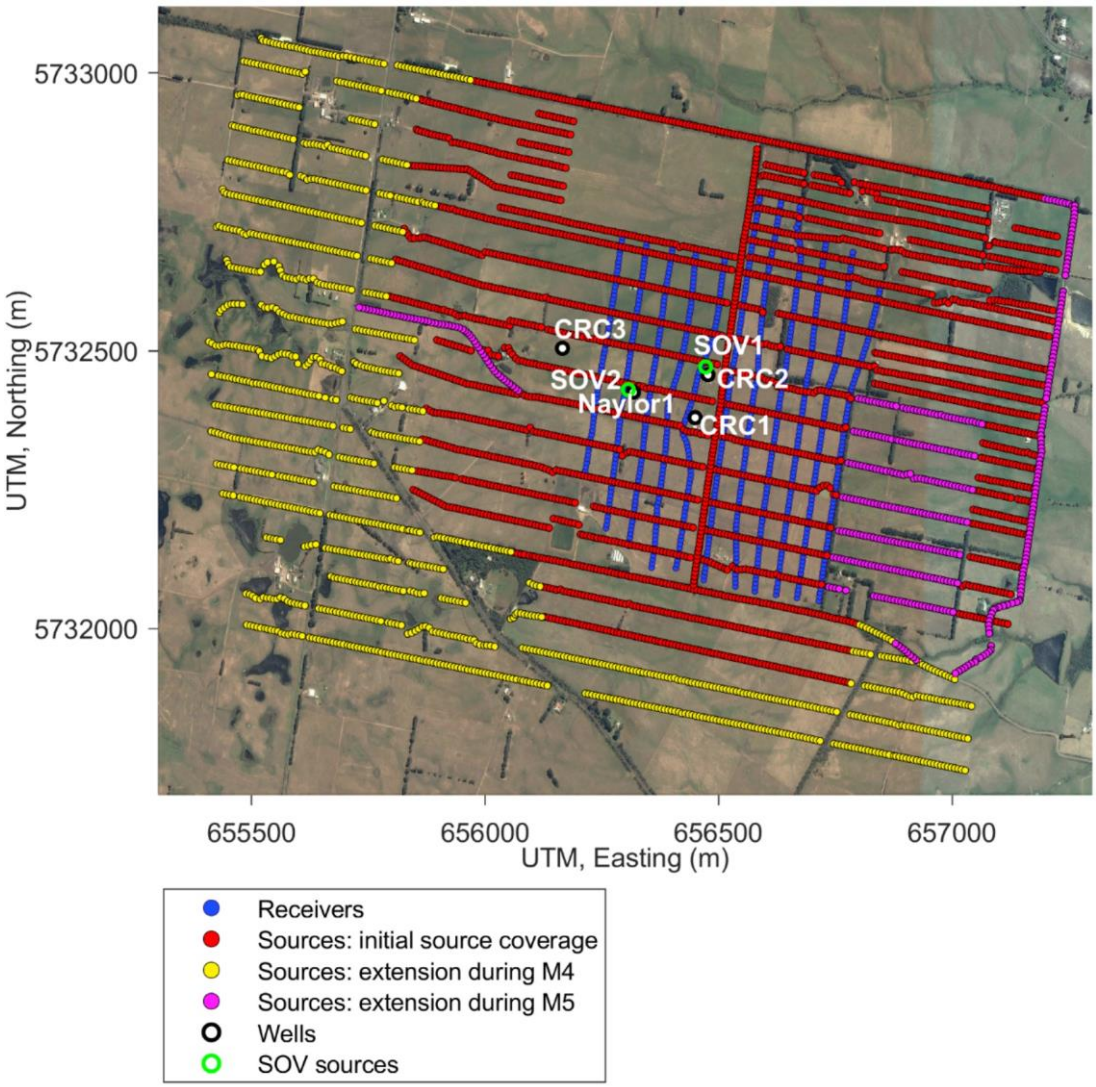

Figure 3.4 CO2CRC Otway Project site acquisition plan and receiver arrays. Wells and permanent sources are also displayed on the figure.

Figure 3.5 Deployed equipment at the Otway site. Surface orbital vibrator source (a); stripped fibre-optic cable deployed on the surface (b); view of the trench along one receiver line while fibre-optic cable deployment (c); view of inside the trench with deployed geophone (orange cable) and fibre-optic cable in a loop (blue cable) (d); helically wound fibre-optic cable (e).

The monitoring strategy for Stage 2C consists of acquiring a combination of 3D surface seismic, 3D VSP, and offset VSP surveys during the baseline survey and after the injection of 5 kt (Monitor 1), 10 kt (Monitor 2), and 15 kt (Monitor 3) of gas mixture, and after 1 year (Monitor 4) and 2 years (Monitor 5) post injection. The 3D surface seismic acquired with the geophones was the main monitoring tool (Pevzner et al., 2017), in conjunction with the 3D VSP acquired with 3-component geophones in the monitor well (CRC-1). Simultaneously with the main surveys, the DAS system was used to acquire 3D surface seismic (Correa et al., 2017c; Yavuz et al, 2016) and 3D VSP using the permanent fibre installation. All surveys were acquired using a 26,000 lb vibroseis source. The source vibration points are displayed in Figure 3.4.

The next stage of the Otway Project, Stage 3, focuses on multi-well monitoring approach to detect the injected plume (Jenkins et al., 2017). For this, a new well (CRC-3 well) was drilled in the beginning of 2017. A fibre cable was installed cemented behind the well casing. A field trial was conducted with the cemented fibre installation, where a series of offset VSP surveys were acquired using DAS and geophones. The field trial shows that DAS VSP acquired with the cemented installation presents similar signal-to-noise ratio to geophone VSP (Correa et al., 2017a). As a consequence of those results, DAS became a strong component in the monitoring for the Stage 3 of the Otway Project.

Table 3.1 lists the field surveys acquired with the permanent fibre-optics array on site that are used in this thesis. During Stage 2C, five surface seismic surveys were acquired with DAS using the surface deployed fibres, as well as five 3D VSP surveys using the tubing deployed fibre in CRC-2 well. The surface and 3D VSP seismic surveys were acquired simultaneously as the fibres are deployed continuously.

As Stage 3 is still in initial phase, we have only performed field trials to this date. The first field trial was performed in May 2017, after the completion of CRC-3 well and installation of the cemented fibre-optic cable. In this field trial, we acquired offset VSPs using the cemented DAS. Additionally, during the Monitor 5 survey, we acquired a 3D VSP with DAS using the cemented single-mode fibre in CRC-3. Moreover, two additional field trials were conducted using SOV sources and the cemented DAS also in CRC-3 well.

In the context of other CCS projects worldwide, the Otway Project is a small-scale project with the objective of testing and demonstrating technologies for CO_2 sequestration. Despite its small storage capacity, the project is committed to applying the latest technologies, such as DAS used for continuous seismic monitoring. Additionally, Stage 3 aims to develop an automated acquisition and data processing flow in order to obtain daily images of the development of the CO_2 plume. This makes the Otway Project unique from other CCS projects world-wide.

Table 3.1 Summary of field surveys at the Otway site analysed in this thesis.

Project stage	**Field survey**	**Acquired datasets**
Stage 2C	Baseline (March 2015)	Surface seismic, 3D VSP (CRC-2)
	Monitor 1 (January 2016)	Surface seismic, 3D VSP (CRC-2)
	Monitor 2 (February 2016)	Surface seismic, 3D VSP (CRC-2)
	Monitor 3 (April 2016)	Surface seismic, 3D VSP (CRC-2)
	Monitor 4 (January 2017)	Surface seismic, 3D VSP (CRC-2)
Stage 3	Field trial (May 2017)	Offset VSP (CRC-3)
	Field trial (March 2018, acquired during Monitor 5 of Stage 2C)	3D VSP (CRC-3)
	Field trial (May 2017)	Offset VSP (SOV sources; CRC-3)
	Field trial (November 2017)	Offset VSP (SOV sources; CRC-3)

3.3 National Geosequestration Laboratory

The NGL is an Australian research collaboration aimed to test varies technologies associated with CCS, focused on storage. The NGL test facility is located at the Curtin University Bentley campus, in Perth, Australia.

The NGL test site contains various seismic tools for testing of seismic monitoring technologies, including three-component geophone shuttles (Figure 3.6a), 24 level hydrophones string (Figure 3.6b), and a 26,000 lb vibroseis source (Figure 3.6e). An interesting aspect of the NGL site is the availability of a DAS system that can be used for field tests. At the site's test well, a fibre-optic cable is cemented behind the well casing, containing a set of single-mode and multi-mode fibres (Figure 3.6c). Additionally, a reel containing standard straight single-mode fibres is also available on site (Figure 3.6f). To acquire the DAS data, we use an iDAS v2 interrogator unit (Silixa Ltd) (Figure 3.6d).

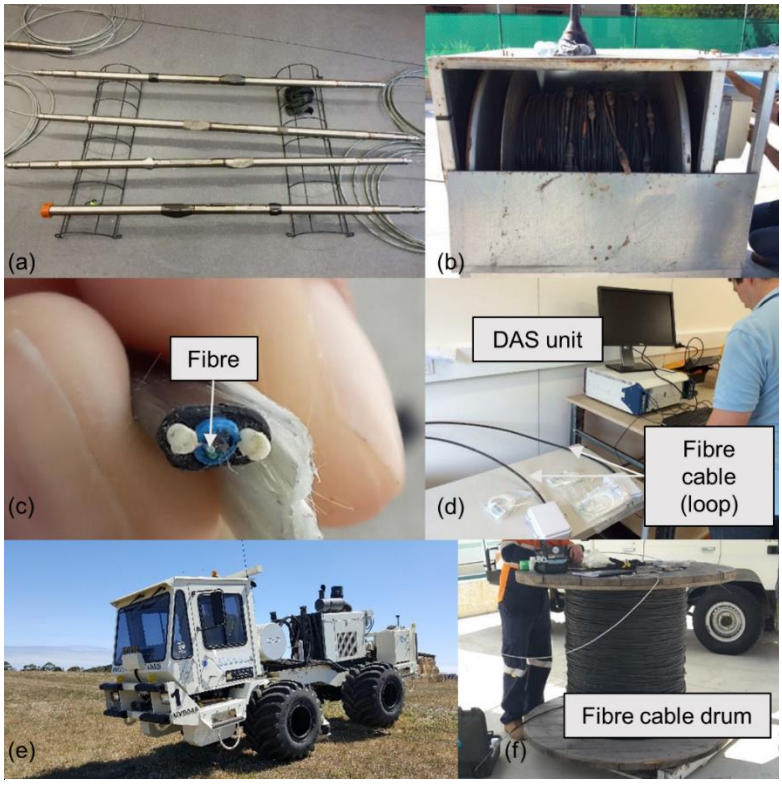

Figure 3.6 Seismic equipment used at the NGL facility. Three-component geophone shuttles (a); 24 level hydrophone string (b); Fibre-optic cable containing single-mode and multi-mode fibre cemented along the well (c); DAS interrogator unit (d); 26,000 lb vibroseis source (e); standard straight single-mode fibre optic cable on reel (f).

CHAPTER 4 QUALITATIVE COMPARISON OF DAS AND CONVENTIONAL SEISMIC RECEIVERS – A CASE STUDY FROM THE NGL TRAINING FACILITY

Here, I provide a qualitative comparison between geophone, hydrophone and the DAS in the context of VSP acquisition. To this end, a series of experiments were conducted at a controlled test facility (NGL) with the aim of understanding the differences in the measurements between all three types of receivers and assess the practical limitations inherent to the geophones, hydrophones and DAS in a borehole seismic acquisition geometry. These experiments were acquired in different occasions and their analyses were published as extended abstracts (Van Zaanen et al., 2017; Bona et al., 2017; Correa et al., 2017b; Correa et al., 2017d; and Correa et al., 2018). The objective of this chapter is to compile the findings from these experiments at the test site in order to explore the main differences, advantages, and limitations of each borehole sensor type. As DAS is still considered a novel technology in relation to geophones and hydrophones, I hope to contribute to a broader knowledge of this method, as well as to assist with choice of borehole receivers and planning of future borehole seismic acquisitions. A more detailed discussion on the physics of each receiver can be found on Chapter 2.

4.1 Acquisition site

The data acquisition was carried out at the National Geosequestration Laboratory (NGL) test well facility. The well is a ~900 m deep vertical borehole with fibreglass casing. Behind the well casing, a fibre-optic cable is installed along the entire extension of the well in a loop, totalling approximately 2 km of fibre length. The installed cable contains a set of single-mode and multi-mode straight fibres.

The stratigraphy along the well consists of 26 m of weathered material at the top, and eight formations, comprising of a combination of siltstone (Kings Park Formation Tk), sandstone (Kings Park Formation Tkc), mudstone with intercalations of siltstone (Leederville Formation Kwlw and Kwlm), and shale (South Perth Shale Kst) (Figure 4.1).

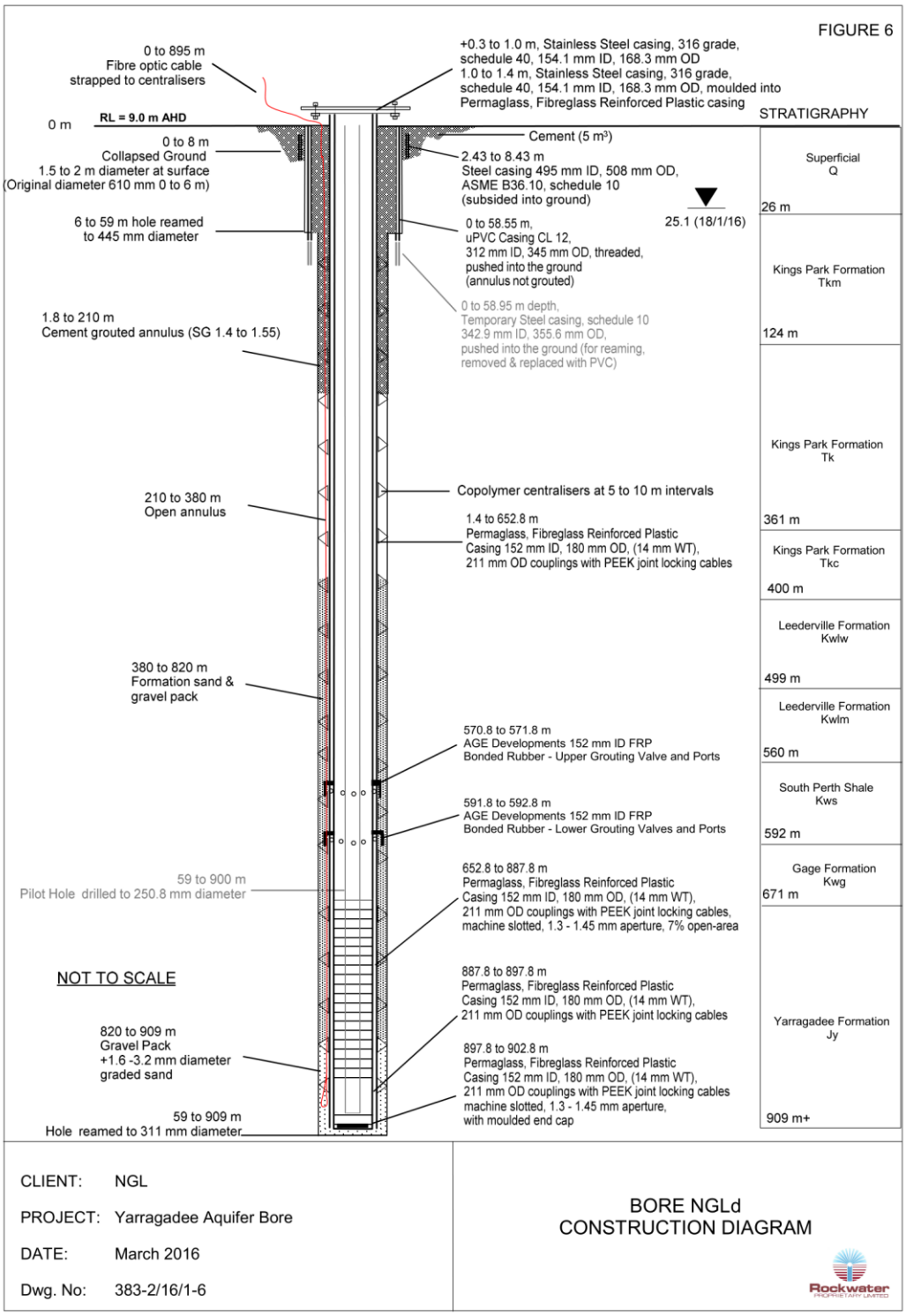

Figure 4.1 Well diagram and stratigraphy (Rockwater, 2016).

4.2 Field experiment

A series of experiments were conducted with the objective of testing the performance of different borehole receivers at a near offset (165 m from wellhead) and a far offset (600 m from wellhead) shot point locations. The experiments were acquired at different occasions. Table 4.1 summarizes the datasets acquired and their acquisition parameters. A 26,000 lb vibroseis truck was used as a seismic source.

At near offset, four datasets were acquired using a 3-component (3-C) geophone tool, a hydrophone string, and DAS. DAS was acquired using two separate cables, the first cable was cemented behind the well casing, and the second cable was deployed suspended in the well and coupled by the well fluid. Both fibres were standard straight single-mode fibres. The geophone data and the DAS cemented data were acquired simultaneously.

Table 4.1 Acquisition parameters for each type of borehole sensor.

	Acquisition parameter	**Geophones**	**Hydrophones**	**DAS, cemented**	**DAS, suspended**
Offset 165 m	Spatial sampling	10 m	2 m	0.25 m	0.25 m
	Maximum depth	640 m	862 m	900 m	645 m
	Source sweep	8 – 150 Hz	8 – 80 Hz	8 – 150 Hz	8 – 150 Hz
Offset 600 m	Spatial sampling	10 m	N/A	0.25 m	0.25 m
	Maximum depth	610 m	N/A	900 m	645 m
	Source sweep	8 – 150 Hz	N/A	8 – 150 Hz	8 – 150 Hz

The geophone VSP survey (Figure 4.2c) at near offset was acquired using a SlimWave (Sercel SA) downhole array. The borehole tool has a 3-C geophone sensor,

equipped with a gamma ray tool (normally used for depth calibration). In total, four geophone shuttles were connected along the wireline with 10 m separation. To acquire the geophone VSP data, the tool was deployed to the maximum depth of 640 m and pulled upwards in steps of 40 m up to a depth of 10 m depth. In total, 16 sweeps were acquired using frequencies from 8 to 150 Hz.

The hydrophone VSP survey was acquired using a twenty-four channel hydrophone string (VCable LLC) also at the near offset point (Figure 4.2a). Each hydrophone tool was spaced at every 2 m. The hydrophone VSP data was acquired until the depth of 862 m. Twenty-two sweeps were needed (more than the geophone survey as the hydrophone acquired almost the entire well), however, using frequencies from 8 to 80 Hz.

A Silixa iDASv2 interrogator unit (IU) was used to acquire all DAS datasets. The DAS VSP survey with the cemented cable (Figure 4.2b) was acquired for the entire extent of the well. The data was acquired with 0.25 m spatial sampling. As DAS records the data simultaneously along the fibre cable, one sweep is needed to acquire the VSP data. Nonetheless, DAS cemented at near offset was acquired simultaneously with the geophone, therefore, while the geophone survey was being acquired, multiple sweeps were recorded with DAS.

To acquire the suspended DAS, an additional fibre cable was deployed in the well. It contains a set of standard single-mode fibres, wrapped around the cable axis in 11 degrees wounding. A weight was attached on one end of the cable to provide downward force (Figure 4.2d). The cable was then lowered inside the well, until reaching neutral buoyancy at the depth of 645 m. The suspended DAS was acquired with 0.25 m spatial sampling, using sweeps from 8 to 150 Hz. 19 repeated single sweeps were acquired (simultaneously with the geophone near offset VSP).

At far offset shot point position, the VSP data was acquired using the 3-C geophone tool, DAS cemented, and DAS suspended. The geophone tool was deployed to maximum depth of 610 m, and acquired also with 10 m interval. The DAS cemented and DAS suspended were acquired using the same acquisition parameters as the near offset data. A total of 19 repeated sweeps were acquired with both DAS datasets.

The DAS IU used 50 ns pulse length with 10 m gauge length. The pulse repetition frequency (PRF) used for the acquisition was 6 kHz. The PRF parameter in the DAS box determines how fast the laser is fired from the IU. The maximum PRF depends on the length of the fibre, as the emitted pulse needs to return to the IU before firing the next pulse. Given a 2 km cable and speed of light in glass of $2x10^8$ m/s, the maximum PRF possible for this acquisition is ~50 kHz (200000 km/s ÷ 4 km). The IU was set to output the DAS response in differential strain (strain rate).

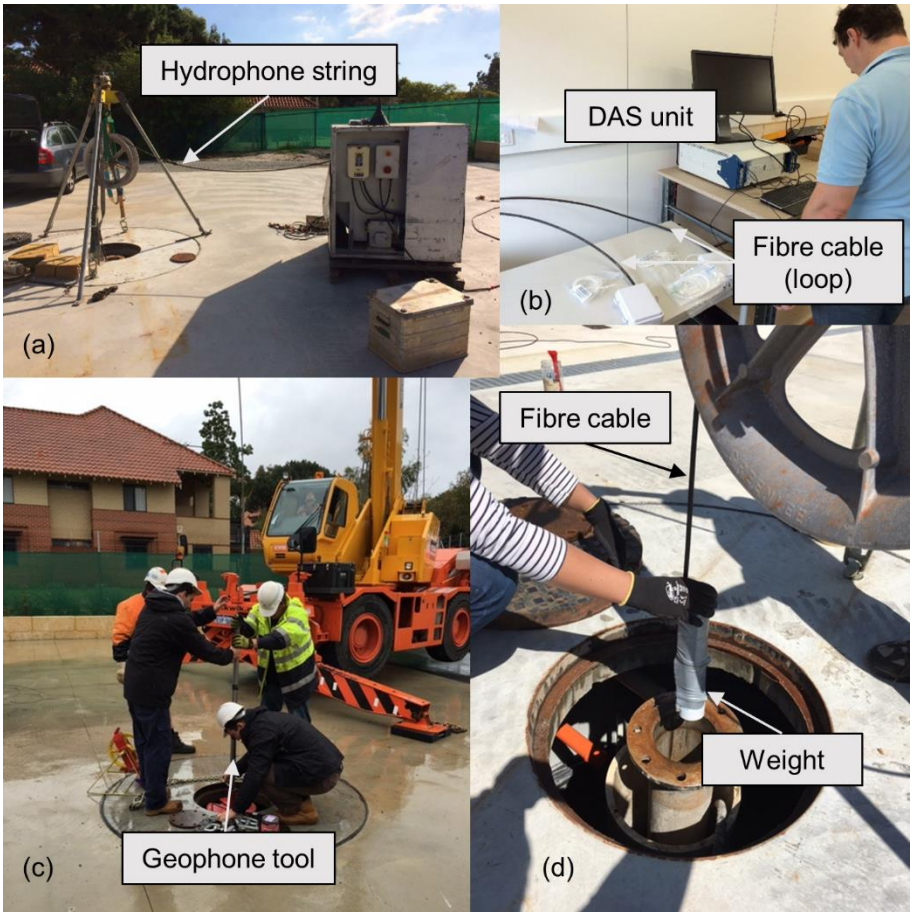

Figure 4.2 Hydrophone acquisition on site (a); DAS interrogator unit connected to the cemented cable (b); deployment of the geophone tool (c); deployment of the loose fibre-optic cable (d).

4.3 Data processing

The intent of this chapter is to compare "raw" data. For this reason, no frequency or amplitude filtering were applied. The datasets were loaded into seismic processing software and the geometry was assigned. Only the vertical component of

the geophone was used for this analysis. After loading the datasets, they were correlated with the sweep-signals to obtain a zero-phase wavelet. The processing applied to the DAS datasets is slightly different from the other receivers. As the acquired DAS response is strain rate, for convenience, the datasets were integrated in time to obtain the strain response. Then each dataset was correlated and the geometry applied.

DAS records all depths simultaneously along the fibre length, while the other receivers need to be moved along the well. This means that DAS can acquire multiple repeated VSP datasets in the same duration of time needed to acquire a single-shot geophone or hydrophone VSP data. For this reason, I decided to stack a range of 19 repeated shots to increase the signal to noise ratio (S/N) of the DAS data, considering that 19 sweeps acquired on DAS took approximately the same amount of time to acquire the geophone and hydrophone data.

4.4 Wavefield comparison

I compare the VSP datasets acquired using the geophones, hydrophones, DAS with the cemented cable, and DAS with the suspended cable, in order to assess their ability to detect the various elastic waves. For this comparison, I used the geophone and hydrophone data acquired with single sweep per level, and DAS data after vertical stacking of 19 repeated sweeps.

At near offset, geophones are able to properly record P-wave reflections, both upgoing and downgoing, with apparent low levels of noise across the record (Figure 4.3a). However, their sparse spatial sampling yielded an aliased wavefield, as seen on the recorded S-waves and reflected P-waves. The hydrophone data acquired at near offset (Figure 4.3d) also contains reflected P-wave energy; however the record contains high level of noise, especially from zero to 50 m, and between depths of 500 to 550 m, which is related to an incident on the cable causing a sudden movement. As the hydrophone tool is suspended in the well fluid, the record contains strong tube wave noise. It also contains strong reverberation along the record, likely caused by wind affecting the cable above the ground. Both DAS VSP datasets present similar wavefield records as the geophone (Figure 4.3b and c). DAS is able to record downgoing waves and upgoing reflections, not only in the cemented fibre but also in

the suspended fibre. The cemented DAS dataset also has clearly recorded downgoing and upgoing P-wave reflections, with a very low level of noise across the record (Figure 4.3b). As DAS is able to acquire data with dense spatial sampling, reflections are visually better pronounced on the cemented DAS record than on the geophone record. DAS was also able to record P-S converted, seen at approximately 125 m depth. DAS using the suspended cable also shows P-wave reflections (Figure 4.3d), however noise levels on the suspended DAS are considerably higher, due to the poor coupling of the cable to the formation. As the cable is suspended in the well fluid, the data also contain tube wave noise, but much less intense than in the hydrophone data.

At far offsets, all datasets present significantly lower levels of signal due to the increased distance (Figure 4.4), which means the noise becomes more visible. The geophone record is able to record upgoing and downgoing waves (Figure 4.4a), however the sparse spatial sampling clearly compromises the quality of the recorded reflected waves. The geophone data also present noisy traces along the record. This was a result of a defect in one of the levels in the geophone tool, which recorded mostly noise. Data acquired with the cemented DAS cable contain high level of random noise (Figure 4.4b). The decrease in sensitivity in the cable with distance results in higher relative amplitudes of the random system noise, which is common for DAS technology. Despite the noise, DAS is able to clearly record upgoing and downgoing reflections. Data acquired with suspended fibre optic cable (Figure 4.4c) also contain clear upgoing and downgoing reflections. Tube wave noise is strongly present in the data, however this does not compromise the detection of reflected waves, which are still evidently visible in the record. The coupling of the suspended cable is done through the fluid in the well, though, the cable is loose and possibly also touching the well casing. Therefore, it is also possible to note partial conversion of energy into shear waves.

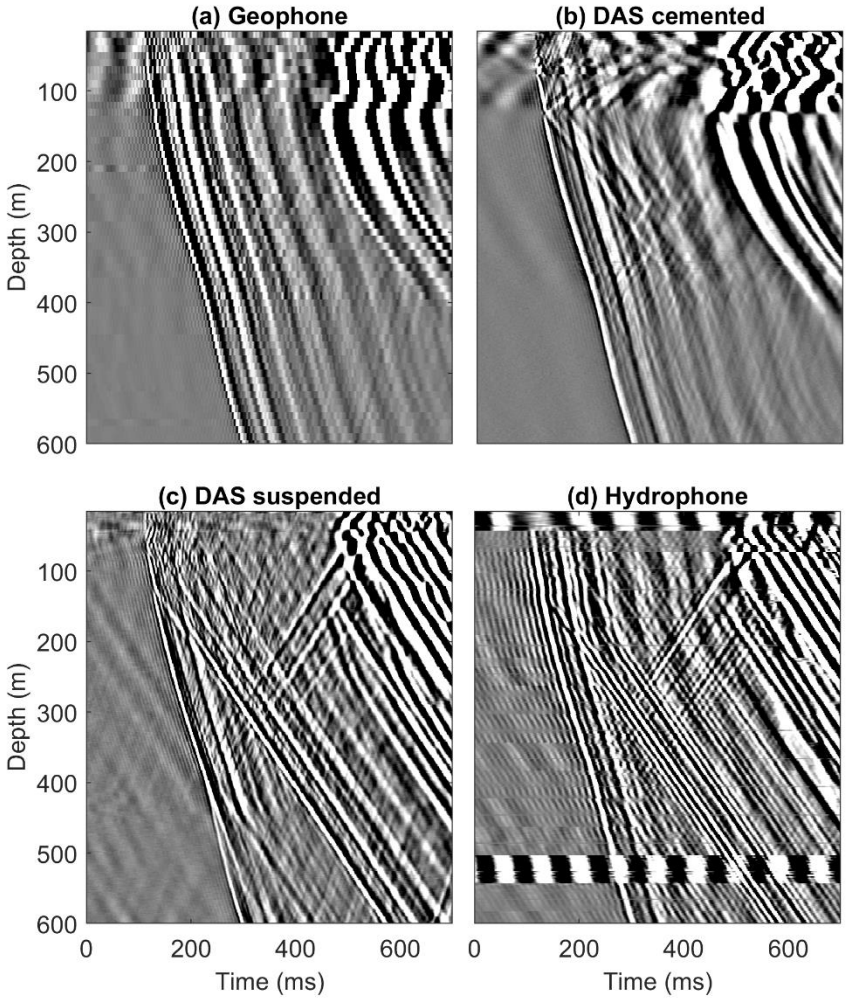

Figure 4.3 VSP acquired at near offset using the vertical component of geophones (a), DAS with cemented cable (b), DAS with suspended cable (c), and hydrophones (d). Amplitudes are normalised.

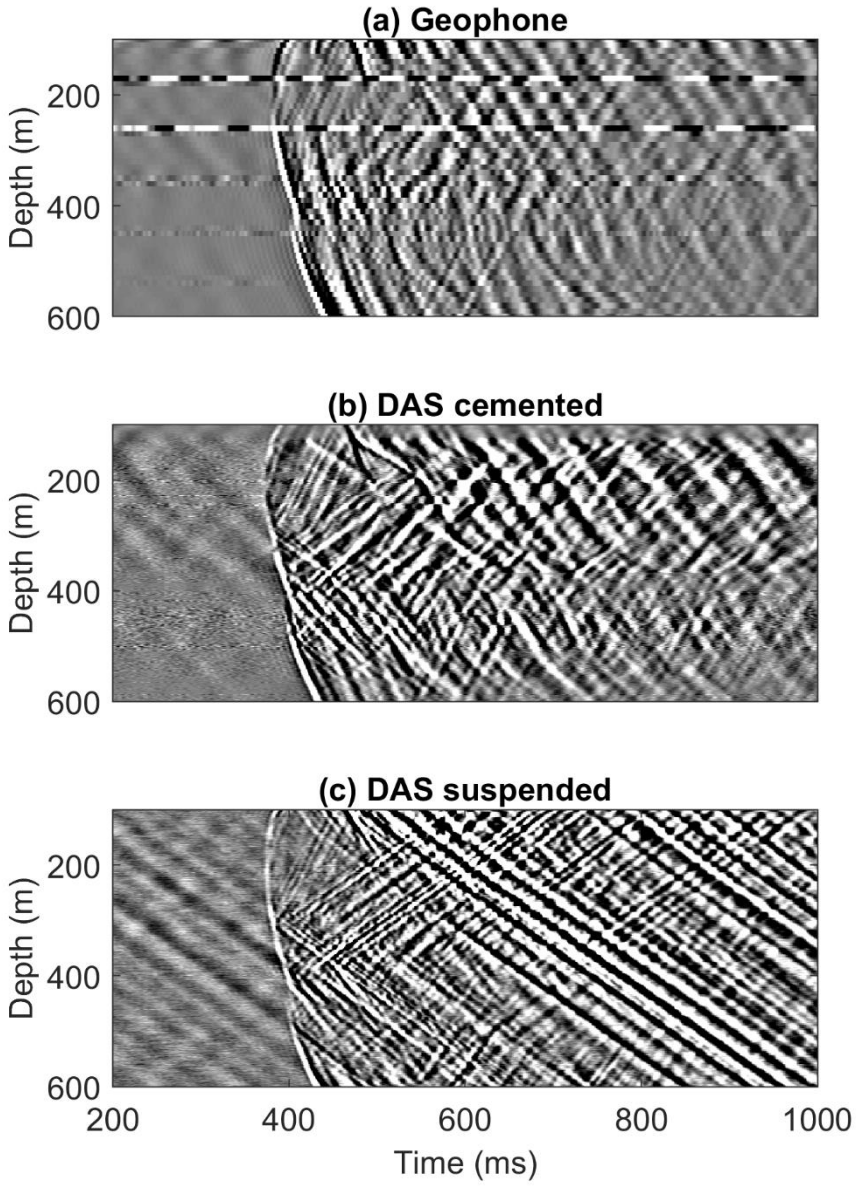

Figure 4.4 VSP acquired at far offset using geophones (a), DAS with cemented cable (b), and DAS with suspended cable (c). Amplitudes are normalised.

4.5 Wavelet comparison

To analyse the polarity and phase characteristics of each receiver, I compare the shape of the wavelet of the data acquired with geophones, hydrophones, and DAS (cemented), using the near offset datasets. To estimate the wavelet, the first breaks were aligned at 100 ms. Next, the traces from 200 m to 400 m depth of each dataset were stacked to attenuate possible random noise and accentuate the signal. As the

hydrophone was acquired using a different source sweep, the wavelets were filtered using a 0-20-70-80 Hz Ormsby band pass filter, so they can be compared within the same frequency band. The amplitudes were normalised by their maximum value.

Figure 4.5 shows the estimated wavelet for the geophone, DAS, and hydrophone data. DAS and hydrophone wavelets present similar shape. Though, the DAS wavelet shows stronger side lobe arriving before, and weaker side lobe arriving after the first break. Several factors can contribute to such differences in the DAS wavelet, including how the acquisition parameters changed for each data set. Such differences could also be attributed to the gauge length in the DAS, which acts as a moving average filter.

As geophones acquire particle velocity and DAS acquires strain, the geophone wavelet should have 90 degrees shift in relation to DAS. The relation between strain and particle velocity is given by a derivative (see Chapter 2). To compare both receivers, the DAS wavelet was shifted by 90 degrees by calculating its Hilbert transform. After the phase shift, the DAS wavelet presents similar shape in comparison to the geophone. Additionally, correlation side-lobes can be seen before the direct arrival in all receivers.

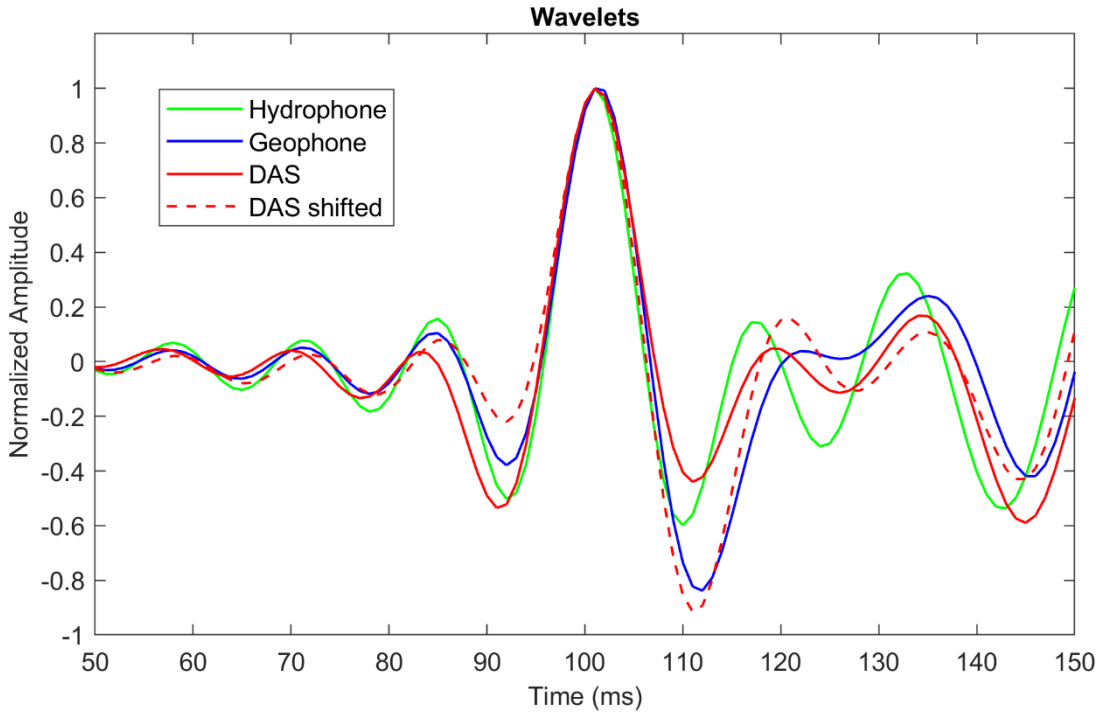

Figure 4.5 Estimated wavelet for hydrophone data (green), geophone data (blue), DAS (red), DAS phase shifted in 90 degrees (hashed red line). Amplitudes are normalised.

4.6 Signal to noise ratio

The S/N was estimated based on the correlation between the two consecutive traces (Hatton et al., 1986), assuming that the noise is mean-zero and uncorrelated:

$$SN_i = \sqrt{\frac{(g_{i,i+1})_{MAX}}{1-(g_{i,i+1})_{MAX}}}, \qquad (9)$$

where i is the trace number, $(g_{i,i+1})_{MAX}$ is the maximum value of the normalised cross-correlation function between i and $i+1$ traces. The S/N was computed over a 60 ms window. Vertical stacking of traces was applied to all datasets to obtain the same geophone spatial sampling (10 m) before S/N calculation. The gauge length on the DAS datasets is 5 m in each side of the trace (10 m in total), which means that it does not intersect with the next DAS trace after vertical stacking.

The geophone data at the near offset presents S/N ratio of approximately 20 to 30 dB close to the first breaks, which decreases to approximately 10 dB with recorded

time (Figure 4.6a). The S/N analysis shows a striped pattern before the first breaks, which suggests that the geophone tool had a noisy shuttle.

DAS is often reputed to have low sensitivity and high noise levels. The cemented fibres usually provide an optimal S/N due to good coupling with the formation. Here, the cemented DAS data recorded at the near offset shows similar, or even superior, S/N than geophone data (Figure 4.6b). This higher S/N is a result of stacking repeated sweeps; S/N of a single DAS shot would be significantly lower. S/N of the cemented DAS data around the first breaks is approximately 30 dB, comparable to the geophone S/N in the same area. The recorded noise, prior to the direct wave, has very poor correlation, which suggests noise is mostly random in nature.

The DAS data from the suspended cable contains a lower level of S/N than cemented DAS, showing approximately 20 dB around the first breaks (Figure 4.6c), and decreases significantly on reflected waves. Tube wave noise response is strong due to its high amplitudes and repeatability across traces. S/N on first breaks in hydrophone data is comparable to S/N in the suspended DAS, however it decreases rapidly along the record due to its high level of correlated noise (Figure 4.6d).

At the far offset, S/N of all data decay significantly as a result of attenuation and spherical divergence of the signal (Figure 4.7). DAS amplitudes are further affected at high angles of incidence, as it decays as cosine squared of the angle of incidence, as opposed to cosine on geophone data (Kuvshinov, 2016).

S/N of geophone is approximately 15 to 20 dB close to the first breaks. However, due to the presence of noisy traces, the S/N decays in these areas to below 0 dB (more noise than signal) as the geophones recorded no signal. The S/N of cemented DAS data at the far offset is lower than S/N of geophone data along the first breaks, most likely due to the high angles of incidence, though, S/N of reflected waves on cemented DAS data is comparable to that in the geophones data. Suspended DAS has the lowest S/N amongst the datasets due to the combination of weak coupling and directionality.

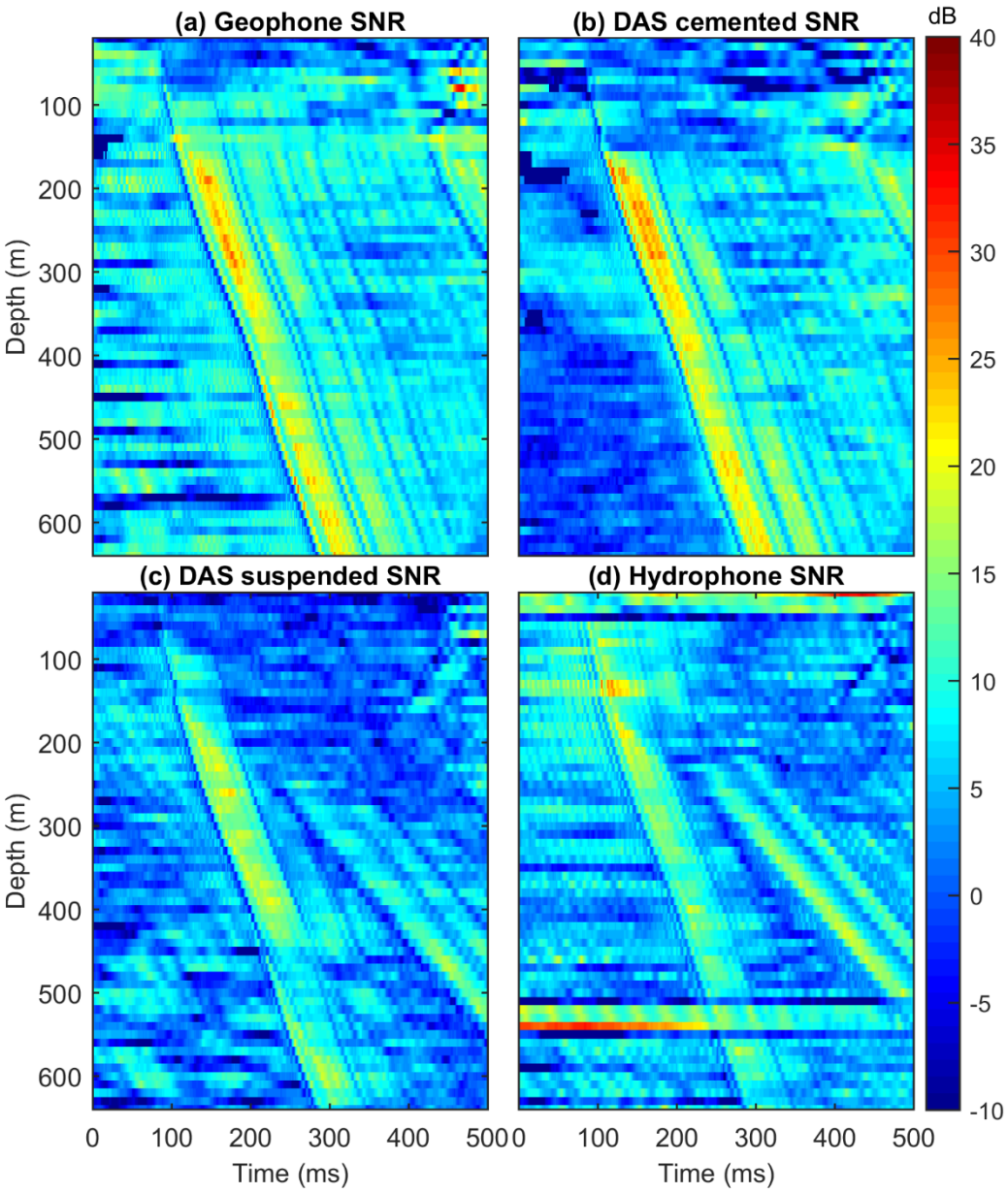

Figure 4.6 Signal-to-noise ratios for geophones VSP record (a), DAS VSP record with cemented cable (b), DAS VSP record with suspended cable (c), and hydrophones VSP record (d) at the near offset.

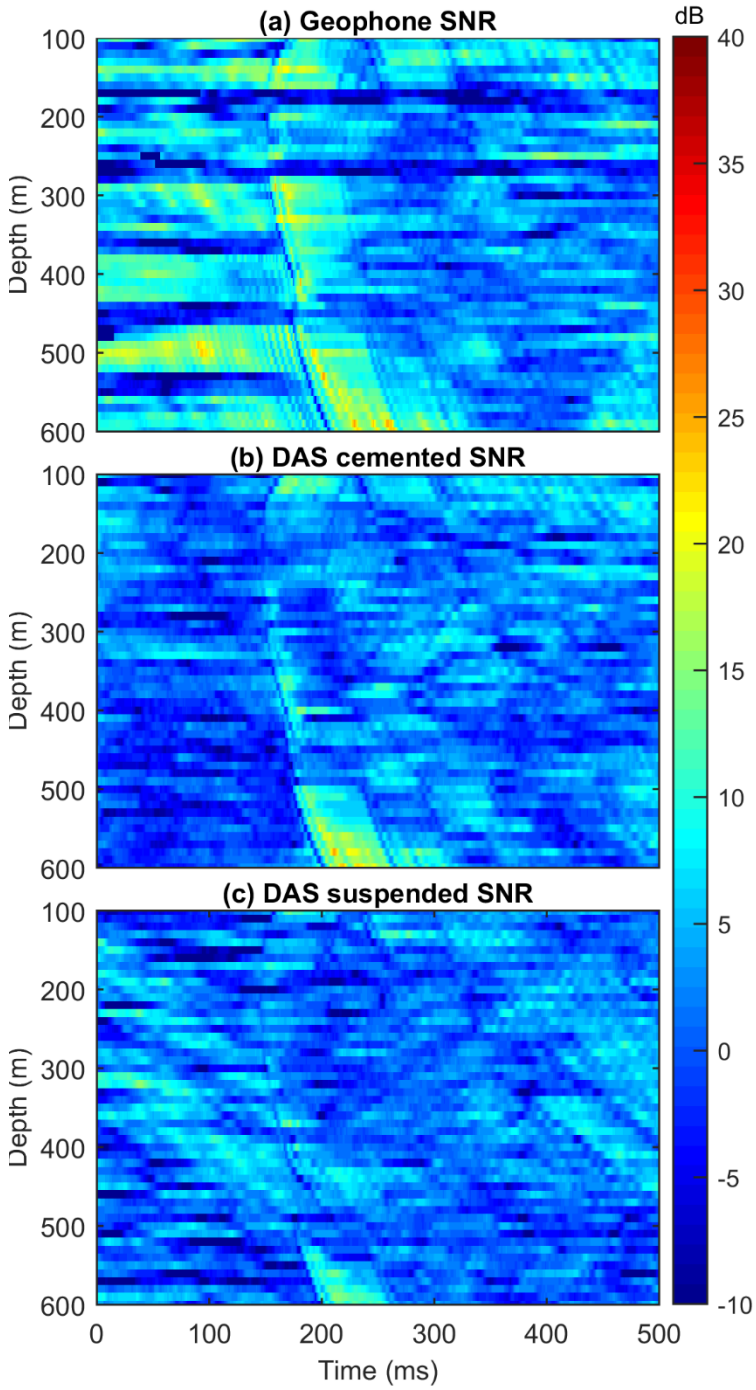

Figure 4.7 Signal-to-noise ratios for geophones (a), cemented DAS (b), and suspended DAS (c) at the far offset.

4.7 Frequency spectra

DAS amplitude responses are intrinsically controlled by effects of the gauge length and pulse length (Dean et al. 2016a). The gauge length acts as an averaging filter on the data, reducing its sensitivity to high frequencies. In some IU systems, the gauge length can be modified, which changes the averaging factor and increases (or decreases) the frequency limit of the acquired data (the smaller the gauge length, the higher the frequency).

The power spectrum of each record shows that geophones give the most broad band dataset at the near offset (Figure 4.8). Geophones show a slight decay in higher frequencies, as a result of attenuation and spherical divergence. At the same offset, cemented DAS shows weaker sensitivity at high frequencies, compared to the geophone data. This decay is likely due to effects of the gauge length on the seismic signal. Suspended DAS, due to low coupling, has the fastest decrease of the amplitudes at higher frequencies. Hydrophone data only contain signal up to 80 Hz due to the parameters of the source sweep. At the far offset, geophones have a greater loss of high frequencies compared to the near offset. The power spectrum of cemented DAS is similar to the spectrum of the geophones. The hydrophone data was not acquired at the far offset.

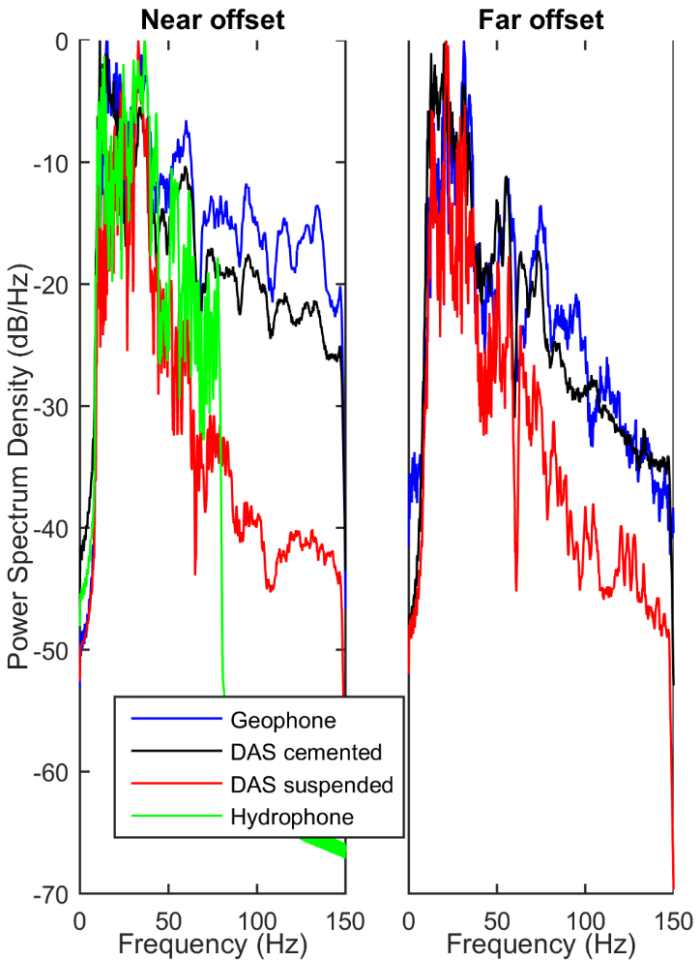

Figure 4.8 Frequency spectrum of VSP records at near and far offsets.

4.8 Depth accuracy

Depth uncertainty is a common issue that affects both DAS and hydrophones. Geophone sensors are usually equipped with a gamma ray tool, which is used as a depth reference (in conjunction with the wireline gamma-ray log). Hydrophones and DAS, however, rely on the measured cable length to assign the depth. This leads to fluctuations in the positioning of the traces since the cable can suffer stretch or slack in the well. Furthermore, for DAS systems, the positioning of the traces calculated by the optical systems depends on the refractive index of the fibre. Thus, small variations in the environment, such as temperature, could slightly change the speed of light in the glass, causing small positioning errors. These depth accuracy issues can be seen as an obstacle to the broader adoption of the DAS technology (Verliac et al., 2015).

To minimize uncertainties in the depth calibration for DAS data, tap tests are usually performed in the attempt of pinning a known position of the cable to a known

depth. Since the geophones provide a good depth accuracy as it uses a gamma tool for calibration, the geophone data was used to adjust the depth of the other data sets. Recent studies suggest that calibrating the depth with two known points provides a sufficiently accurate depth match (Ellmauthaler et al., 2016).

I compare the depth accuracy on each borehole sensor, considering the geophones as the sensors with the best accuracy (Figure 4.9). To this end, I pick the first break times and calculate the difference between hydrophone and geophone, cemented DAS and geophone, and suspended DAS and geophone. Figure 4.9 illustrates the variations in the first break times for each dataset. DAS acquired with cemented cable was able to deliver the most accurate depth control, as the first break variations were less than 1 ms (Figure 4.9c). For the other datasets, first break differences were increasing with depth, reaching up to 4 ms mismatch. This suggests that, for the hydrophone string, the cable could be stretching with depth as more cable is deployed. For the suspended DAS, as it was deployed until neutral buoyancy, the cable could have too much slack and slightly looping at the bottom.

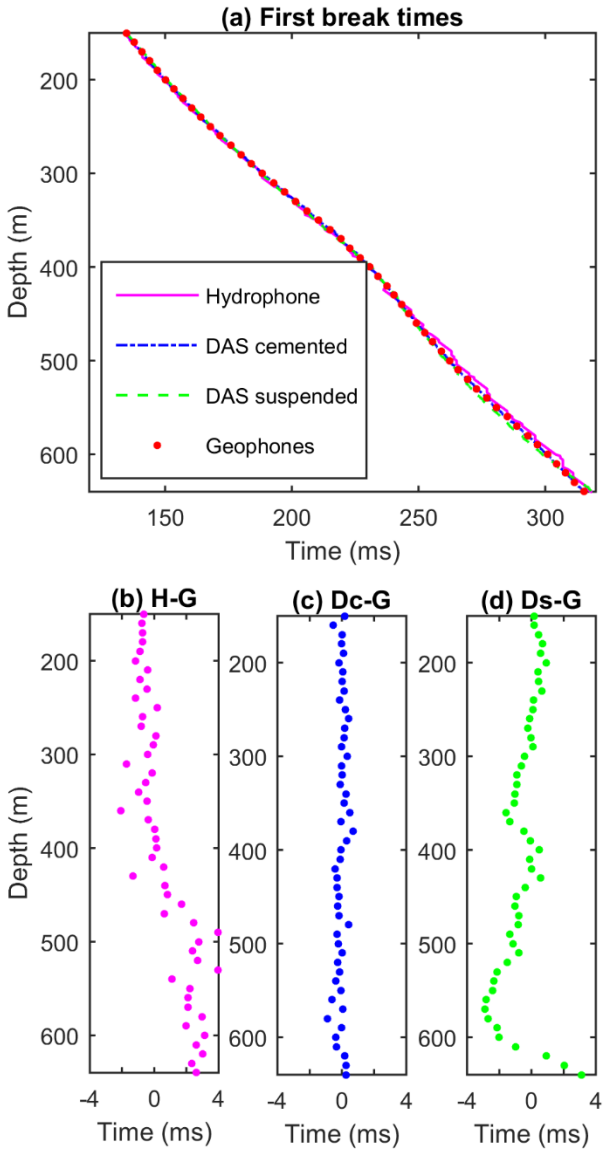

Figure 4.9 Picked first break time of Hydrophone data, DAS cemented, DAS suspended and Geophones (a). Difference between hydrophone first breaks and geophone first breaks (b); difference between DAS cemented first breaks and geophone first breaks (c); and difference between DAS suspended first breaks and geophone first breaks (d).

4.9 Interval velocities

VSP datasets are routinely used to compute the interval velocities from the first break times, since VSP data contains information of both time and depth. I assess the quality of the interval velocities calculated from the DAS data by comparing it with the interval velocities from the geophone data. Only DAS cemented and geophone

datasets acquired at near offset were used for this comparison as they present similar S/N and low levels of noise.

To compute the interval velocities, I use the first break picks and measured depth of each dataset. As the datasets were acquired 165 m from the well, the first break times were projected to zero offset. To calculate the interval velocity from the geophone data, the measured depth between pairs of receivers were divided by their zero offset projection of the first break times. Due to the dense spatial sampling of the DAS data, the calculation of the interval velocities using the same method as the geophones results in unstable interval velocities. In order to reduce this variation, the interval velocities were taken by first calculating the zero-offset projection of the first breaks; then the derivative of the function between the first breaks and the measured depth was taken over a window of 18 m. The calculation over the range of 18 m was chosen as it presented the best velocity estimation.

The interval velocities calculated from the geophone and DAS data agree well (Figure 4.10b). The changes in velocity for both datasets correspond to the stratigraphic description of the well (Figure 4.10b). The interval velocities from the DAS data present finer resolution when compared to the geophone due to its dense spatial sampling.

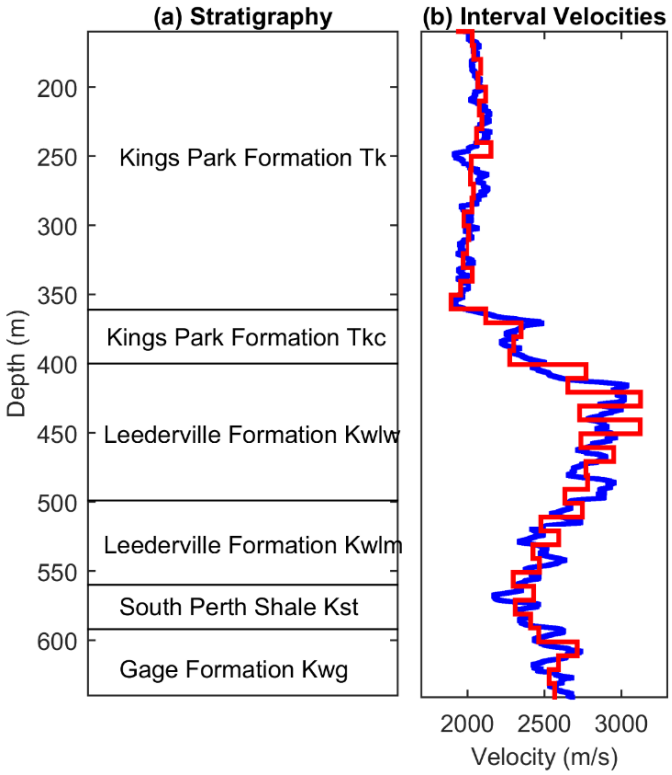

Figure 4.10 Stratigraphy along the well (a). Interval velocities calculated using the geophone data (red) and DAS data (blue).

4.10 Signal to noise ratio as a function of stacked sweeps

DAS data can contain high level of noise originated from the optical system. A single shot acquired with DAS data may give low S/N when compared to conventional receivers, such as geophones. Li et al. (2015) suggest that S/N can be increased by reducing the noise floor of the interrogator unit, using a strong acoustic source, or by simply stacking a combination of repeated sweeps so there is constructively interference of the signal, and destructive interference of the incoherent noise.

In order to understand the noise characteristics of the DAS system, I calculate the S/N of DAS data for different numbers of stacks, varying from one to 50. S/N in this case was calculated by dividing the root mean square (RMS) amplitude computed in 20 ms window around the first breaks with 20ms of noise in the beginning of the record.

Figure 4.11 shows the improvement of S/N with stacking of repeated sweeps. The black curve shows the theoretical S/N increase, $20\log_{10}\sqrt{N}$, with N being the number of stacks. The theoretical curve shows that after stacking 50 shots the S/N should increase by 17 dB.

The increase in S/N in the DAS data was extracted at depths 128 m, 386 m, and 643m. DAS S/N, shows an improvement of approximately 15 to 16 dB in S/N. This suggests that the noise characteristics present on DAS data are mostly random.

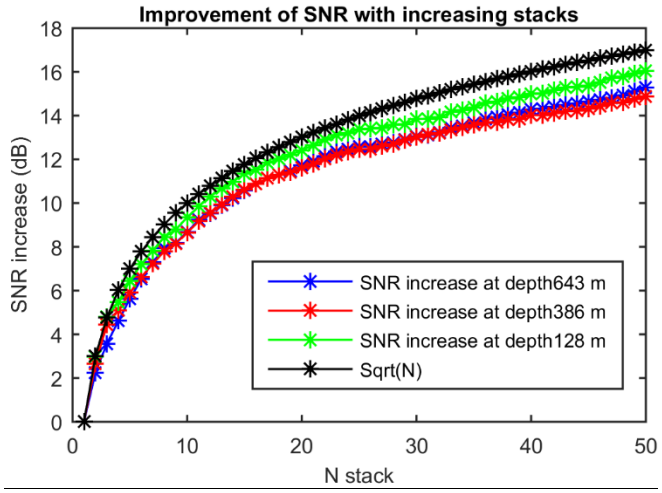

Figure 4.11 Improvement in S/N of DAS data after stacking of repeated shots. Blue, red, and green curves show the improvement at depth 643 m, 386 m, and 128 m, respectively. Black curve shows the theoretical increase in S/N assuming random noise.

4.11 Discussion

The seismic industry is continuously seeking cost-effective alternatives to borehole sensors, as the current conventional options take a long time for surveys and require cumbersome equipment. This study provides a comparison of two commonly accepted borehole sensors (geophone and hydrophones) with the new emerging DAS technology in two different deployment types: with fibres cemented behind a well casing and fibres suspended in the well fluid. Such studies are needed to establish a benchmark of quality for the DAS technology and help its broader acceptance in the seismic industry. Though, comparing principally different measurands is not trivial. For this reason, I mainly make qualitative comparisons, instead of quantitative, by using S/N, for instance.

Different types of borehole sensors have diverse features that are also important to consider when planning a VSP survey. Geophones measure the approximate particle velocity, while hydrophones measure pressure, and DAS measures the approximate strain rate. Table 4.2 summarizes the main characteristics of each measurement, as evidenced in this study. As could be seen in the presented datasets, all the three sensor types, including DAS acquired with suspended cable, were able to detect downgoing and upgoing P-wave reflections.

The main differences in each VSP dataset are their S/N values and sensitivity to high frequencies. Geophones typically have higher S/N per single shot when compared to other borehole sensors. However, DAS data acquired with cemented fibre was able to deliver comparable or even superior S/N with similar source effort than the geophone VSP (geophone VSP acquired with 16 shots; cemented DAS VSP stacked with 19 repeated shots). In VSP acquisition, a significant amount of time is needed to move the geophone tool along the well, which increases the rig time needed for such acquisitions, and thus, increasing the cost. Therefore, even though the DAS and geophone data sets present similar S/N for the same source effort, VSP acquisition with DAS can significantly reduce the total acquisition time - and cost - since DAS data is acquired simultaneously along the entire extension of the well.

The controlling factors that dictate the frequency range largely depend on the design of the sensor. For geophones, the stiffness of the spring, the type of mass and damping are factors that control its frequency range. VSP with hydrophones can acquire frequencies as high as several kHz, which is considerably beyond the usual "seismic frequency range" (approximately from 10 Hz to 120 Hz). The frequency limit depends on the transducer, but it is common for hydrophones to be able to acquire up to hundreds of thousands of hertz. Hydrophones usually show lower S/N, mostly due to the strong presence of tube wave noise, which obscures the signal from reflected waves. Nevertheless, the high frequency range characteristic of hydrophone sensors make them particularly suited for shallow well applications and high-resolution surveys.

DAS sensitivity can vary in relation to the design characteristics of an interrogator unit and parameter settings, such as the gauge length, pulse length, laser power and laser repetition rate. The laser repetition rate is especially a major

controlling factor of the maximum frequency in the data. If the laser is fired at 5000 Hz, the strain on the cable will be sampled at 5000 Hz. Therefore, the faster the laser is fired from the IU, the higher is the sampling frequency. This allows for the recording of high frequencies in the DAS data, comparable to the hydrophone frequency limit. However, the amplitude of the recorded frequencies may vary depending on the fibre sensitivity. DAS also allows for the acquisition of data using a very small spatial sampling, down to 0.25 m depending on the interrogator unit. The spatial sampling is also variable.

Table 4.2 Summary of main characteristics of borehole sensors.

Characteristic	**Geophones**	**Hydrophones**	**DAS**
Physical property	~Particle velocity	Pressure	~Strain
Components	3C	1C	1C
Directivity	Cosine	Omnidirectional	Cosine squared
Coupling	Clamped	Borehole fluid	Cemented, borehole fluid
Upper frequency limit	~300 Hz	~ n*1 kHz	~100 Hz [+]
Typical spatial sampling	~10-20 m	~2-10 m	> 0.25 m
Depth calibration	Reference log (e.g. gamma ray)	Measured cable length	Tap test
Cost	$$$	$$	$

[+] The frequency sensitivity will vary depending on the PRF, gauge length, and pulse length.

Another major controlling factor for the sensitivity of DAS data is the coupling of the cable with the formation. DAS VSP acquired with the cemented cable at the NGL well shows significant attenuation of high frequencies, possibly due to the averaging effect caused by the gauge length. However, such attenuation seems to have a minor effect on the overall quality of the record, given that the cemented cable shows a satisfactory S/N level.

DAS acquired with a suspended cable can be an option if a cemented cable is unavailable. The fibres can be easily deployed and retrieved from the well, and the acquisition time considerably outperforms the geophones and hydrophones. However, DAS with a suspended cable gives lower S/N, and it shows a considerable attenuation of high frequencies in comparison to other sensors.

Additionally, care should be taken when assigning depths to DAS, especially when using a suspended cable. For the cemented fibre, the depth calibration is a significantly more precise than for the other methods, making it possible to provide a more accurate time-depth curve. Moreover, amplitudes on DAS data (on straight fibres) decay as a factor of cosine squared of the angle of incidence. This amplitude dependence should be taken into consideration when designing surveys with DAS, as they should affect angle dependent applications, such as AVO analysis. Lastly, strain response as acquired by DAS presents a shift of 90 degrees in phase from particle velocity as acquired by the geophones.

4.12 Conclusions

In this work, I presented a comparison between VSP records at near (165 m) and far (600 m) offsets, acquired using a 3-C geophone tool, a hydrophone string, DAS acquired with a cemented cable, and DAS acquired with an additional cable suspended loosely in the well fluid.

DAS acquired with cemented cable has similar recorded P-wave reflections and similar S/N to geophone data, at both near and far offsets. Due to the high spatial sampling, DAS performs better than geophones, especially at the far offset as it properly records the incident reflections. Noise levels on cemented DAS at the near offset are mostly low and comparable to that in the geophone data.

Cemented DAS shows better data quality than suspended DAS, as it provides better coupling with the formation and lower noise levels. Suspended DAS has lower sensitivity and higher noise; however it was still effective in recording reflected waves. Both DAS records show attenuation of high frequencies, most likely as an effect of the gauge length. VSP record with hydrophones shows high level of noise. In this experiment, both cemented and suspended DAS provide higher quality records and higher S/N ratios than hydrophone data.

Due to the Gaussian characteristic of the random noise commonly present on DAS data, stacking of repeated sweeps is an effective method for noise attenuation. Cemented DAS data of the stacked 19 sweeps provide a superior dataset quality than the one recorded with geophones.

CHAPTER 5 3D SURFACE SEISMIC STUDY ON BURIED FIBRE-OPTIC CABLE AT THE OTWAY PROJECT SITE

3D surface seismic is possibly the most common method used for subsurface imaging and monitoring. It provides detailed information of the geology in subsurface, at the scale of meters. A major, yet obvious, advantage of the surface seismic is that data can be collected entirely on the surface, dismissing the need for expensive wells. Conventional surface seismic surveys usually use thousands of geophone channels deployed on the surface. Marine seismic is also routinely acquired by towing hydrophone streamers behind a boat. Such surveys are routinely acquired with the objective of providing reservoir characterization in hydrocarbon exploration. During surface seismic acquisition, usually receivers are deployed at 10 m to 30 m spacing. An immense effort is required for the acquisition of surface seismic, especially for the deployment and retrieving of equipment. For this, a large number of personnel crew is also needed. Therefore, 3D surface seismic surveys are extremely costly and lengthy, especially on land environment.

DAS has been more commonly used in VSP application due to its increased sensitivity to waves polarised along the fibre axis (Kuvshinov, 2016). As a result, little has been shown towards using DAS for surface seismic as it can often present noisy datasets, insensitive to P-wave reflections. Field trials have demonstrated the use of DAS acquired on surface cables for the applications of earthquake detection (Lindsey et al., 2017; Martin et al., 2017), and near surface imaging (Dou et al., 2017; Hornman et al., 2013). Surface seismic with DAS for deep imaging, however, is uncommon and in experimental stages. There are no published previous attempts using DAS for 3D surface seismic imaging.

At the Otway Project, we work towards finding a cost-effective monitoring technique to image the injected CO_2 plume and track its behaviour in subsurface. For this, during Stage 2C, a permanent seismic array was installed on-site early 2015, consisting of 908 buried geophones. 3D surface seismic with the buried geophones were the main monitoring tool (Pevzner et al., 2015), together with the 3D VSP with 3-C geophones (Tertyshnikov et al., 2018). Burying the geophones permanently meant

that some of the issues related to constant deployment and retrieving of receivers on site are minimized, while decreasing ambient noise and improving time-lapse repeatability.

However, we also wanted to test alternative monitoring techniques that could effectively image the CO_2 plume, while being more practical and less expensive than buried geophone sensors. Previous field trials on-site demonstrated that fibre-optics sensing DAS shows significant potential for seismic imaging applied to carbon sequestration projects (Daley et al. 2013; Dou et al. 2016; Yavuz et al. 2016). As a result, we decided to test the performance of DAS for the acquisition of 3D surface seismic. Therefore, approximately 40 km of fibre-optic cable was installed on-site and buried at ~80 cm below the surface, along with the geophones.

In this chapter, I show the results after the processing of 3D seismic surveys acquired using the permanent installation of fibre-optic cables deployed on the surface. 3D surface seismic with DAS was acquired simultaneously with the 3D surface seismic with conventional geophones and with the 3D VSP survey with DAS (DAS in the injector well, CRC-2). As mentioned before, the geophones were the main monitoring tool during the Stage 2C of the project, though, DAS data was acquired simultaneously with the geophone survey. In total, a baseline survey and three monitor surveys were acquired with DAS focusing on the surface deployed fibre. I present the results of the 3D surface seismic acquired with DAS and analyse the suitability of using surface DAS for monitoring at the Otway Project, as well as analysing the lessons learnt with these experiments. The 3D surface seismic data with DAS were part of the first field trials with the permanent fibre array at Otway.

This study was published as an extended abstract in (Correa et al., 2017c).

5.1 Experiment design

The DAS time lapse surface seismic experiment is part of Stage 2C of the Otway Project. In 2015, a permanent monitoring array was installed on site in order to monitor the injection. In total, 908 geophones were buried at 4 m depth at every 15 m. The fibre-optic cable was buried at 0.8 m depth in trenches (with the geophone cables). In total, there are eleven receiver lines, with varying lengths from approximate 890 m to

1460 m, and 100 m cross-line separation. Refer to Chapter 3 for information on the Otway Project.

The fibre-optic cable deployed on the surface contains a set of single-mode fibres; the fibres are wounded along the cable axis at 11 degrees pitch. A helically-wound cable (HWC) was also deployed along approximately half of receiver line 5; the HWC contains a set of single-mode fibres wound along the cable axis at 30 degrees pitch (Figure 5.1). The fibres deployed in the well are standard straight fibres. Each line and well has the cable deployed in a loop, symmetrically. The fibre-optic cable on the surface was deployed in two sections of roughly 20 km each, where each section was connected to an interrogator unit. Figure 5.2 shows the diagram of the deployment of the fibre cable connected to interrogator unit 1 (iDAS-1). The iDAS-1 unit was responsible to interrogate the well deployment, line 4, line 5, line 5 with HWC cable, line 6, and line 7. The other section of cable, deployed on the remaining lines, was connected to a second interrogator unit (iDAS-2).

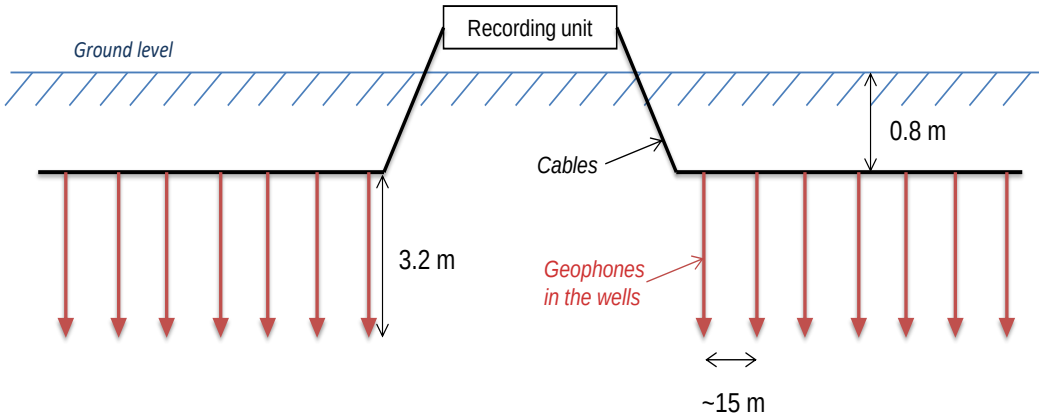

Figure 5.1 Vertical section of deployment (Pevzner et al., 2015).

The monitoring plan for Stage 2C of the project consists of acquiring a series of 3D seismic surveys, 3D VSP and offset VSP with geophones. Although the geophones are the main tool to acquire seismic data in the project, DAS data was acquired using the same source effort. To monitor the evolution of the injected plume, in total, a baseline and five monitor surveys have been acquired to this date for Stage 2C. DAS acquisition parameters were focused on the surface deployment only during Baseline, Monitor 1, Monitor 2, and Monitor 3 surveys. Channel separation for DAS

was 0.5 m for all monitor surveys, and 1 m for the baseline. Source positions are displayed in Figure 5.3, along with receiver line positions and the location of HWC cable.

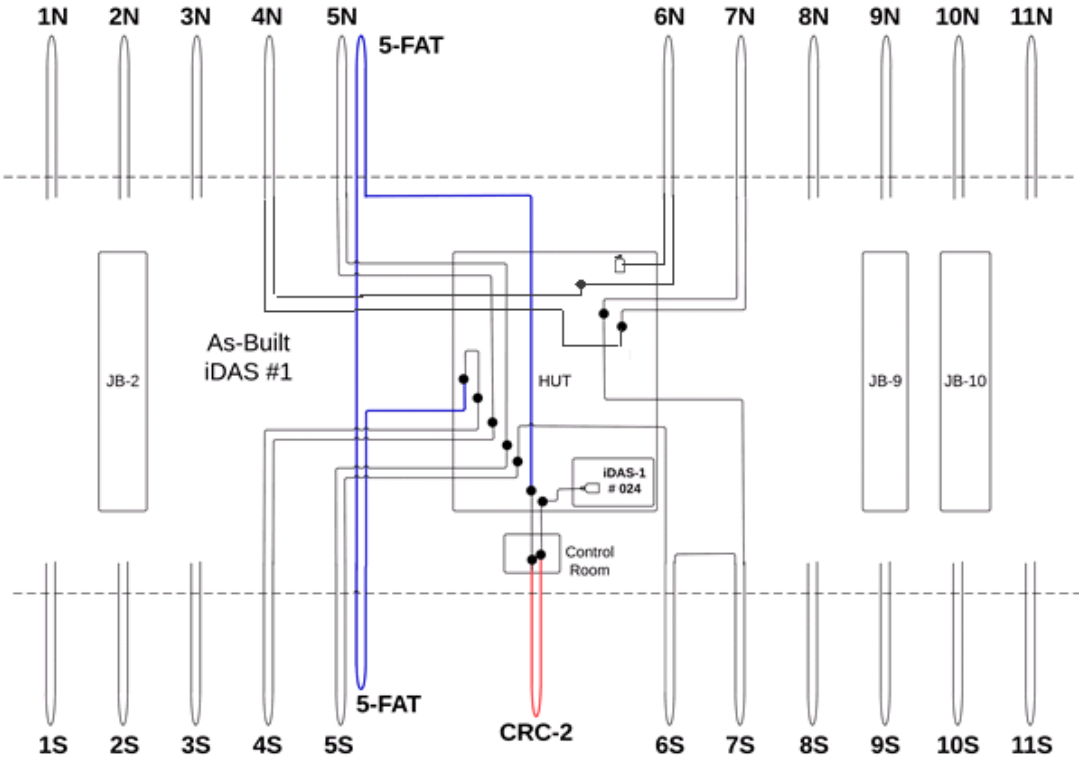

Figure 5.2 Diagram of fibre connections for interrogator unit iDAS-1.The 30 degree helically wound fibre is in blue, and the well deployment in red. N stands for the north section of the cable, and S for the south section (LBNL, n.d.).

A DAS interrogator unit (iDASv2) is used to acquire DAS data. The interrogator unit is also at times referred to as the DAS box. Several key parameters are defined in the IU, such as receiver gain, optical power, and pulse repetition rate. The interrogator unit records the data in GPS time with microsecond precision. As DAS was being acquired as an experiment for surface seismic and imaging, we chose different parameters depending on the survey in an attempt to determine the best set of parameters. However, this resulted in small variations in data quality across surveys.

The Baseline survey was first acquired in continuous acquisition, as it was not connected to the vibrator truck trigger. In continuous time acquisition, the record length is specified to infinite and each file is 30 s. Halfway through the baseline survey,

however, we connected the DAS IU to the trigger from the vibroseis truck. The trigger is a signal sent from the vibrator truck with a time break for the start of the record. For monitor 1, monitor 2, and monitor 3 surveys, DAS was also being triggered.

Figure 5.3 Acquisition design at the Otway site: receiver lines (blue), shot points (red).

5.2 Positioning of DAS traces

DAS determines the position of each trace by analysing the travel time of the backscattered signal. The exact position depends on the velocity of the light in the glass, which varies with the glass refractive index. The actual geographical position of each trace is unknown by the system. There are a few methods that can be used to determine a known location on the fibre to a geographical position. A common method is the "hammering method", or also called the tap test. The tap tests consists of physically tapping a known location on the cable several times and recording the response. I use the tap test method to identify the location of the start, end, and backbone (located approximately at half of the line) positions along the fibre. Their geographical position was recorded with a GPS and assign to the DAS data geometry.

An algorithm to assign DAS trace positions was developed in MATLAB. After assigning coordinates from the tap test, I use the surveyed geophones coordinates to obtain the geometry for the DAS traces. Using the geophone coordinates to assign DAS traces takes the curvature of the lines into account. I then interpolate the known

coordinates of the geophones, with receiver spacing of 15 m, to fit DAS positions, with spacing of 0.5 m (except for baseline survey, which has receiver spacing of 1 m).

5.3 Seismic processing

DAS 3D datasets were processed using SeisSpace/PROMAX seismic processing software. The processing flow applied to DAS is a simplified version of the geophone data processing (Popik, et al. 2018). In fact, I used buried geophone array data processing to guide DAS data processing by using same velocities, static corrections and parameters in some procedures. I believe this is a fair approach for monitoring applications as we can assume that a limited dedicated geophone survey can be acquired in addition to DAS for this purposes.

Table 5.1 shows an overview of the main processes applied to the DAS data. Due to the very large volume of data (approximately 15 Tb), the amount of DAS traces was reduced by stacking five consecutive traces for the monitor datasets. For the baseline data, as the spatial sampling was different, 3 traces were stacked. This also contributed to increasing the signal to noise ratio as the stacking processes destructively interferes on random noise and constructively interferes on the signal. After vertical stacking of adjacent traces, the new spatial sampling was of 2.5 m intervals. Geometry was then applied to the data to assign 3D grid coordinates to each trace. Following geometry assignment, elevation statics was applied to correct topographical variation, with new datum chosen to be 30 m above the sea level.

A simple noise attenuation flow was applied to the DAS data. F-X Median Noise Burst Removal was applied to remove spikes, with a band pass filter from 10 to 150 Hz following. To attenuate the strong ground roll present on the data, Surface Wave Noise Attenuation process was tested; optimal parameters attenuated velocities up to 900 m/s, from 6 to 35 Hz. Lastly, an FK filter was applied to attenuate further noise and separate P-wave reflections.

In the next stage of the processing, DAS shot gathers were sorted in CDP domain, and the residual statics was applied. Amplitudes were compensated for attenuation and spherical divergence by applying true amplitude recovery process. Normal moveout correction (NMO) was then applied to the data, using the velocity field generated from the geophone data.

Due to the directional pattern of DAS, the fibre-optic cable is more sensitive to waves arriving close to the cable axis (Kuvshinov, 2016). This means that most of the possible detectable signal comes from far offsets. Because of this, different NMO stretch mutes were tested to try to include most far offsets possible; the optimal results were when using 200% stretch, which means all far offsets were included, although having considerable stretch. This inevitably affects the resolution of the obtained image.

In the next process, traces for each CMP bin were stacked together. Additionally, FXY deconvolution was applied to the stacked data to attenuate random noise, prior to Phase Shift Post Stack Time Migration. The interval velocity field used in migration was also generated from the geophone data analysis, as the geophones present less noise, providing more reliable velocity field. After migration I used a 3D FKK filter to reduce some migration noise and artefacts.

Table 5.1 Seismic processing flow.

Process	**Parameter**
Vertical stacking of adjacent traces	2.5 m (stacking of 5 traces)
3D geometry assignment	7.5 m square bins
Elevation statics	30 m above sea level
F-X Median Noise Burst Removal	Spike removal. Replaced amplitude up to 50 Hz.
Band pass filter	10-20-120-150 Hz
Surface Wave Noise Attenuation	900 m/s, 6 – 35 Hz
FK	Polygon filter. Frequency = 9.5 to 140 Hz; wavenumber = 0 to 0.4
CDP sort	Sorting shot gathers to CDP domain
Residual statics	n.a.
True amplitude recovery	15 dB/sec
NMO	200% stretch mute
Stack	3D stack
FXY decon	Filter frequency = 1 to 250 Hz
Post stack migration	Phase shift 3D time migration. Up to 90^o dip;
3D FKK filter	

5.4 Data analysis

Figure 5.4 shows three shots acquired with geophones and DAS, before and after the noise attenuation flow. The three shot point locations were selected to contain near to far offsets. The geophone data exhibits strong direct arrivals, as well as clear P-wave reflections for all three shots, as expected. Strong surface waves are seen on the geophone data, though, they appear aliased, which might compromise how efficiently this noise can be removed. Reflections on the DAS raw data are mostly weak. DAS data presents mostly direct arrivals in all three shots, though, on the farthest offset, the direct arrival is almost not visible. Ground roll and S-waves are strong on the DAS data. Note that they present slightly different signature than the geophones. The different distribution of wave types recorded by DAS and geophones can be attributed

to the different wave components each sensor records. The geophone record shows the vertical component of the wavefield, whereas the DAS record shows mostly the horizontal component since the fibre is wounded in 11 degrees along the cable axis.

After the FK processes during the seismic processing flow, the surface waves were attenuated, though, still presenting strong amplitudes in comparison with the direct arrivals. At this stage of the processing, most of the coherent noise is filtered from the data, as seen on source line 17 and shot point 70. DAS also contains high levels of random noise, which ultimately influence the quality of the dataset. At this point, no P-wave reflections can be seen on DAS data. Note that, for the DAS data acquired on receiver line 5 for source line 29 and shot point 30, DAS records direct arrival on one side of the data from the closest offset, but not from the other side, although the distance between source-receiver should be the same. This is due to the directionality of DAS as receiver line 5 is not straight, having certain sections where the direct arrival is reaching the cable closer to the axis of the fibre. It is difficult to identify the presence of body waves in DAS records.

To analyse the events on the shot record, I calculate the FK spectrum for receiver line 5 acquired for source line 29, shot point 30 (Figure 5.5). The spectrum shows the frequency content of the data in relation to the wavenumber. Strong events seen as low frequency and low dip on the spectrum represent most of the amplitudes coming from the DAS record. This event is probably related to ground roll as this type of noise has low velocity. Also, other dips can be identified on the data up until approximately 120 Hz. This event is probably associated with the direct arrivals. No apparent P-wave reflection can be identified on the FK spectrum.

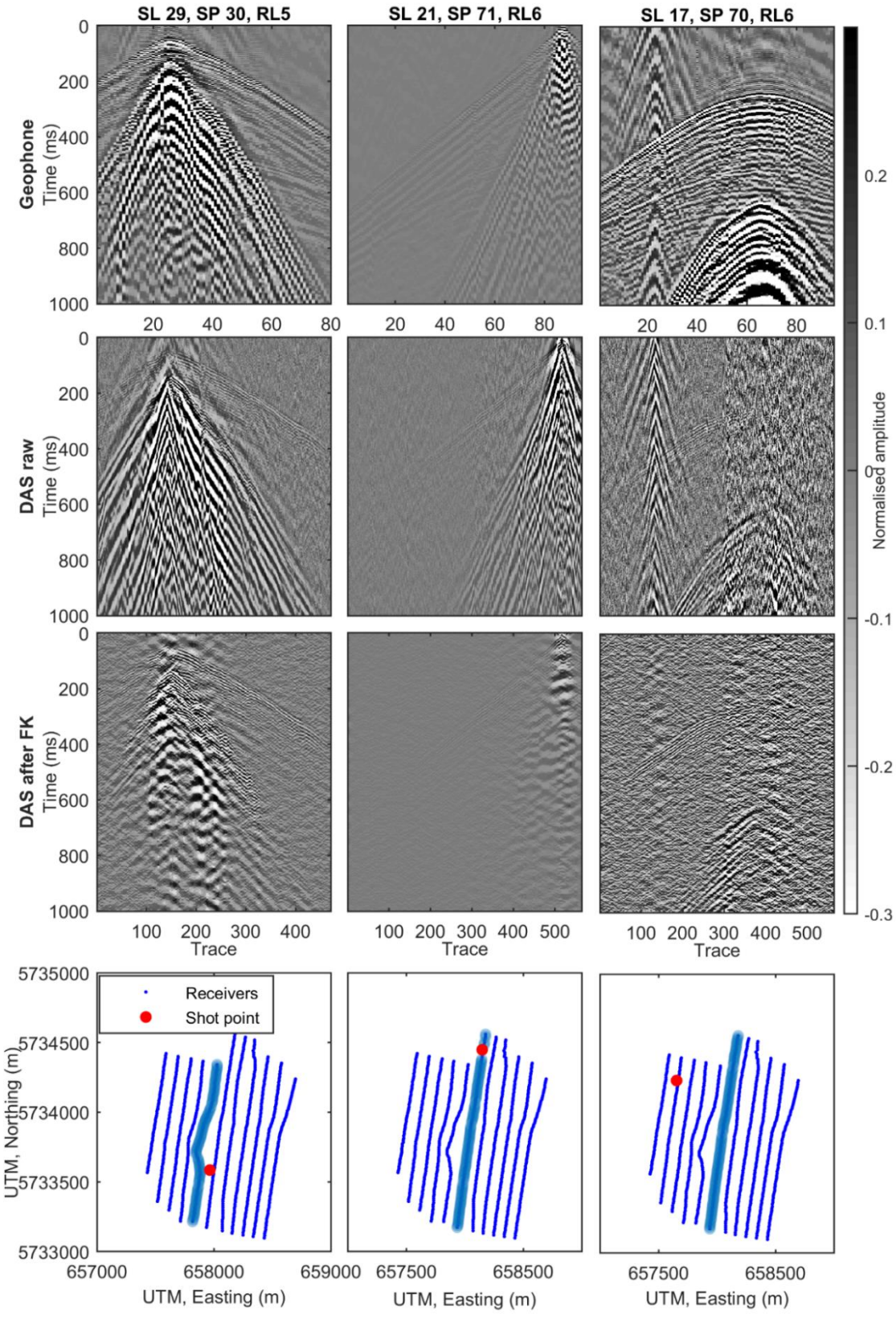

Figure 5.4 Shot gather examples of the geophone data, DAS, and DAS after FK filtering. Last row shows the location for each shot. Receiver line displayed is highlighted.

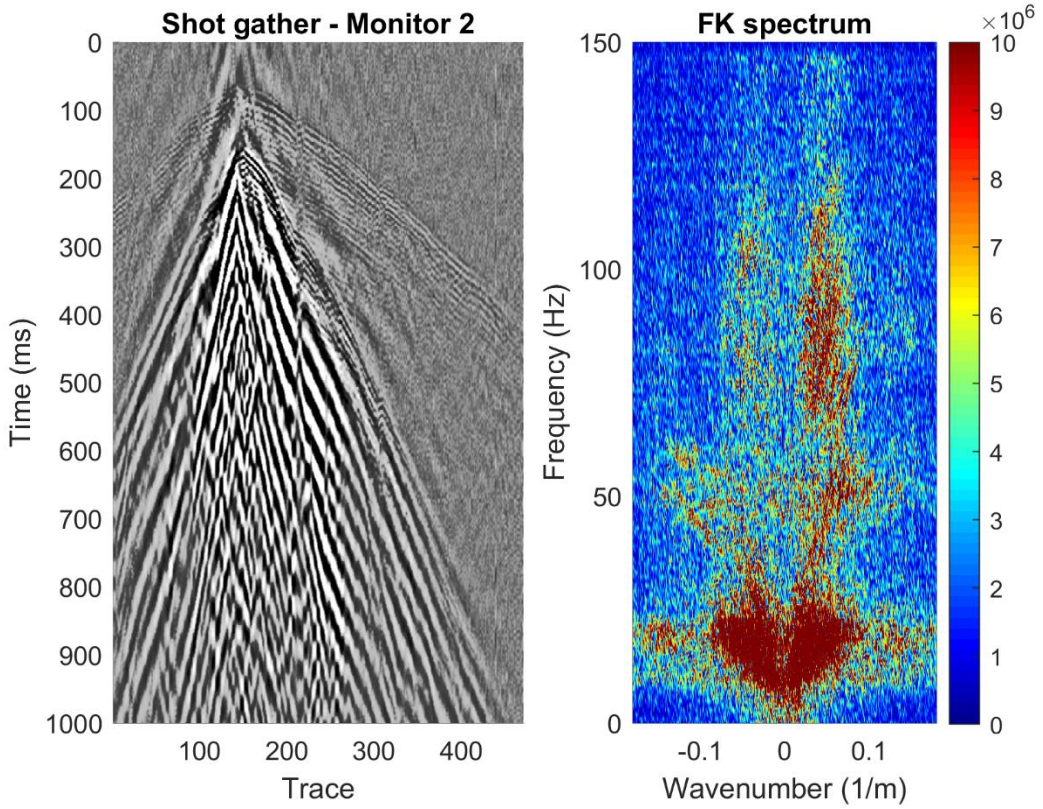

Figure 5.5 FK spectrum for DAS acquired on receiver line 5, source line 29 and shot point 30.

Figure 5.6 shows the same shot on receiver line 5, and source at line 29 and point 30, acquired during the baseline, monitor 1, monitor 2, and monitor 3 surveys. Monitor surveys present visually comparable quality shot recorded. The baseline survey contains noisier traces in comparison with the monitor surveys. As each data set presents high levels of random noise, no difference analysis is done at this point.

After migration, the noise on the data reduces considerably due to the stacking effect migration performs on the data (Figure 5.7). This suggests the system noise present on DAS is mostly random. Reflections that were not identifiable in the shot domain can be seen after stack. Inline 71 on DAS data shows a strong reflection at approximately 500 ms that matches well with a reflection seen on the geophone data. This reflection on DAS, though, has much lower frequency content due to the high NMO stretch mute applied in the processing. Other weaker reflections can be seen on shallow parts of the data and at approximately 600 ms.

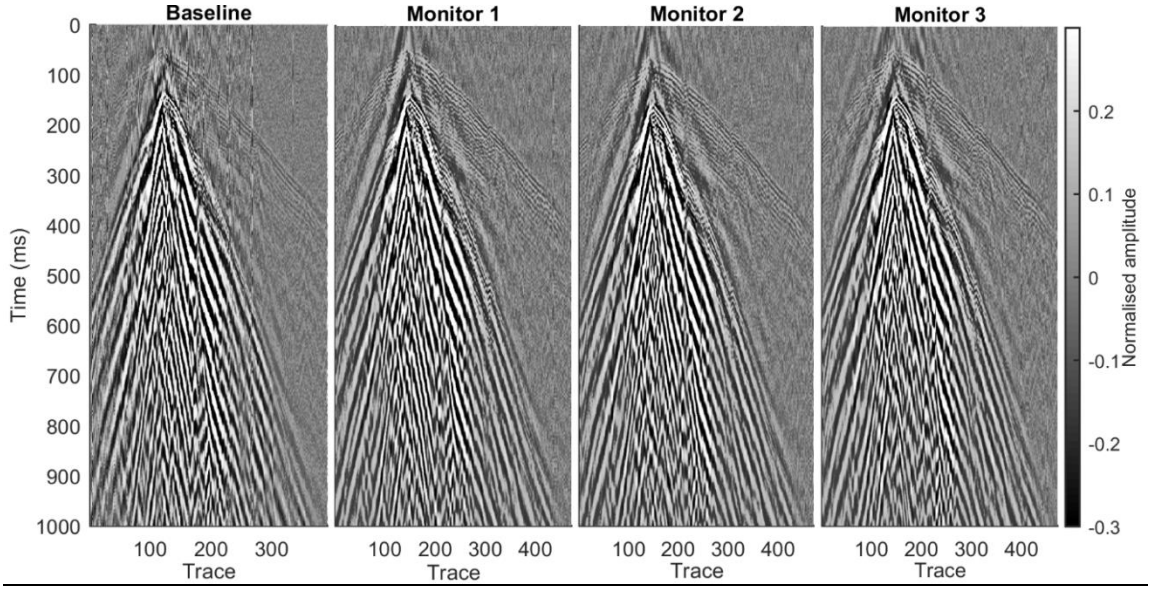

Figure 5.6 Receiver line 5 acquired with DAS for source line 29 and shot point 30 during the baseline, monitor 1, monitor 2, and monitor 3 surveys.

Figure 5.8 shows inline 90 for the first, second and third monitor surveys. The baseline was not included as it was acquired with different parameters. The same strong reflection at 500 ms is prominent across all the surveys. It is also possible to notice reflections at 300 ms and 600 ms, although weak. Strong noise still remains on the data.

To measure the repeatability across survey, I calculate the normal root-mean-square (NRMS) metric by

$$\mathrm{NRMS} = 200\,\frac{\mathrm{RMS(b-m)}}{\mathrm{RMS(b)+RMS(m)}} \qquad (10)$$

where RMS (b) is the root-mean-square of the first survey and RMS (m) is the root-mean-square of the second survey. The NRMS metric was calculated for each monitor data using a window of 40 ms. The NRMS values represent how repeatable a survey is in comparison with a baseline; the higher the value, the worst is its repeatability. DAS presents NRMS of approximately 40% until 500 ms. For most of the dataset, NRMS is approximately 120 to 140%, which means mostly random noise was recorded. The injection interval is located a time of approximately 1200 ms, which makes the surface DAS data unsuitable for monitoring in this particular case at Otway.

To improve the angle sensitivity of DAS, either for surface applications or for use in horizontal wells, a special design of cable, called the "helically wound cable", can be used. The HWC contains a set of fibres that are wound around the cable axis. Their sensitivity to P-wave reflections increase as the angles on incidence are smaller due to the winding of the fibres. Field tests on the HWC show that it can be used for broadside wave detection (Hornman, 2017).

On the Otway Project site, a loop of HWC fibre-optic cables along the northern half of receiver line 5 was installed as a trial. The HWC contains a single mode fibre, wrapped with a 30^{o} pitch in respect to the cable axis. The HWC is deployed alongside the standard DAS cable and the geophones. I would like to compare the P-wave sensitivity of the HWC cable and the standard fibre-cable used for the surface seismic acquisition. To analyse the differences in broadside wave detection, I analyse two shot records acquired with the standard cable and HWC (Figure 5.9). Source line 18 was chosen for the comparison as it intersects the start of both cables on the north end of the line. Significant noise is present on both cable types. The HWC cable seems less sensitive to direct arrival and surface waves, which suggest its angle sensitivity is different from the standard cable. P-wave reflections are not seen on the shot record, probably due to the high level of noise.

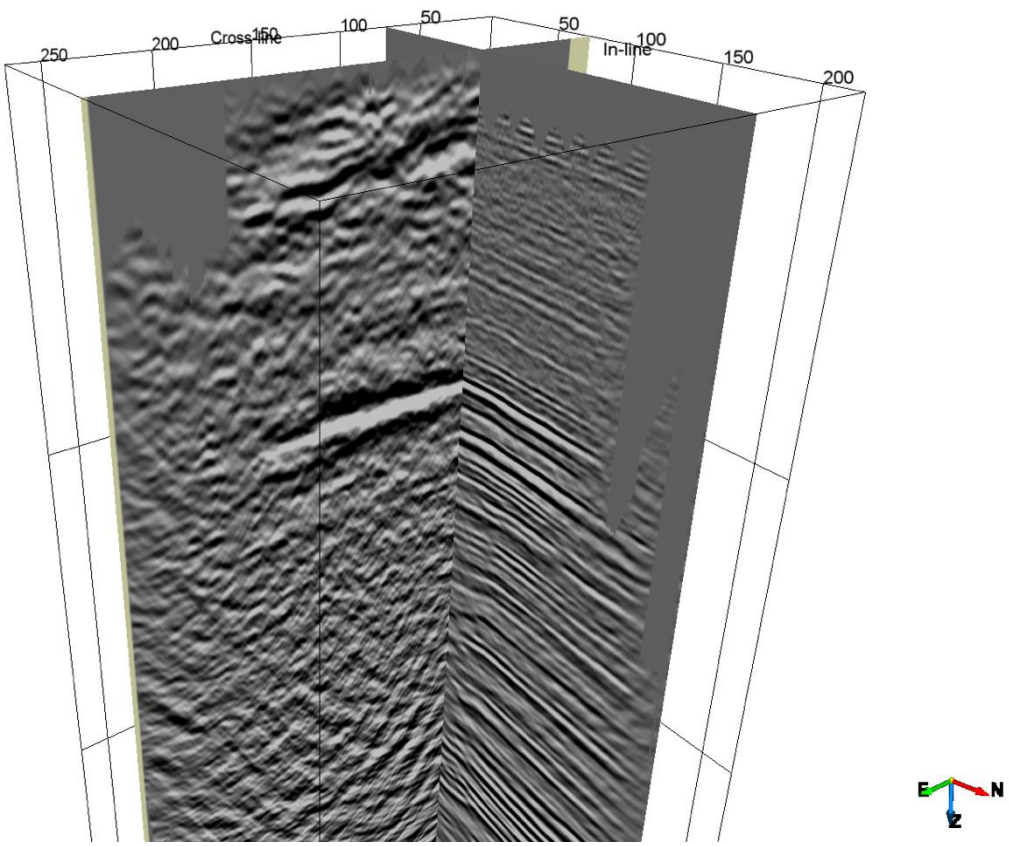

Figure 5.7 DAS stacked data on inline 71 intersected by a crossline from the geophone data, both datasets were acquired during monitor 2.

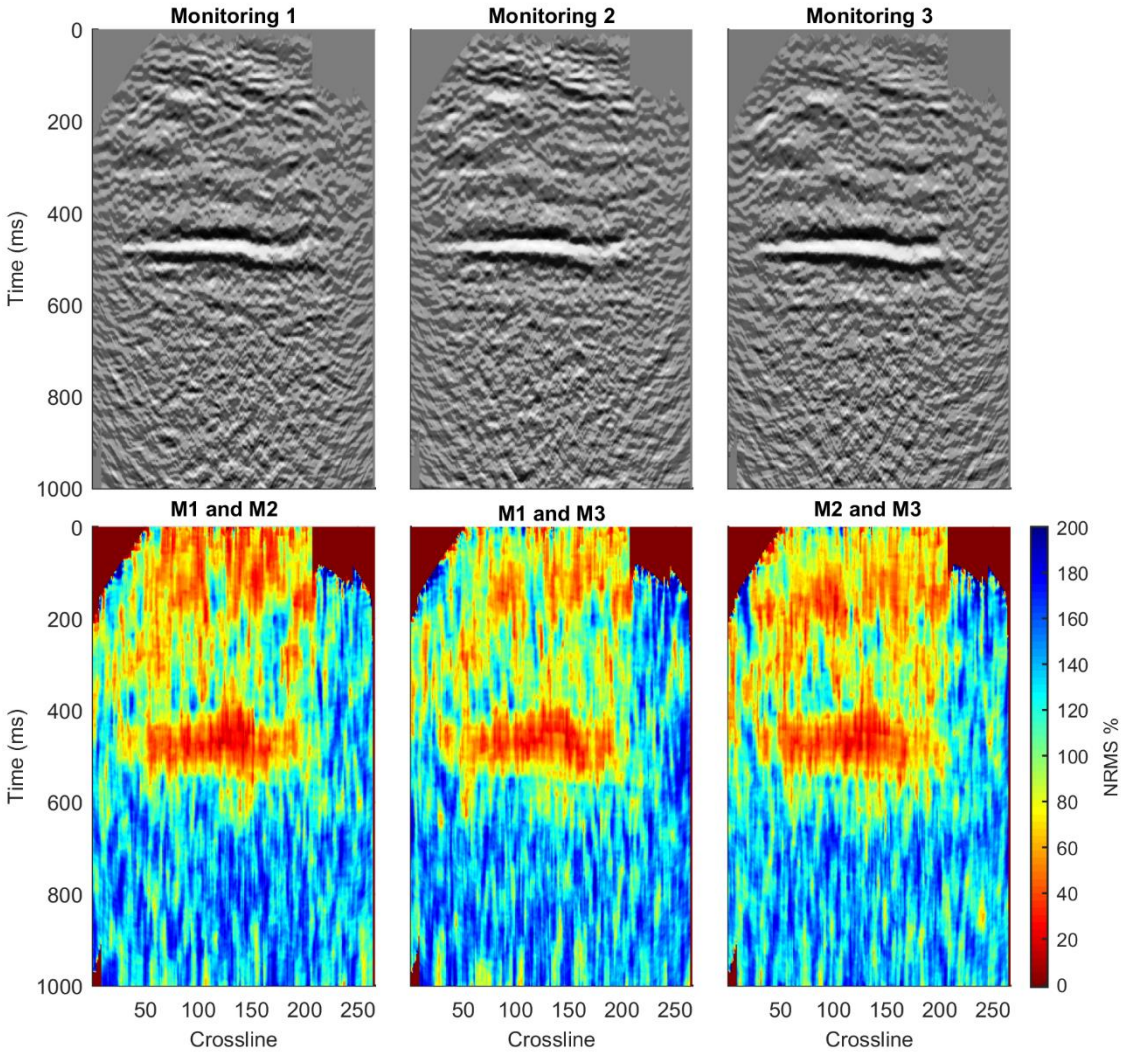

Figure 5.8 Inline 90 from the first, second and third monitor surveys, respectively.

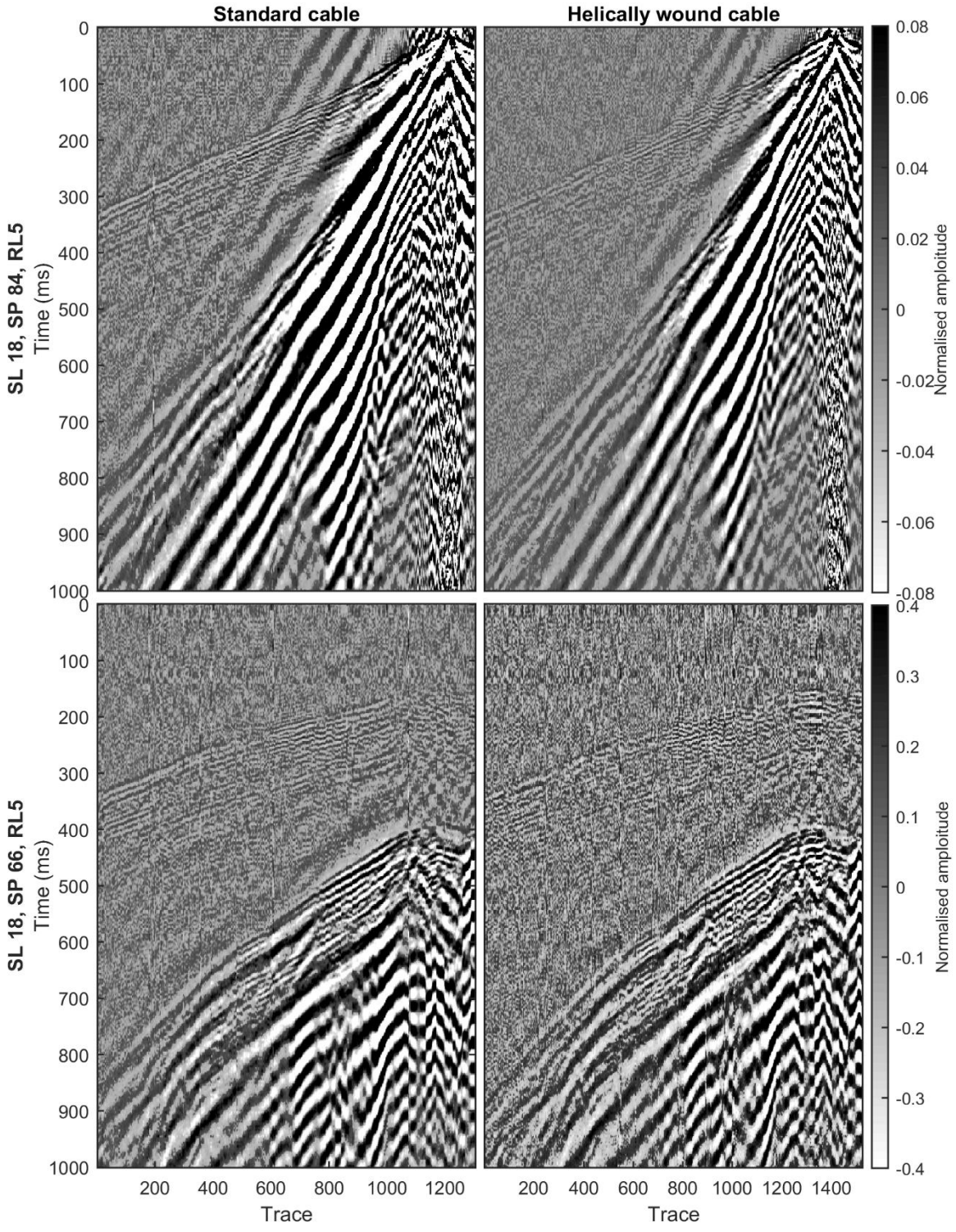

Figure 5.9 Shot gathers acquired with the standard fibre-optic cable (deployed along the surface spread) and the HWC cable.

5.5 Directionality

The directionality pattern in DAS surveys is narrower compared to geophones. Since DAS measures strain along the fibre, it is almost insensitive to a wave arriving perpendicular to the fibre. According to Kuvshinov (2016), for straight fibres, the amplitude in DAS decays as a factor of cosine squared of the angle of incidence to the fibre for P-waves (refer to Chapter 2 for details). Hence, it is understandable that DAS would present different sensitivities depending on the trace azimuth, since each azimuth presents different incidence angles.

In order to identify which azimuth is contributing to the reflections on the stacked image, I divided DAS data into azimuth bins to analyse the signal contribution according to the azimuth. The DAS data was divided into 20° azimuth bins (azimuth from shot-receiver direction to north direction). The azimuth bins show that the fibre detects signal mostly at 0° to 60°, and then at 140° to 180° (Figure 5.10). As the receiver lines azimuth is approximately 10°, DAS could only detect signal up to 50^{o} of azimuth (60^{o} minus 10^{o}). Beyond 50 degrees azimuth, DAS records mainly noise. Figure 5.11 illustrates the angle sensitivity shown on the data.

I analyse if excluding “noisy” azimuths would influence on the quality of the datasets. The stacked data was selected to contain azimuths up to 40 degrees and then migrated. A slight improvement on data quality can been seen, where it is possible to identify a reflection up to approximately 750 ms (Figure 5.12). This reflection was not seen on the original migrated data.

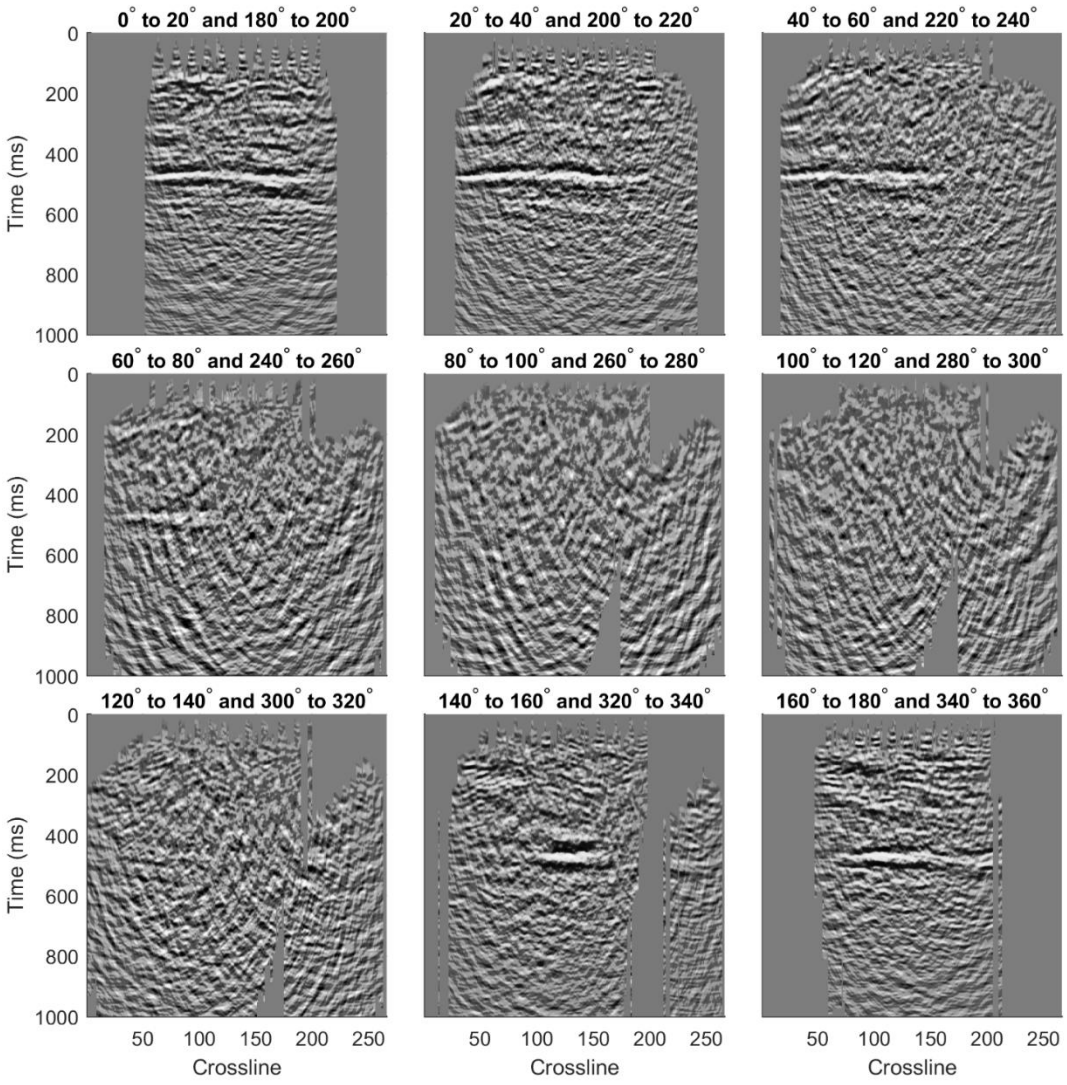

Figure 5.10 Monitoring 2 data showing inline 90. Each section is an azimuth bin of 20 degrees.

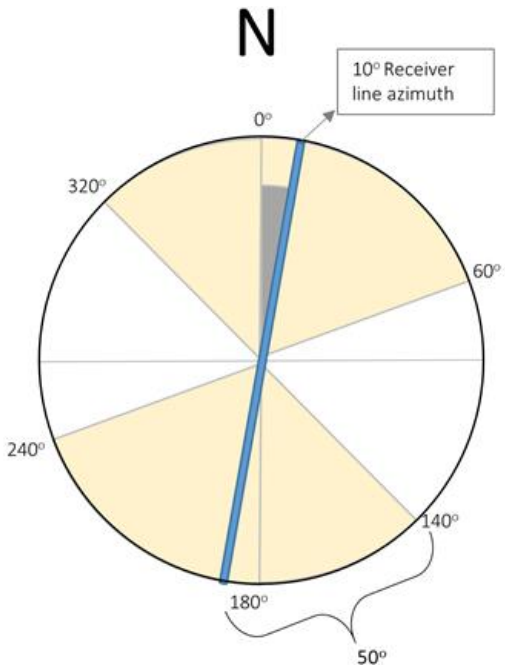

Figure 5.11 Illustration of angle sensitivity of acquired DAS data.

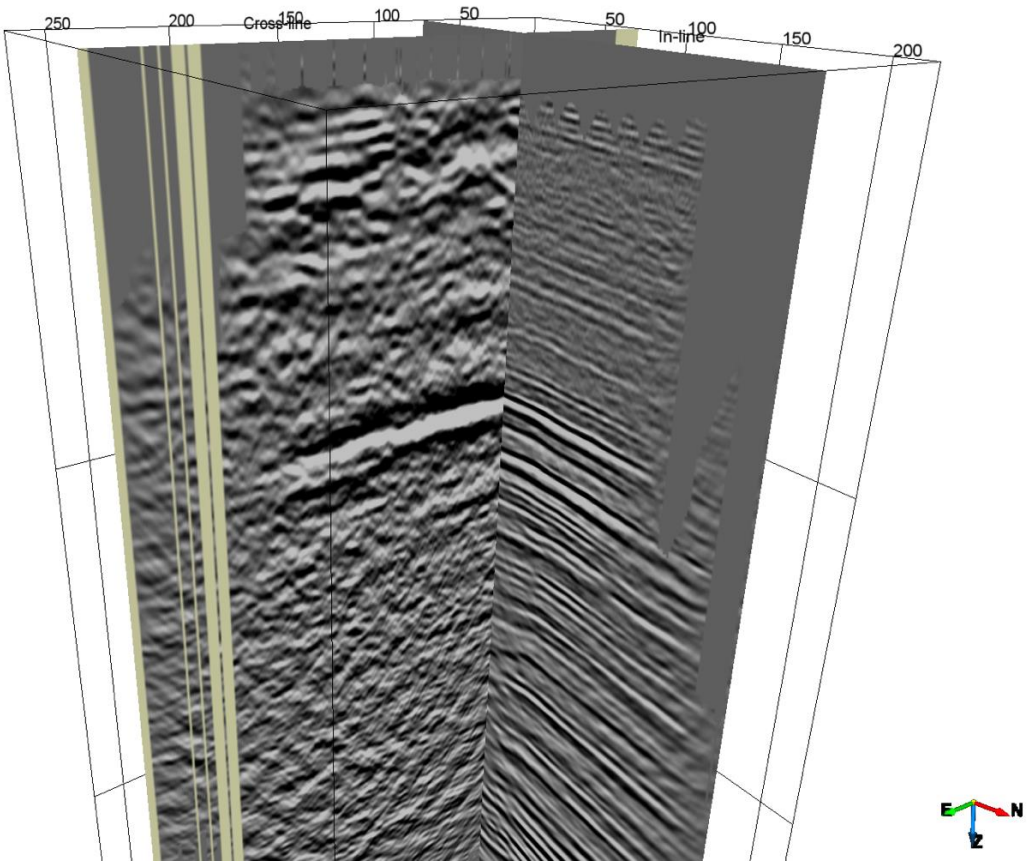

Figure 5.12 DAS stacked data using azimuths up to 60 degrees. Inline 71 from DAS intersected by a crossline from the geophone data. Both datasets acquired during monitoring 2 survey.

5.6 Discussion

Distributed Acoustic Sensing is a technology that can potentially be used for continuous seismic monitoring as it can be installed permanently and offer increased spatial sampling. Currently, seismic applications of DAS are often related to VSP acquisition. Due to the reduced sensitivity of the fibres to broadside waves, the application of DAS to surface seismic is limited. The low sensitivity to P-wave reflection translates to high levels of noise on DAS data, making applications of DAS to surface seismic restricted to near surface imaging or earthquake detection. However, there are many ways one can improve the signal to noise ratio in such applications. The source force can be increased to improve the signal or especially engineered fibres can be used to increase sensitivity. Though, it is important to understand the specifications of the survey before designing the fibre optic array.

As the laser pulse is sent along the cable, it backscatters in the core of the fibre throughout its course. As the light backscatters, it constantly loses its power as it travels further in the fibre. The longer the cable is, the more loss the light suffers. Therefore, the loss determines how far DAS can sense. In the Otway site, we have installed approximately 40 km of fibre optic cables. Each half of the deployed fibre (~20 km) was connected to and interrogated with a DAS interrogator unit. The long cable length contributed to the low quality of the data set. For future experiments, it is preferred to disconnect each receiver line and interrogate them separately, so optimal parameters on the IU can be set. Certain parameters of the interrogator unit aim to compensate the loss of power in the light. For example, the optical power parameter increases the amount of power in the light. However, there is a maximum amount that can be input until it starts creating non-linear effects. The long length of the interrogated fibre dictates how the optical power can be set. Non-linear effects can be seen on the end of the fibre if optical power is set too high, causing unstable changes in phase.

Another parameter that affects the IU output is the pulse repetition rate (PRF). The PRF parameter is the frequency with which a pulse can be sent along the fibre, reach the end of the fibre, and return to the IU. This controls the amount of light pulses that can be sent along the cable. This parameter can be used to improve the data quality; however, it is also dependent on the fibre length. The low quality of the DAS

data acquired on the surface fibre in Otway is a result of the narrow angle sensitivity of the fibre, and the chosen IU parameters. Due to the long length of the fibre, the parameters of the IU that control the quality of the data were limited. This resulted in the poor sensitivity seen on DAS.

5.7 Conclusions

Due to the large volume of data, vertical stacking of adjacent traces was applied to the 3D surface DAS to reduce the size, and then the data was processed. Assigning the correct geometry to DAS traces required the interpolation of the geophone sensors coordinates, as only the start, backbone, and end of the receiver line positions were known. By analysing the DAS shot gathers, P-wave reflections are not seen on the data, while most of the recorded response comes from S-waves and ground roll. After migrating the data, a strong reflector is seen at approximately 500 ms. Random noise improves after migration, though, the 3D seismic cube remains mostly noisy.

I analyse azimuth bins to identify the source of the signal recorded on DAS. Signal on DAS comes from azimuths below 60°, which suggests the fibre was only sensitive to waves up to 50° incident angle (given the receiver line azimuth of 10°). For angles above 50°, the fibre records mostly noise. Developments in cable design, such as the 30° helically wound cables, are expected to improve the angle sensitivity on DAS. I compare two shot gathers acquired by the standard cable and the HWC. Although the shot gathers on HWC present no evidence of P-wave reflections, the cable seems to be less sensitive to direct waves, which suggests the angle sensitivity pattern of the HWC is different from the standard cable. This largely agrees with what has been presented in the literature, although, each work shows a slight variation on the signal to noise ratio.

CHAPTER 6 3D VSP ON TUBING CONVEYED CABLE

The installation of permanent receivers in wells is a common trend in the seismic industry that allows for constant reservoir surveillance (Lumley, 2001). However, permanent installation of conventional receivers is expensive, and it involves the associated risk of a failure of the equipment's electronic components. Distributed Acoustic Sensing (DAS) avoids many of the problems associated with conventional seismic sensors, utilizing an unobtrusive small sensing element that can be permanently deployed in the wellbore annulus. Optical fibre is remarkably robust and avoids the risks associated with downhole electrical and mechanical components.

The use of DAS in borehole seismic, in particular, offers certain advantages over geophones and hydrophones, such as equipment long-life, dense spatial sampling, and full well coverage, making it especially suited for permanent reservoir monitoring. However, DAS is a rapidly developing technology, and currently has some disadvantages, such as a lack of broadside sensitivity.

Fibre-optic cables can be permanently installed in boreholes, e.g. cemented behind the casing. Cemented fibre-optic cable installations provide better coupling to the formation, thus resulting in higher signal-to-noise ratio. However, in some cases, it might be operationally impractical to cement the cable, particularly when using a pre-existing well. In such cases, DAS data can be acquired using a fibre cable clamped on the well tubing. Deploying the cable on the tubing is a semi-permanent deployment that can avoid some of the complexity of cementing a cable outside the long casing string (Li et al., 2015). The installation on tubing avoids interfering with perforation operations, and the cable can be retrieved and replaced in case it is damaged. Barberan et al. (2012), Didraga (2015), and Daley et al. (2016) have demonstrated that fibres deployed on tubing can be used to acquire offset and walk-away VSP. Mateeva et al. (2017) demonstrated the feasibility of using DAS on tubing installation for 4D VSP.

In the CO2CRC Otway Project (described in more detail in Chapter 3), I hope to use DAS to detect the time-lapse seismic signal of an injected CO_2 plume. For this, approximately 40 km of fibre-optic cable were deployed on the surface, as well as on the tubing of the injector well. However, tubing installations of fibre-optic cable

usually present low coupling, which leads to poor quality of the DAS data. The future stage of the project (Stage 3) focuses on multi-well monitoring where several wells will be drilled and instrumented with DAS (Jenkins et al., 2017). Therefore, using the current DAS on tubing would be beneficial as it would increase the seismic fold during the next monitoring stages.

I analyse the results of a 3D VSP data acquired with DAS on tubing installation at Otway. I investigate the quality of the data acquired with the current tubing deployed DAS and discuss whether it is able to image the target interval. Also, I discuss the limitations associated with the current installation and what can be done to improve data quality for future surveys.

This chapter contains work peer-reviewed and accepted for publication in (Correa et al., 2019a).

6.1 Data acquisition of 3D VSP DAS on tubing

In this study, I focus on the VSP data acquired with DAS on tubing installation in CRC-2 well during Stage 2C of the project. The CRC-2 well is a 1500 m deep vertical well, cased with 5.5 inch diameter, and fluid filled from top to bottom. The fibre was installed clamped on the tubing, along the entire extent of the well. The cable was looped at the bottom, and returning to the top of the well, where it was spliced to the surface fibre array. A DAS interrogator unit (Silixa iDASv2) was connected to the borehole end of the fibre, interrogating approximately 20 km of fibre-optic cables (the well deployment and part of the surface deployment). The IU was located close to CRC-2 well. The installed fibre cable is straight single-mode. Temperatures in the well do not exceed ~56 ˚C, therefore, issues with sensitivity due to hydrogen darkening in the fibres is unlikely at this point.

As DAS was a technology on trial during Stage 2C, we experimented with acquisition parameters during each survey. The acquisition parameters in the DAS IU, such as power of the optical transducer, and brightness of the emitted light, were set differently for each survey, which ultimately degraded the signal repeatability. For baseline, monitor 1, monitor 2, and monitor 3 surveys, the acquisition parameters were chosen in order to optimize the 3D surface seismic acquisition. However, this

compromised the quality of the 3D DAS VSP, as the DAS box was interrogating 20 km of cable while the well section was only in the first 3 km of the fibre cable.

Another important issue caused by the length of the cable is the maximum possible laser pulse repetition frequency (PRF). In order for the light to reach the end of the fibre and return, the maximum PRF for 20 km is ~5 kHz (considering speed of light in glass of $2x10^8$ m/s), while for 3 km we could increase it by a factor of almost seven. The actual PRF used in the acquisition was only 3 kHz due to the software limitations. During the fourth monitor survey, the parameters of the DAS box were changed to optimize the quality of the borehole fibre array; this, however, did not include PRF as no changes in splicing of the array was performed and the length of the fibre remained the same.

Due to the above history, this study focuses on the 3D VSP acquired with tubing deployment during the fourth monitor survey of Stage 2C, which was optimized for well acquisition. The DAS VSP data was acquired at 1 m spatial sampling. We used a 26,000 lbs vibroseis truck as the seismic source, with a single linear 24 s sweep from 6 to 150 Hz per shot point. There were approximately 3000 shots in total at a vibration point interval of 15 m (Figure 6.1).

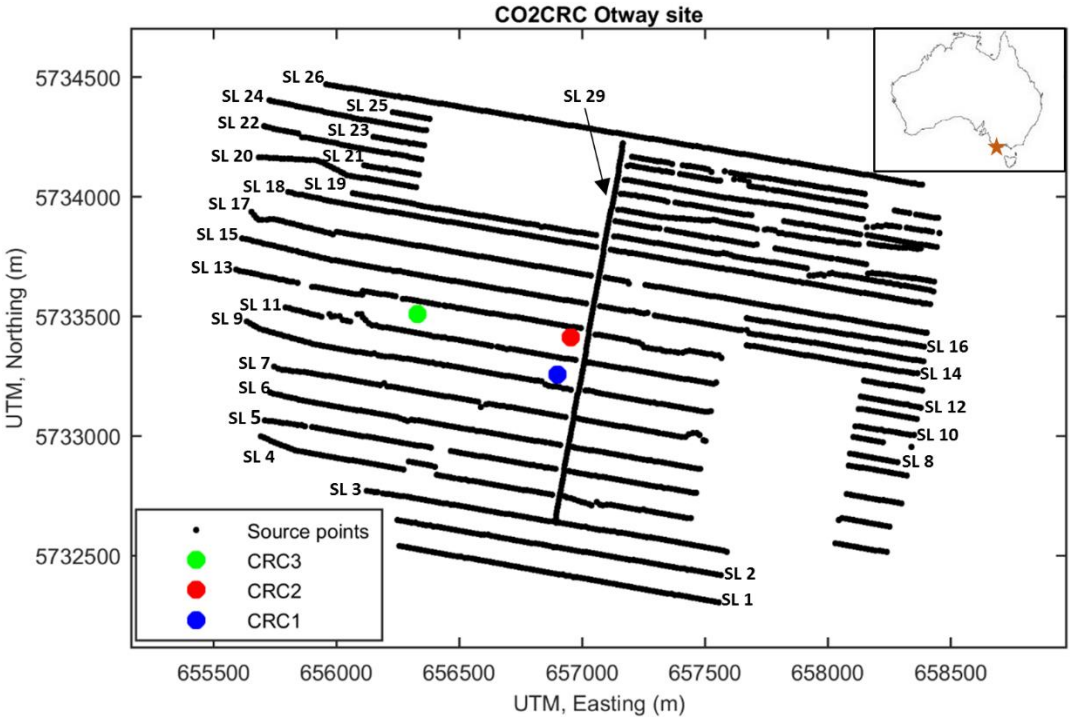

Figure 6.1 CO2CRC Otway Project site. Source point locations are displayed on the map in black. In total, there are 27 source lines (SL), which are labelled on figure.

6.2 DAS records and signal quality

I aim to analyse the acquired DAS datasets and understand what limits the signal quality. A major factor impacting the quality of DAS datasets is the coupling of the cable with the formation. Cementing the fibre-optic cable in the well provides the optimal coupling (Li et al., 2015). The on tubing DAS VSP records acquired in the CRC-2 well exhibit high levels of noise relative to the signal (Figure 6.2). Such poor data quality could be partially explained by the poor coupling, as the cable is deployed along the well tubing.

Figure 6.2 shows an example of four different shots ranging from a far offset to near offset (a – d), after the correlation with the sweep signal. High levels of random noise are seen on all shots, especially at the far offset, when the signal level is relatively weaker. Areas with noisy channels can be seen at depths of 600 m, 750 m, and 950 m on all shots.

Despite the noise, DAS was able to record direct P-waves for shots until offsets of approximately 1000 m (Figure 6.2a), though, at these offsets mostly downgoing P-

waves are visible. The closer the shot is to the well, the stronger the signal. At a closer offset (Figure 6.2b), downgoing and upgoing P-wave reflections become visible, including an upgoing P reflection at 1500 m, coinciding with the injection interval, although showing weak amplitudes.

Upgoing P-wave reflections can be seen at the nearest offsets (Figure 6.2c and d). At 470 m from the well (Figure 6.2c), random noise is still strongly present on the data. The random noise is significantly less apparent at 100 m from the well (Figure 6.2d) as the signal becomes stronger.

The data suffers not only from high incoherent noise, but also by tube waves. Tube waves travel along the fluid-solid boundary in a borehole (Hardage, 1981), masking the desired P-wave reflections. They are source generated tube waves, and can be seen mostly at near offsets (Figure 6.2c and d). Not only downgoing, but also upgoing source generated tube waves can be observed on the nearer offsets. Additionally, vertical stripe-like noise is apparent in the data. The "stripe noise" originates from small movements happening in the surroundings of the DAS box. The tube waves and the "stripe" noise are both indicated on Figure 6.2 (c and d).

To analyse the data quality, I calculate the signal-to-noise ratio (S/N) for every shot point throughout the 3D survey. The S/N was calculated by dividing the RMS amplitude of a 20 ms window around the first breaks with the RMS amplitude of a 100 ms window of noise in the beginning of the record. To reduce the number of points and attenuate outliers, I bin the calculated S/N in 1 ˚ angles of incidence and 20 m distance from shot to receiver, and then average the values in each bin.

"DAS on tubing" presents S/N up to 30 dB, when the incidence angle is small (wave propagation close to the direction of the fibre), at approximately 10 degrees, and at a distance of approximately 500 m (Figure 6.3). S/N decreases with incidence angle, naturally, as DAS measures only one diagonal component of the strain tensor (along the fibre axis). S/N decays also with increased distance from the source. For waves arriving close to the fibre axis, S/N decays to 10 dB or lower at a distance of approximately 1500 m. The darker blue area on the plot indicates when the S/N level is below 0 dB, meaning that the signal is equal or lower to the noise level. This means

that, at a certain angle of incidence and distance from shot, DAS is unable to acquire any signal.

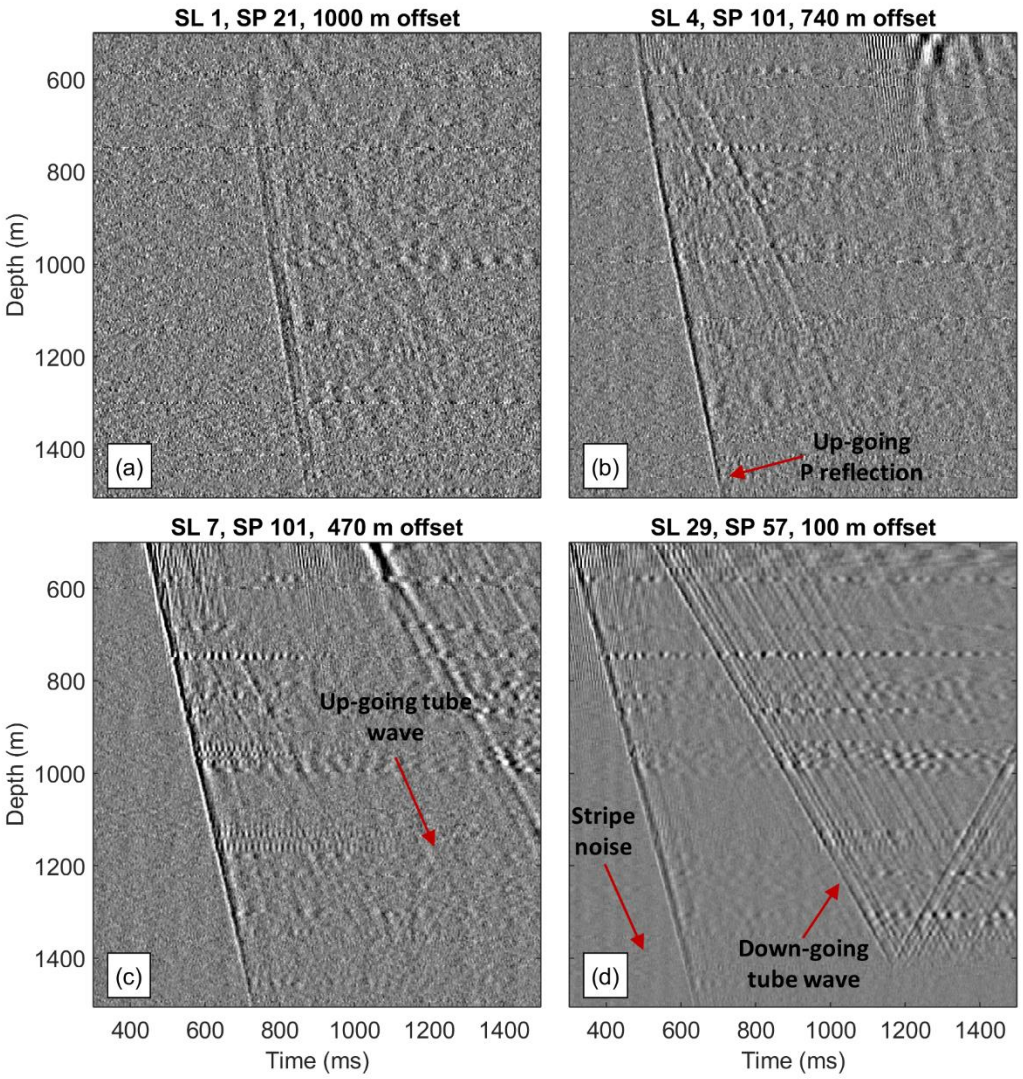

Figure 6.2 Example of shots acquired with DAS VSP on tubing, no signal processing applied after correlation. Displayed shots range from offset of 1000 m (a), 740 m (b), 470 m (c), and 100 m (d).

Although DAS on the tubing was able to acquire sufficient signal at near offsets, its low sensitivity at further offsets is a huge limitation for this type of deployment, especially when considering monitoring applications. With the current data quality, applications such as velocity model building from first breaks can be considered. The overall S/N of DAS can be increased by improving the coupling of the cable with the formation, or by limiting the contrast of acoustic impedance of the cable with the surrounding materials. Additionally, S/N can be improved by vertical

stacking, as a significant portion of the noise presented on DAS is randomly generated by the IU (Bakku et al., 2014b; Li et a., 2015).

An important consideration is that I believe the low quality of the on tubing 3D DAS VSP is mostly attributed to the long cable length (20 km), which means a small PRF was used in acquisition. Reducing the cable to 3 km (only well deployment) could increase the PRF by a factor of almost 7. This means that S/N could increase up to almost 8 dB.

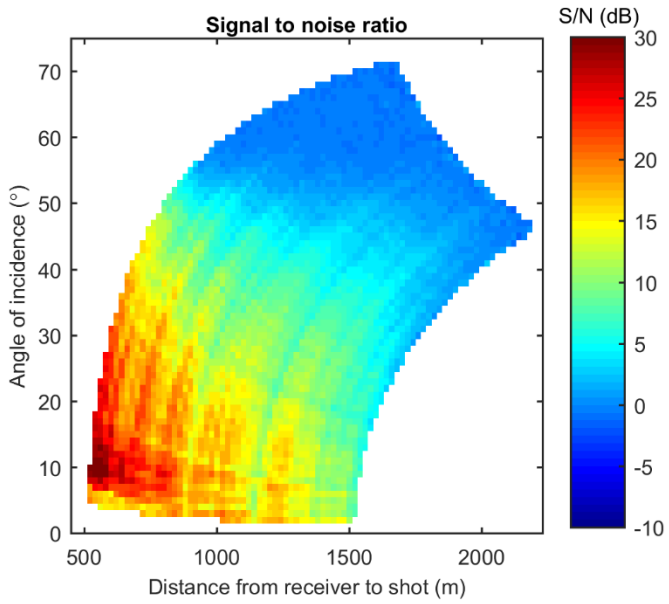

Figure 6.3 Signal to noise ratio calculated from the first breaks of all shot points, as a function of angles of incidence and shot-receiver distance.

6.3 Processing and imaging

The DAS data acquired by the cable on the tubing went through three main stages of processing (Table 6.1). I first used a MATLAB script to read the datasets in its native format and assign the geometry to the DAS traces. The depth on DAS traces were calibrated by doing tap tests on the fibre cable to pin point a specific position on the cable with a known geographical location. As the VSP and surface seismic were acquired simultaneously, each dataset contains the well data, as well as sections of surface lines, so the script selects the area of interest along the cable.

The DAS IU had no communication with the vibroseis truck. As the geophone and DAS surveys were acquired simultaneously, I match the GPS time of the sweeps

(recorded in the first trace of the geophone records) to the GPS time on the DAS data in order to assign shot point numbers and coordinates to each DAS record. As the DAS IU native measurement is the strain rate, the DAS record is converted to the strain response by integrating each trace over time. The strain data is then correlated with the source sweep signal and saved to SEG-Y files.

Table 6.1 VSP processing flow.

Procedure	**Parameter**
Data input	Native iDAS format
Geometry	Coordinates applied from geophone SEGD's
Conversion from strain rate to strain	Integration in time
Correlation	Correlation with source sweep
Band pass filter	5 to 100 Hz
2D spatial filter	Alpha-trimmed mean. 30%, 101 traces. Three passes were applied with same parameters, targeting tube wave noise and "stripe" noise.
2D spatial filter	Alpha-trimmed mean. 30%, 51 traces (targeting first breaks).
Spectral shaping	Flattening frequency spectrum
FK filter	Wavefield separation
3D migration	Kirchhoff

In the next step of the processing, the data is loaded into seismic processing software. A simple noise attenuation flow is applied to the DAS VSP datasets, consisting of a 5 to 100 Hz band pass filter and three passes of 2D spatial alpha-trimmed mean filter. The 2D spatial filter was targeting mainly tube wave noise and the vertical "stripe" noise present in the raw data. Prior to each pass, each component (upgoing and downgoing) of the tube wave was flattened so the filter would distinguish the noise. The "stripe" noise was also attenuated by using a 2D spatial filter with the same parameters. To obtain the upgoing P-wave reflections, I flatten the first

breaks and apply 2D spatial filtering, followed by f-k filter. Spectral shaping was applied to the data to flatten the frequency spectrum.

Figure 6.4 shows four shot points with varying offsets (same shot points as displayed in Figure 6.2), raw after the correlation with the source sweep (a – d), after noise attenuation (e – h), and after wavefield separation (i – l). Downgoing and upgoing PP reflections are difficult to identify on the raw records (Figure 6.4a-d). After the noise attenuation (Figure 6.4e-h), most of the coherent noise was attenuated. The tube wave noise that quite pronounced in source line 29 and shot point 57, was mostly attenuated. P-wave upgoing reflections are still difficult to identify and high levels of random noise still remain in the data.

Figure 6.4i-l shows the upgoing P-wave reflections after wavefield separation. Upgoing P-wave reflections are present along the well, however, reflections are weak and noise is still an issue. Reflections can be identified mainly at depths 1150 m and 1500 m, the latter coinciding with the depth of the gas injection. These reflections are clearer at the nearest offset (Figure 6.4l).

The upgoing wavefield data was migrated using a modified version of 3D Kirchhoff migration algorithm. The Kirchhoff migration implementation has a cosine term to account for the angle between the direction of the travel and the vertical (Sheriff and Geldart, 1995). In order to take into account the dependency of DAS sensitivity on the angle of incidence, I modify the migration algorithm by adding an additional cosine to the weight term. I migrate the data using a 3D grid consisting of 219 inlines, and 265 crosslines, with 7.5 x 7.5 m bin size, and 2 m depth bin. The migration was set to image the depth range from 760 m to 2400 m, in order to reduce the run time while focusing on the target area. Additionally, the amplitude polarity of the migrated dataset was reversed.

After migration, most of the random noise present on the shot gathers was attenuated (Figure 6.5) due to the stacking nature of the migration algorithm. Figure 6.5a shows inline 119 and crossline 119 from the migrated DAS VSP cube. DAS is able to image the reflections along the well, until over 2000 m depth. The injection interval, corresponding to ~1250 ms reflection, was also imaged. A time slice at 1250 ms (Figure 6.5b) was extracted from the volume, which shows the spatial extension of

imaging at the injection interval. The image presents quite a narrow illumination range, of approximately 300 m from the wellhead, as a result of the weak signal at the far offsets. Despite the low quality of the raw datasets, DAS acquired by a cable on tubing was able to produce a good image of the subsurface around the well.

In order to evaluate the reflections imaged by DAS, I compare an inline from the DAS migrated cube with a check-shot recorded by geophones in CRC-2 (this check-shot was acquired during Stage 1, as discussed previously). Geophone upgoing waves are recorded with different polarity than DAS upgoing waves as geophones measure the particle velocity vector, thus distinguishing also the direction of the particle movement. To compare DAS and geophones, the polarity of the DAS was flipped during the processing so it would match the polarity of the geophones.

Additionally, I produced a corridor stack from the DAS data in order to identify matching reflections with the DAS migrated cube and the geophone check-shot. A single sweep recorded with DAS showed nearly no visible reflections. In order to improve the quality of the corridor stack, I selected the nearest offset shots and stacked them to improve the S/N. For this, I selected the shots after wavefield separation, up to 120 m radius from the well (33 shots in total). VSP normal move-out (NMO) correction was applied to the selected shots to correct them to zero offset, then they were stacked. After stacking the shots, 15 adjacent traces on the resulting data set were also stacked to further improve S/N. From the resulting data set, I produced the corridor stack.

Figure 6.6a shows half of an inline from the DAS cube, coinciding with the well location. Figure 6.6b shows a corridor stack produced from the DAS data, Figure 6.6c shows a corridor stack produced from the geophone check-shot. Figure 6.6d shows the geophone check-shot after NMO correction, and Figure 6.6e shows the DAS upgoing P-waves after NMO correction (after stacking NMO corrected shots). Only half of the DAS inline is shown for comparison purposes.

Reflections on the inline from the DAS migration have good correspondence with the reflections recorded by the geophone check-shot, as seen at 850, 900, 1200, 1250, and 1600 ms. This shows that DAS was able to record upgoing body waves. A strong reflection at ~1250 ms, corresponding to the injection interval in Paaratte

Formation, is clearly seen on both DAS inline and geophone check-shot. DAS is also able to clearly image the reflection related to the Waarre C Formation at ~1600 ms, which was the target interval for the previous stage, Stage 1.

The corridor stack produced with the DAS data (Figure 6.6b) also shows good correspondence with the geophone corridor stack, with matching reflections at ~900, 1000, 1200, 1250, and 1600 ms. However, at ~1400 and 1500 ms, DAS and geophone corridor stacks show different behaviour, possibly due to high levels of noise on DAS data. The geophone VSP NMO (Figure 6.6d) and the DAS VSP NMO data (Figure 6.6e) also present good correspondence for the stronger reflections (at 1000, 1200, 1250, 1600 ms), meaning that, although DAS records show low levels of signal, it was still clearly able to record upgoing body waves. Though, the VSP NMO from the DAS data shows poor event continuity. It also seems to contain a narrower bandwidth when compared to the geophone VSP NMO, as the reflections present a lower frequency character.

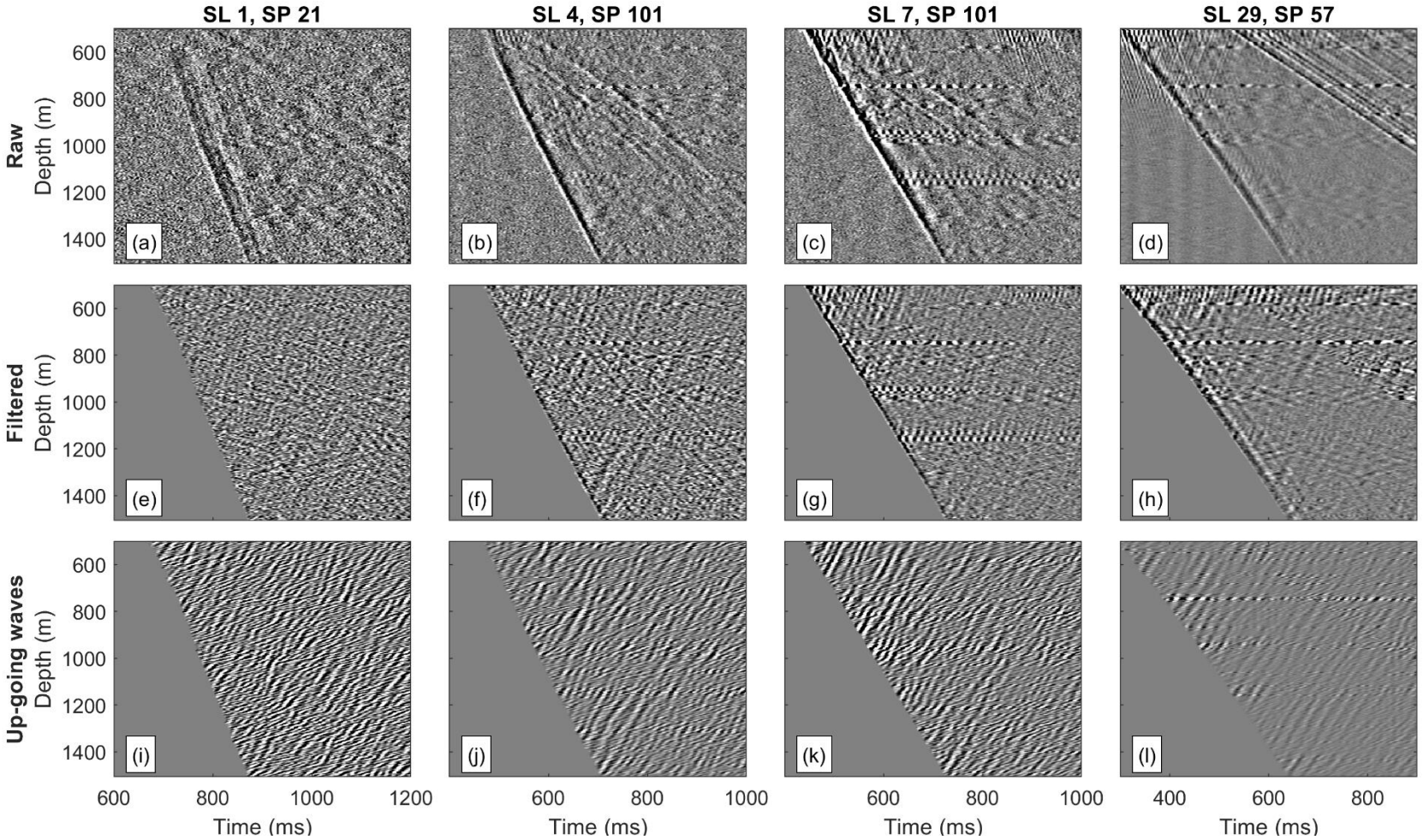

Figure 6.4 Examples of shot records acquired with DAS before noise attenuation (a-d), after noise attenuation (e-h), and after wavefield separation (i-l).

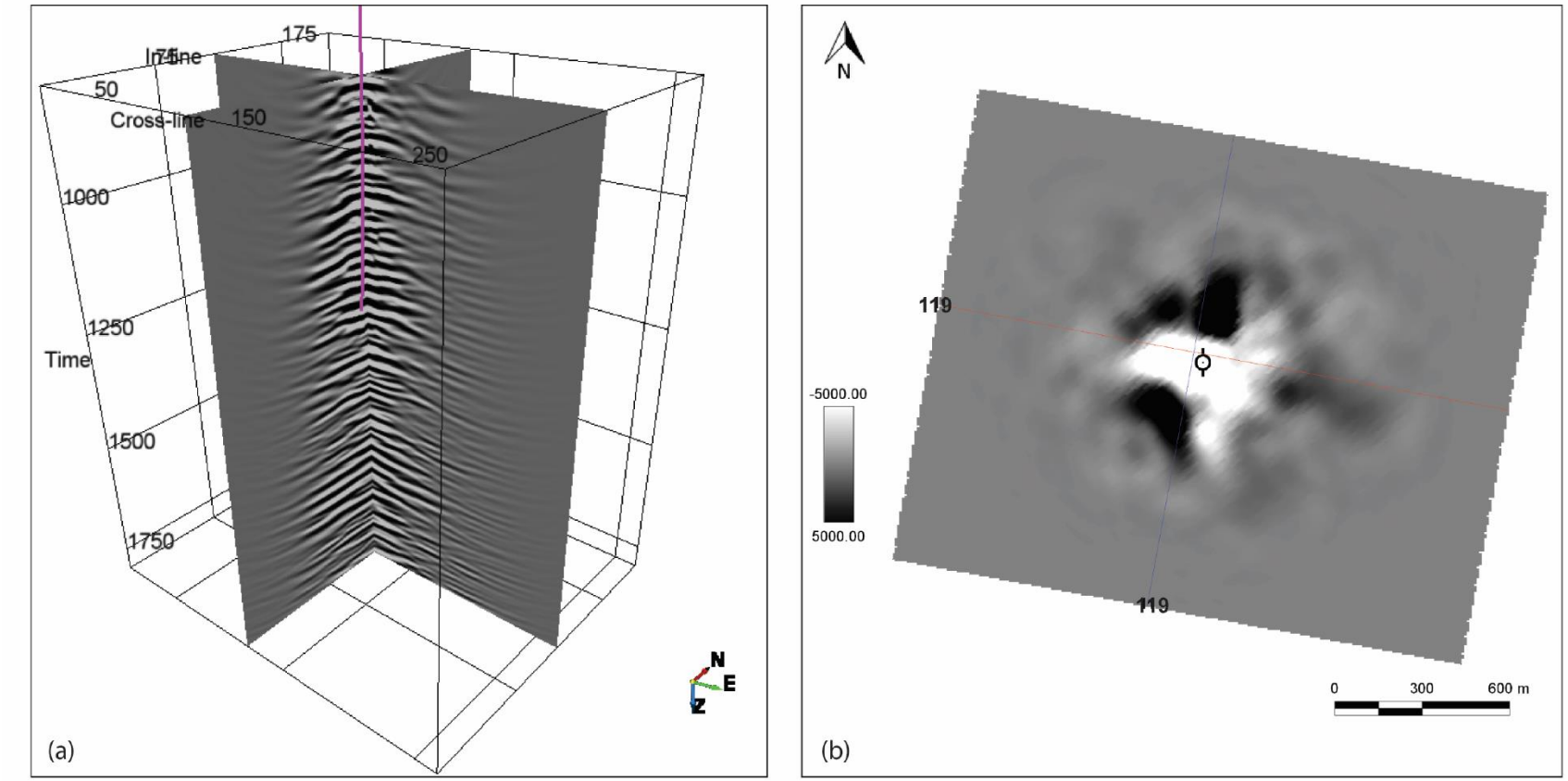

Figure 6.5 Migrated cube (a) displaying inline 119, crossline 119, and CRC-2 well path in magenta. Time slice at 1250 ms (b).

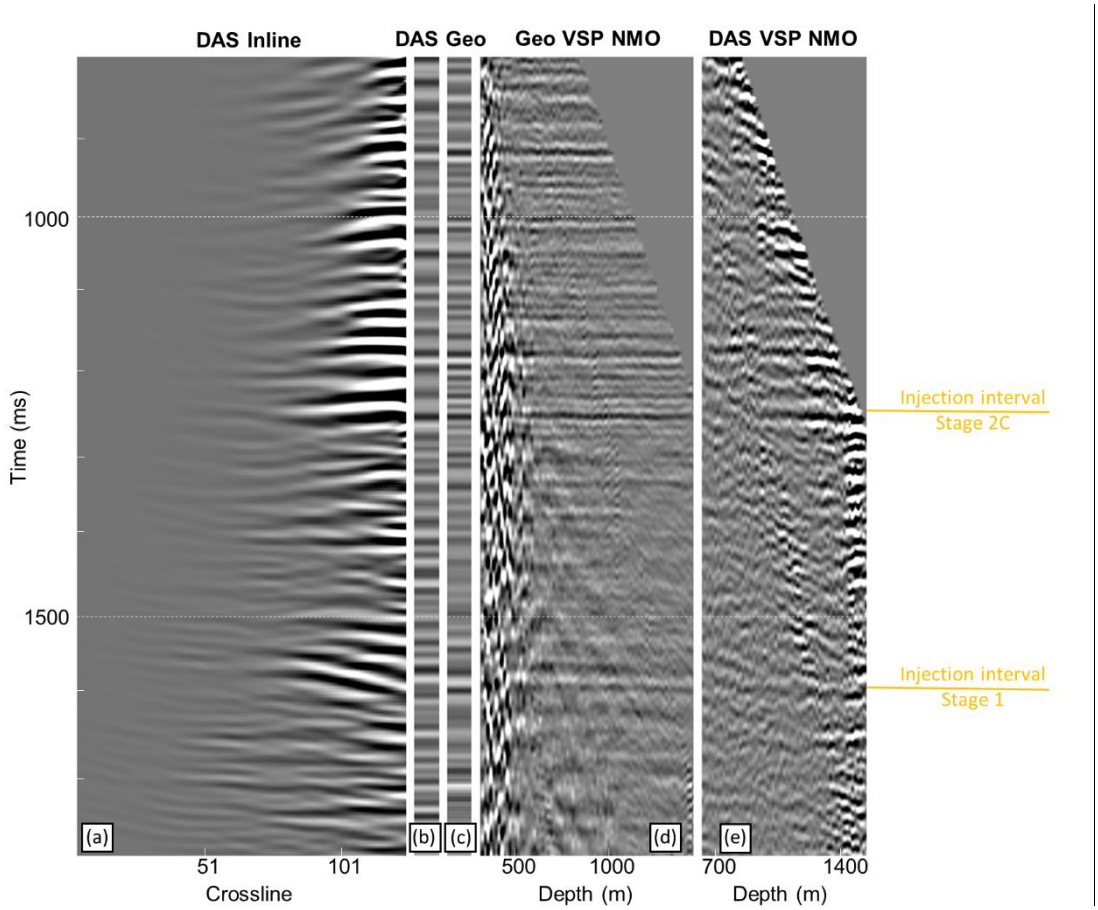

Figure 6.6 Migrated data shown on the inline crossing the borehole from DAS VSP acquired by cable on the tubing (a). Corridor stacked produced from shots acquired with DAS (b). Corridor stacked produced from check-shot acquired with geophone array (c). Check-shot acquired with geophones after NMO (d). DAS upgoing P-waves after NMO (e).

6.4 Conclusions

I have demonstrated the results of a 3D VSP survey acquired using a standard fibre-optic cable deployed on the production tubing. The on tubing deployment of fibre has the advantage of being retrofittable and replaceable, while not compromising well integrity. In this chapter, our aim was to determine whether the on tubing deployed DAS has sufficient S/N to image the injection interval of a gas plume during Stage 2C of the Otway project. Moreover, I provide lessons learnt from our experience with the deployed fibre-optics array on site and ways to maximize the signal acquisition.

The DAS data has significantly lower bandwidth, S/N and event continuity than the geophone data. There are several reasons for this: the reduced coupling

between the cable and the formation, and the long fibre length and insufficient source effort. These result in the raw DAS records having low levels of signal and P-wave reflections are barely detectable on the raw records. Though, strong direct P-wave can be seen on the shot records. After processing, the upgoing P-wave reflections can be identified.

The S/N of the individual records show that signal levels are similar to noise levels (0 dB) for incident waves above 55˚ at 900 m distance, to incident wave of 45˚ at distances of 1500 m. This clearly indicates that the angle sensitivity of DAS needs to be taken into consideration when planning DAS VSP surveys. Due to the nature of the noise in the data, S/N could be substantially improved by stacking multiple shots, or by maximizing the laser pulse repetition frequency in the IU.

The 3D dataset containing the upgoing waves was migrated using a modified version of the Kirchhoff migration algorithm. After migration, the random noise in the data decreases due to the stacking nature of the migration algorithm. The illumination range provided by the DAS tubing deployment, however, was relatively narrow as a result of its reduced sensitivity at far offsets, imaging up to 300 m from the well.

At this point we cannot verify if tubing deployed DAS has sufficient repeatability to monitor the injection due to differences in the acquisition parameters between the baseline and monitor surveys,. However, the results show that the migrated 3D DAS VSP data recorded by cable installed on tubing was able to image the interfaces beyond the injection depth. This was demonstrated by comparing the DAS migrated inline and the DAS corridor stack with the geophone corridor stack.

Additionally, I believe the results of the 3D DAS VSP were strongly affected by interrogating the whole extent of the cable (~20 km). Thus, for further acquisitions, it is desirable to consider reducing the fibre length by detaching fibre-optic configuration in the well from the surface configuration in order to increase the laser pulse repetition rate of the interrogator unit. Potentially, an improvement in S/N from the use of the shortened cable could be close to a factor of $\sqrt{7}$ – approximately 8 dB – due to the increase in the pulse repetition by a factor of approximately 7. This tells us that we may consider using the tubing installed DAS for future monitor surveys at Otway, including the next stage of the project, Stage 3.

CHAPTER 7 PERFORMANCE OF DAS IN OFFSET VSP GEOMETRY

To understand how DAS can be used in monitoring applications, it is important to know how it behaves with varying offsets and incidence angles. In this chapter, I show the data from different field trials that took place within the framework of the CO2CRC Otway project. The CO2CRC Otway Project and monitoring program are reviewed in more detail in Chapter 3.

In the first section of this chapter (7.2), I discuss the results from an offset VSP field trial in Otway where a series of offset locations were acquired using a combination of single-mode fibre and an "enhanced-sensitivity" fibre. The cable containing the fibres are cemented behind the casing of CRC-3 well. This field trial was conducted using a conventional vibrator source.

The last section (7.3) aims to analyse the data acquired with a unique type of vibroseis source, the Surface Orbital Vibrators (SOV). The SOV sources are permanently installed on site at two different locations. Two recent field trials were conducted at Otway with the objective to analyse the performance of DAS/SOV configuration for monitoring applications. The first field trial tests the performance of SOV sources acquired with standard fibre and enhanced fibre-optic cable. In the second field trial, a series of SOV sweeps were tested for optimal parameters, as well as different SOV source types.

7.1 Offset VSP on cemented fibre using conventional vibroseis source

Stage 3 of the Otway Project aims to establish cost effective solutions for monitoring of injected CO_2, focusing on multi-well VSP acquisitions. The first appraisal well for Stage 3 (CRC-3) was drilled in early 2017, with additional wells scheduled to be installed in 2018. The CRC-3 well was instrumented with two fibre-optic cables cemented behind the casing. The cables carry a combination of multimode fibres for temperature measurements, standard single mode fibres and a newly developed fibre with increased sensitivity.

Here I show the results of an offset VSP survey acquired using both types of fibre (standard single mode and increased sensitivity fibres) and a conventional 3-component geophone tool. The aim is to compare DAS response from both systems and understand how the data behaves with varying offsets and incidence angles. The results from this survey will assist decision making when designing monitoring surveys with DAS technology.

Subsection 7.1 contains work peer-viewed and published in (Correa et al., 2017a).

7.1.1 Survey design and acquisition

The VSP data acquisition was conducted in May 2017 to improve seismic characterisation of the subsurface, appraise the capability of the fibre optic system, estimate its performance in different survey geometry configurations and compare it with a conventional seismic locking arm geophone array. The survey was conducted in the CRC-3 well, the first injector well for Stage 3 of the Otway Project. CRC-3 was drilled in Q1 of 2017 to a total depth of 1667 meters. The completed CRC-3 well is instrumented with several designs of fibre optic cables, which are clamped along the string of casing and cemented in place.

During the survey, the seismic signal was recorded with two different optical interrogators. The second generation DAS interrogator developed by Silixa Ltd is referred to as an iDAS v2, which was connected to the standard single mode straight fibre. The latest version of Silixa's iDAS, which is refered to as iDAS v3, consists of an interrogator with optimized architecture for use with a proprietary optical fibre (Constellation), exhibiting engineered backscattering properties. The Constellation fibre was designed to allow more backscattered light to reach the interrogator with an optimal ratio between forward propagating and reflecting laser energy. Sercel's SlimWave (Nantes, France) downhole array consisting of eight shuttles with three component geophones (Omni-2400 15 Hz) was deployed in CRC-3 well and acquired data simultaneously with the fibre-optic systems.

Five locations for the offset VSP shot points, SP0, SP1, SP5, SP6 and SP7 (using continuous offset shot point numbering for all stages of the project; SP0 and SP1 were used in previous surveys) were chosen to cover a range of various azimuths

and distances for the experiment (Figure 7.1). Shot points SP7 and SP0 are check shot positions for the CRC-3 and CRC-1 wells, respectively. Far offsets were mainly employed to explore potential limitations of DAS sensitivity at large distances.

Offset shot points locations:

- shot point 7 ~50 m from CRC-3 well;

- shot point 0 ~680 m from CRC-3 well;

- shot point 1 ~970 m from CRC-3 well;

- shot point 5 ~1025 m from CRC-3 well;

- shot point 6 ~2000 m from CRC-3 well;

For every offset shot point, the geophones depth range in the well is 295 – 1600 m, with a receiver spacing of 15 m. Both DAS records acquired the entire length of the well (0 – 1667 m) with a 1 m recording spatial sampling.

A walkaway VSP (WVSP) survey was also acquired along existing roads, using 369 vibration points. The WVSP was conducted using 26,000 lb Inova UNIVIB vibrator trucks, with source parameters set to 6 - 150 Hz linear 24 s sweep with a 4 second listen time. In total, 5 sweeps were shot per vibration point at the offset locations.

Figure 7.1 Survey map for the VSP acquisition in CRC-3 well, CO2CRC Otway research site.

7.1.2 Conversion of DAS response to vertical particle velocity and comparison with geophone measurement

One of the main goals is to quantify the difference between the data quality of DAS and geophone measurements. Since DAS and geophones measure different physical quantities, a conversion from one to the other is necessary for such a comparison. Herein DAS data is converted to the particle velocity, which is measured by geophones within an appropriate frequency range. Moreover, converting DAS data to particle velocity allows one to apply existing processing and imaging routines to the converted DAS data. An example of such a technique is full waveform inversion (Egorov et al., 2017; Virieux and Operto, 2009).

DAS measures strain, or its rate of change, in the optical fibre (Parker et al., 2014). The DAS response (strain rate) can be approximated as (Bona et al., 2017):

$$\frac{\partial \varepsilon_{zz}}{\partial t} = \frac{d}{dt}\int_L \left(u\left(z - \frac{G}{2} + l, t\right) - u\left(z + \frac{G}{2} + l, t\right)\right) w(l)dl, \quad (11)$$

where u is the displacement along the direction of the fibre, G is the gauge length, L is the pulse width and $w(l)$ is the function that defines the laser pulse shape.

Several techniques may be used for the conversion of DAS data to particle velocity. Time integration is one of the methods commonly used for that purpose. In this case, the integral of the data is calculated in respect to time, which can be done in the frequency domain. Daley et al. (2016) apply rescaling of the time-integrated data using the local propagation velocity of seismic waves for the comparison with geophones. This technique requires the knowledge of seismic velocities and does not automatically account for the wave propagation direction. Another approach is to integrate the data along the cable length. Herein, we use the conversion derived from the previous equation, where the displacement u is given by a monochromatic plane wave $Ae^{-i(\omega t-\vec{k}\vec{x})}$. The derived DAS response is similar to that used by Bakku (2015) and Dean et al. (2017), with the exception of including the pulse length:

$$A_z e^{-i(\omega t-k_z z)} \frac{\omega}{k_z}(e^{\frac{ik_z L}{2}} - e^{\frac{-ik_z L}{2}})(e^{\frac{ik_z G}{2}} - e^{\frac{-ik_z G}{2}}),$$

which compares to the response of a geophone:

$$-i\omega A_z e^{-i(\omega t-k_z z)}.$$

Thus, the filter converting the DAS response to geophone response is equal to the ratio of the derived DAS response and the geophone response:

$$\frac{ik_z}{4\sin(\frac{k_z L}{2})\sin(\frac{k_z G}{2})}.$$

The filter can be used to process the data directly. To avoid division by zero for certain values of k_z, the filter can be regularized by adding a small parameter γ to the denominator. This parameter is similar to the water-level parameter commonly used in deconvolution. In order to pick γ, first the filter without regularization is applied, which correctly converts the waveforms, but may contain noise in the output. After a test of several γ values, each of the results are compared to the unregularized processing output and the smallest γ that attenuates the unwanted noise while preserving the waveforms of the unregularized result is picked.

For small values of the wave vector component k_z, the filter can be simplified by approximating $\sin(\frac{k_z L}{2}) \approx \frac{k_z L}{2}$ and $\sin(\frac{k_z G}{2}) \approx \frac{k_z G}{2}$:

$$-\frac{1}{ik_zLG},$$

which is simply an integration along the fibre with reversed polarity multiplied by a scalar $\frac{1}{LG}$. As the absolute value of seismic samples is usually given in arbitrary units, that scalar can be dropped.

The presented theory provides an easy way of correcting both for gauge length and pulse width. Dean et al. (2017) show that the effect of a pulse width is significantly more subtle when compared to the effect of a gauge length for the pulse width smaller than approximately half the gauge length. The effect of pulse widths is mostly evident for wave numbers larger than the first zero of $\sin(\frac{kG}{2})$. To compare the results of the different types of conversion procedures, the data for shot point SP0 is used, with offset of approximately 680 m. Figure 7.2a shows a raw DAS gather acquired with DAS v2. This gather is integrated along the time axis (Figure 7.2b) and along the depth axis (Figure 7.2c). After the integration, a median filter is applied in the (x, t) domain to filter out the low-wavenumber artefacts caused by the numerical integration. Figure 7.2d shows the gather corrected using the regularized filter with the regularization coefficient γ =0.0008. As a reference, a gather acquired with geophones in the same well is shown in Figure 7.2e, where the coarse depth sampling is clearly visible.

It is clear from the comparison of time-integrated DAS and geophone gathers that time integration does not correct the polarity of upgoing waves (the upgoing wavefields in Figure 7.2b and Figure 7.2c-e have opposite signs, which is indicated by green arrows). Wavefields in Figure 7.2c-d show that the depth integration and the regularized filter correct both the wavelet shape and the sign of the upgoing wavefield. Another difference between the conversion results is that the time-integrated result contains a visible converted reflected wave from a layer at ~500 m depth (indicated by a red arrows). This wave has very low amplitude on other conversion results and the geophone gather.

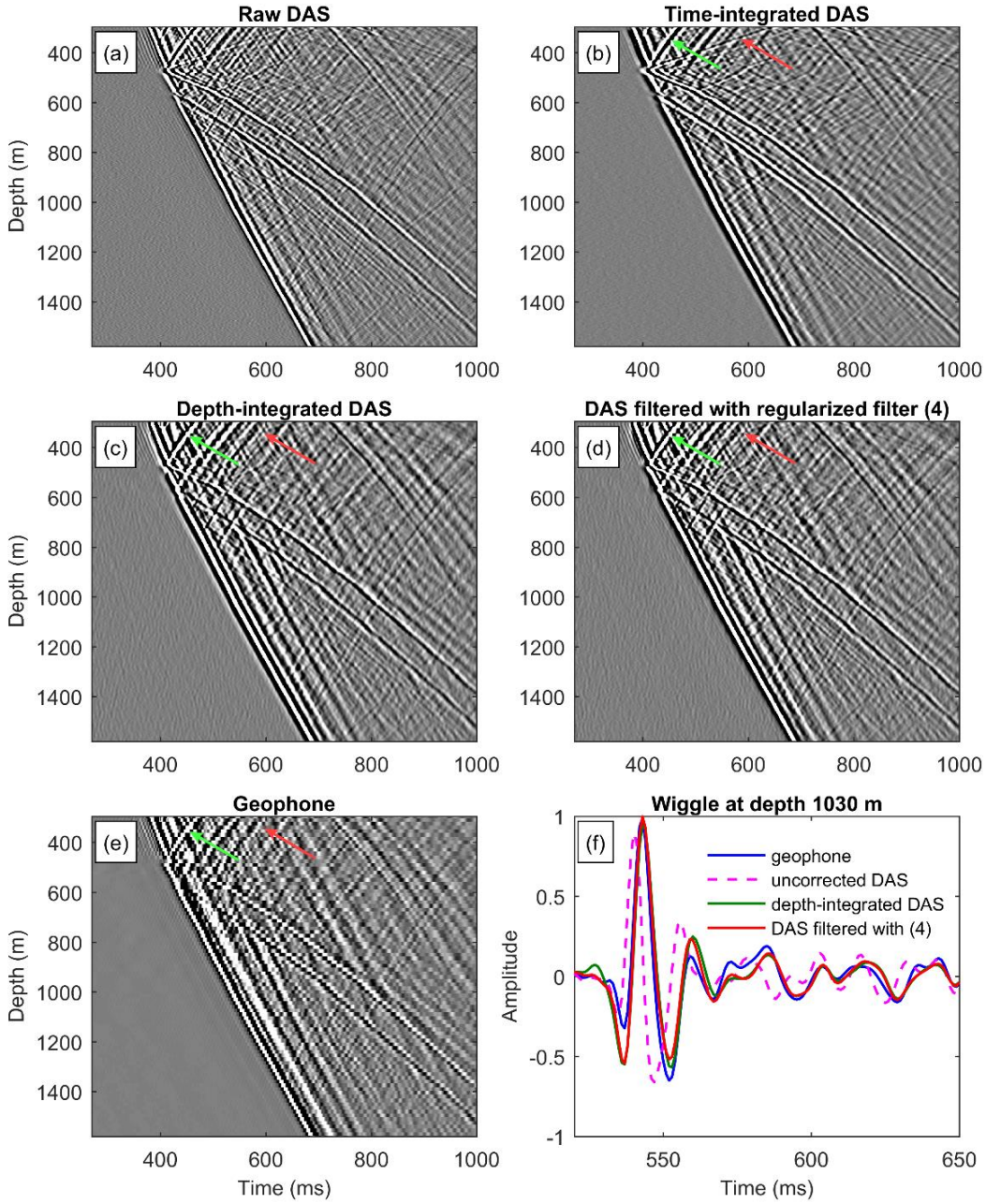

Figure 7.2 Conversion of DAS v2 data to vertical component of particle velocity. Raw DAS gather (a), DAS gather after time integration (b), DAS gather after depth integration (c), DAS gather after correction using regularized filter (d), geophone gather (e), and comparison of traces at the depth of 1030 m (f). Green and red arrows show differences between the conversion results.

A single trace at a depth of 1030 m from the gathers is chosen and a comparison of these traces is illustrated in Figure 7.2f. This comparison shows that, for the displayed gather, the depth integration and the regularized filter produce similar results. However, even for these filters there still remains a difference between the converted DAS traces and the geophone trace.

Comparison of the wavefield acquired from both DAS systems and geophones shows that for the nearest offset SP7 (Figure 7.3a, b and c), the three acquired datasets look similar. The geophones are able to clearly record P-wave reflections along the well, as expected. The level of noise on the data is low, except for the presence of the side lobes resulting from the cross-correlation with the vibroseis sweep, which are present in all three datasets. Geophone data is affected by tube wave noise as the tool is suspended in the well. On DAS gathers, the tube wave is almost absent (indicated by green arrows). DAS v3 shows a defect in the fibre at 1400 m, which occurred during the optical fibre fabrication process.

For the VSP acquired at a medium offset at shot point SP0, at approximately 600 m distance (Figure 7.3d, e, and f), differences between geophones and DAS wavefields become more obvious due to differences in directional sensitivities of the receivers. For this shot point both DAS systems are able to acquire the same PP-wave reflections as acquired by the geophones. The main difference between the DAS systems and geophones at this offset is seen at approximately 500 m depth, where DAS also acquires PS-wave reflections.

At shot point SP5 (Figure 7.3g, h and i) and SP6 (Figure 7.3j, k and l), at approximately 1 km and 2 km distance, DAS v3 and v2 still compare reasonably well to geophone data. DAS is able to record upgoing and downgoing waves, as well as PS-waves. DAS v2 shows a significantly higher level of random noise when compared to DAS v3. Some events that arrive almost parallel to the fibre (indicated by red arrows) were not reconstructed by the conversion.

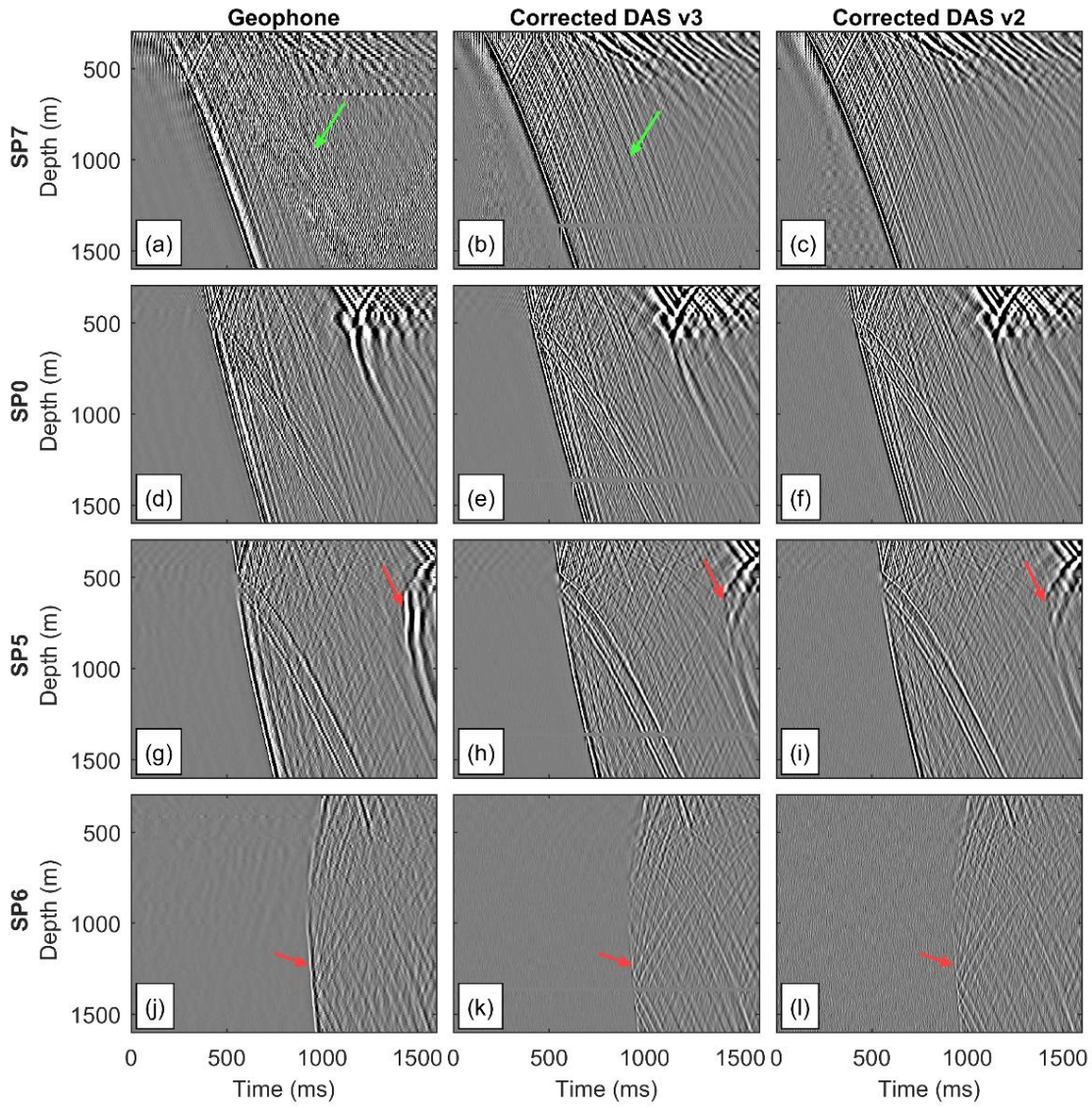

Figure 7.3 Offset points SP7, SP0, SP5 and SP6 for geophone data (a, d, g, j), converted DAS V3 (b, e, h, and k), and converted DAS V2 (c, f, I and l). Green and red arrows show differences between DAS gathers and geophone gather. Overall, DAS systems are able to record the same PP events as recorded by the geophones.

7.1.3 Comparison of signal to noise ratios

To analyse the performance across all recording systems for different offsets, I compare the VSP records acquired using geophones, iDAS v2 with standard fibre, and iDAS v3 with enhanced fibre, at shot points SP7, SP0, SP5 and SP6 (shown in Figure 7.4). Since DAS senses the strain changes only along the direction of the fibre, I utilize only the vertical component of the geophones for the comparison. Unlike the geophones, DAS acquires the data along the entire length of the well simultaneously. By the end of the geophone acquisition, DAS acquired more than 50 shots for each offset point. To increase the signal to noise ratio (S/N), I stack all the repeated shots for DAS data at each location. While the transformation of DAS measurements to the vertical particle velocity is important for comparison of the waveforms recorded by the different systems, for assessment of the S/N of the systems I opt to use the strain response of DAS, which I obtain by integration of the strain rate along time. I choose to use strain not only due to its wide use in the industry, but also because the time integration does not contain artefacts that can be produced by the conversion to the particle velocity by the zeros in the presented filter. It is important to note that different conversions of the data might result in different S/N values.

S/N values were calculated by dividing the root-mean-square (rms) amplitude of a 20 ms window around the first breaks by the mean rms amplitude of a 20 ms window of noise at the beginning of the record, from depth 1000 to 1200 m. This interval was chosen as it gives a good representation of the background noise, free of correlation side lobe effects. Due to the high amplitude of the first breaks in comparison with reflected waves, this method of S/N estimation could, though, yield optimistic results that do not represent S/N of reflected waves.

Figure 7.4 shows that S/N of geophones, DAS v2, and DAS v3 decreases with distance, as expected. Though, S/N in DAS v2 seems to decrease at a greater rate than geophones when acquiring at further offsets - geophones decay by 10 dB, while DAS v2 decay by 20 dB (Figure 7.4d and l). DAS v3 performance is significantly better than DAS v2 as S/N virtually remains the same. Visually, all systems present good quality records, showing similar reflections.

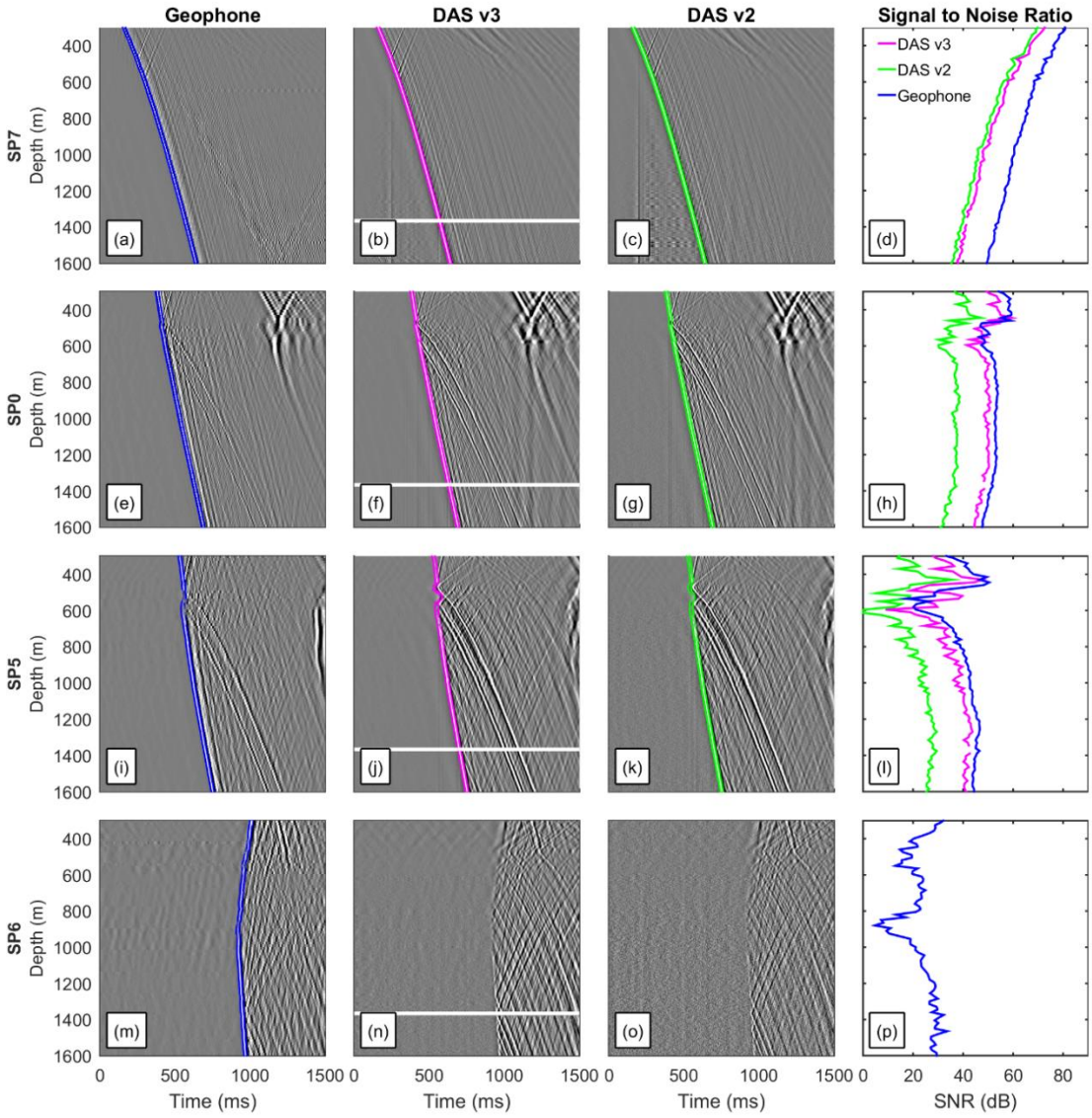

Figure 7.4 VSP record acquired at different offsets with respective recording systems. Geophone vertical component data (a, e, i) acquired at offset points SP7, SP0 and SP5, respectively. DAS v3 (b, f, j) and DAS v2 (c, g, l) also acquired at offsets SP7, SP0 and SP5, respectively. S/N (d, h, m) for each dataset at respective offset points. VSP records normalised trace by trace on the display.

S/N of the geophone data at a distance of 50 m, SP7, is approximately 10dB higher than for the DAS datasets. For this distance, DAS v2 and v3 datasets have no significant difference in S/N (Figure 7.4d). While distance increases to 680 m at SP0, S/N of DAS v2 decreases significantly, showing a decay of approximately 10 dB. DAS v3 shows similar S/N in comparison to geophone data (Figure 7.4h). The apparent S/N discrepancy between DAS and geophones for the near offset can be attributed to the presence of a vertical noise likely caused by the air blast from the source (seen at approximately 200 ms).

At shot point SP5 (Figure 7.4l), 1025 m far from the well, DAS v3 and geophone datasets still have similar quality, while DAS v2 suffers a further 10dB loss. When data is acquired at SP6, at a 2 km distance, geophones S/N further decreases by 10 dB (Figure 7.4p). Because of the directivity, first breaks are not present in the DAS data at offset SP6, therefore S/N were not calculated. Upgoing and downgoing reflections are well imaged in both DAS v3 and DAS v2, despite the high level of random noise present in the latter. Directivity will affect waves closer to normal incidence, such as direct arrivals. However, DAS is still sensitive to reflected waves; they are better captured on DAS data due to the higher spatial sampling.

To increase S/N, DAS data can often be stacked with repeated sweeps so it constructively adds in signal and decreases random noise. S/N is calculated for DAS records after stacking of 5 sweeps and approximately 50 sweeps (maximum number of sweeps for each shot point varies from 48 to 60). Figure 7.5 shows a histogram of the difference in S/N between 5 and 50 stacked shots. The difference represents the improvement after stacking. For both DAS systems, S/N increases by approximately 10 dB. This shows that the improvement in S/N varies close to $\sqrt{N}$, N being the number of traces in the stack. This suggests that the noise on DAS data is predominantly random. For far offsets on DAS v3, however, the improvement is slightly inferior, presenting approximately 7 dB of increase in S/N.

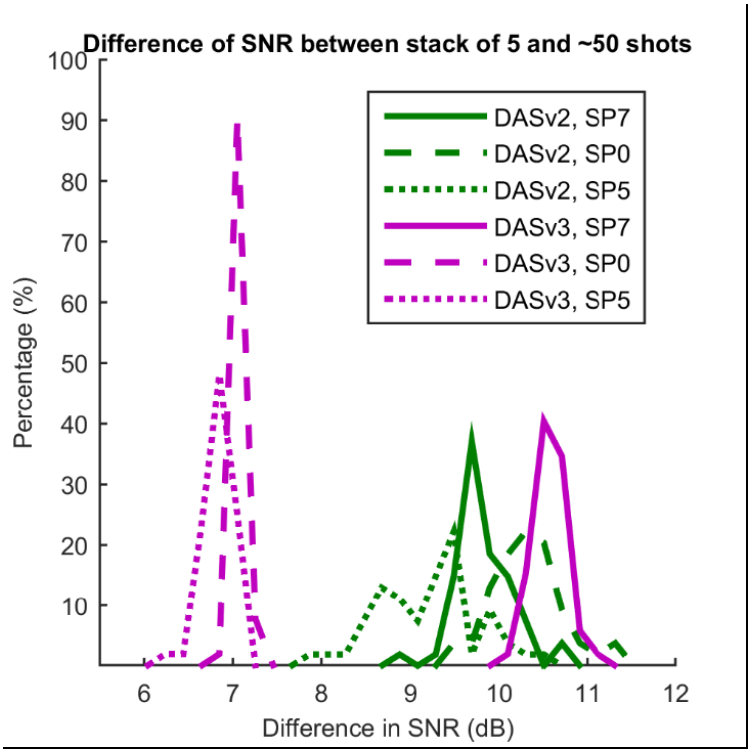

Figure 7.5 Difference in signal to noise ratio between DAS data stacked with 5 sweeps and approximately 50 sweeps. Differences in S/N for DAS v2 are in green, and for DAS v3, in purple. Overall, the improvement in S/N of datasets is close to 10 dB, which corresponds to the square root of number of stacks.

7.1.4 Directional sensitivity of DAS measurements

Direction of particle displacement drastically affects the sensitivity of DAS systems. Figure 7.6 illustrates the decay of first break amplitudes observed in DAS v3 and v2. To highlight the variations in amplitude caused by directivity it is useful to eliminate the effects of the spherical divergence and attenuation. This is done by normalizing the DAS amplitudes by the magnitudes of the geophone 3-C measurements (all components).

At depths from 295 to 1600 m, incidence angles for shot point SP7 vary from 10 to 2 degrees. At offset SP0, angles vary from 67 to 23 degrees; and at offset SP5, from 73 to 31 degrees. Amplitudes for both DAS systems decay approximately as cosine-squared function of the angles of incidence, as predicted by Kuvshinov (2016) for straight single-mode fibres. The scatter in the normalised amplitudes are likely

caused by the interference of the direct and reflected waves, and noise. For small incidence angles, amplitudes show an unexpected trend, probably caused by the normalisation with geophone amplitudes, which are influenced by the compaction of the ground after repeated sweeping at the same location. While geophones acquire the data at one section of the well at a time, its amplitudes present a slight change in source signature along the well.

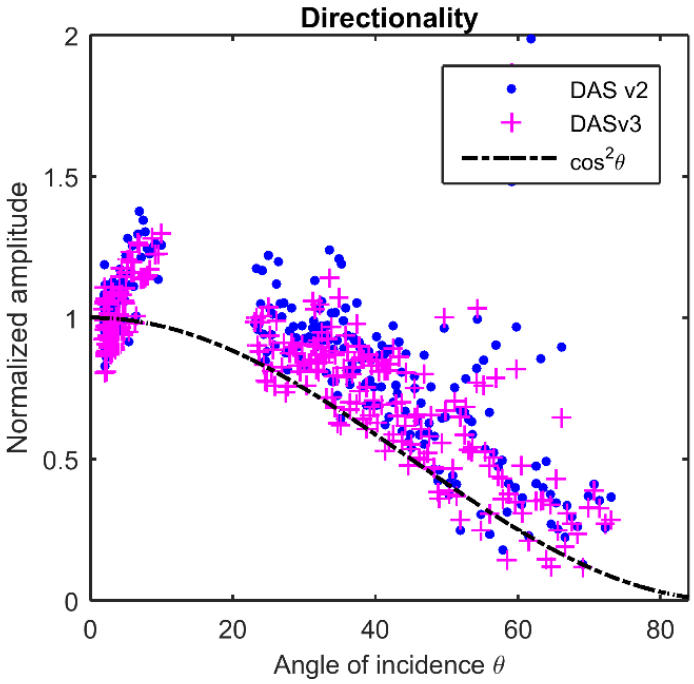

Figure 7.6 Directivity plot showing normalised amplitudes of DAS v3 and DAS v2 against angles of incidence. Theoretical cosine squared curve is plotted with the dashed line.

7.1.5 Conclusions

DAS offers many advantages over the use of conventional geophones. However, it is often affected by the lack of sensitivity and high noise levels inherent in DAS data. Furthermore, straight fibre has a narrower directivity pattern compared to geophones. While these factors still hinder the broader application of DAS in the seismic industry, DAS technology continues to evolve rapidly. Hence it is important to re-evaluate its capabilities in comparison to standard geophones. Understanding

how DAS behaves in respect of varying offsets and how directivity influences in its amplitudes are crucial for a successful adoption of DAS in permanent monitoring.

I show the results of a field trial at the CO2CRC Otway site where VSP data were acquired using both 3-C geophones and DAS cables cemented behind the casing with offset to shot point positions varying from 50 m to 1.8 km. DAS was acquired using a standard single-mode fibre and a new type of fibre with enhanced backscatter.

For near offsets, both DAS systems show similar S/N, with geophones being approximately 12dB higher. This comes with the same source effort used for DAS and geophone acquisition (same number of shots required for the full geophone VSP by moving the seismic string were used to stack DAS data). If we decrease the number of shots on DAS to mimic the number of shots recorded by geophones at each level, the difference would be greater. However, S/N on DAS data is high and the record is visually similar to the geophone record. An important aspect is that, due to the higher spatial sampling, DAS data might provide more detailed velocity information compared to geophones.

S/N for the single mode fibre decreases significantly at far offsets, where it shows a loss of 20 dB at 1025 m distance compared to Constellation, where it remains high at far offsets. Although noise in single mode fibre was significantly higher, reflected waves are well pronounced on all DAS records. There is no doubt that the DAS data can be used for imaging and monitoring purposes. It is also obvious that for the very far offsets (SP6, 1.8 km) reflected waves are better captured by DAS compared to geophones due to higher spatial sampling.

In conclusion, from our prospective, data acquired with fibre optic sensors deployed behind the casing potentially outperforms geophone data for seismic monitoring applications. This is largely valid for both standard single mode and Constellation fibres, but the latter clearly provides higher quality data for the large offsets/incidence angles. However, in many cases deployment of the fibre-optic cable behind the casing is not viable (for instance when the well is already drilled, or there are risks of compromising a newly drilled well integrity by deploying equipment behind the casing). I believe these are the cases where impact of such fibre with higher sensitivity will be the greatest.

To establish an accurate comparison, we have proposed a filter that converts DAS data to geophone equivalent. There are many ways one can convert the DAS data; the conversion presented here was derived from the theoretical response of DAS sensors. The main difference between the conversion done by time-integrating the data and by the filter is that the filter converts for polarity of the upgoing wavefield. After conversion with the filter, DAS signature becomes very close to the geophone signature, correcting for polarity differences of the upgoing and downgoing fields. Such conversion is also necessary when using DAS in applications that require particle velocity response, such as in standard Full Waveform Inversion.

7.2 Permanent reservoir monitoring with orbital vibrator

Onshore seismic monitoring applications ideally involve the deployment of seismic receiver arrays and mobile sources to image the subsurface. Time-lapse surveys rely on accurate positioning source points and receivers to monitor the changes in the reservoir. Common land access issues and the imprecise positioning of seismic equipment might result in significant and irreversible time-lapse signal loss. Furthermore, reservoir monitoring requires significant labour as a large amount of seismic equipment needs to be deployed, and then retrieved on every survey. Permanent reservoir monitoring seeks to overcome the limitations of the conventional approach by fixing either the seismic receivers, sources or both. In CO2CRC Otway project, the use of DAS combined with permanent SOVs is optimised to acquire high quality time-lapse seismic data at relatively low cost and a minimum land impact.

Due to the long-life of the fibre cables and their inherent affordability compared to conventional seismic sensors, the permanent installation of such acoustic receivers is becoming significantly more attractive and viable.

To reduce the cost and environmental impact compared to vibroseis sources, permanent installation of SOVs can be utilised in monitoring surveys. SOVs consist of common AC induction motors. They produce vibrations as an effect of the rotation of eccentric weights, which produces both a vertical and horizontal shear force. The force of the source increases as frequency squared. With their low production and operating cost and adequate force, SOVs can be a good alternative to a common

seismic source. Yet, they have not seen widespread adoption, but only have been explored for niche applications as seismic sources (Daley and Cox, 2001).

In 2016, Freifeld et. al. presented an initial look at DAS/SOV data collected with an aerial DAS/SOV array at the CO2CRC Otway Project site. Clear reflections were visible on the surface fibre, and an initial review of VSP data showed that the tubing deployed DAS cable exhibited poor S/N performance. In this chapter, I present the analysis of a follow-up study at the CO2CRC site using a series of VSP acquisitions performed using a DAS cable cemented behind casing in the CRC-3 well. To compare the impact on data quality, I analyse two distinct SOVs with different power and frequency settings.

Subsection 7.2 contains work submitted for publication in (Correa et al. 2019b).

7.2.1 Field experiment with DAS and SOV sources at Otway

The field experiment was designed in order to test the performance of SOV sources in conjunction with cemented DAS in CRC-3. The field trials should test the imaging capabilities of DAS/SOV in relation to the target horizons (1500m) by testing the performance of a series of OVSP surveys acquired with a standard single-mode fibre and the "enhanced fibre". Additionally, the field trial aims to test different SOV source types and sweep designs in order to come up with the optimum parameters for imaging in Otway.

Two field trials were conducted with DAS and SOV sources (see Chapter 3 for location of the sources). The first field trial was conducted in May 2017 with the objective to compare DAS VSP acquired with a standard fibre and enhanced fibre using the SOV sources. During the first field trial, DAS VSP was acquired using the longer fibre cable (maximum depth 1660 m) in the CRC-3 well. Two DAS interrogator units were used in the trial; DASv2 was acquiring data from the standard fibre cable, and DASv3 was acquiring data from the "enhanced" cable. SOV1 and SOV2 sources (with large motors) were used in the acquisition. The sources were set to produce sweeps of 155 seconds (30s upsweep, 5s hold, and 120s downsweep), from 0 to 80 Hz (Table 7.1), which produce approximately 10 t force at maximum frequency. SOV1

source is located at ~630 m from the well, and SOV2 is located at ~380 m from the well.

The objective of the second field trial, conducted in November 2018, was to test source sweep designs in order to decide on optimal parameters to be used during the future monitoring program. DAS VSP was acquired using the shorter cemented cable, where a standard single-mode fibre was connected to the DASv2 interrogator unit, at 0.5 m spatial intervals. Two different motors were used for SOV1 and SOV2 – small and large motors. Large motors are capable of spinning to at least 80 Hz and produce approximately 10 t force at 80 Hz, smaller motors can achieve frequencies of 160 Hz or more and provide approximately 4 t force at maximum frequency.

SOV1 was set to produce sweeps from 0 to 80Hz using large motors (30% peak force setting corresponding to ~10 t force), and from 0 to 120 Hz using small motors at their 50% peak force setting. SOV2 was set to produce sweeps also from 0 to 80Hz with large motors, and with small motors from 0 to 120Hz, and from 0 to 160Hz, both at 50% peak force (Table 7.2). Multiple sweeps for each sweep setting were acquired.

Table 7.1 Acquisition parameters for May 2017 field trial.

SOV 1	**SOV 2**
Large motors, 0 – 80Hz	Large motors, 0 – 80Hz

Table 7.2 Acquisition parameters for November 2017 field trial.

SOV 1	**SOV 2**
Large motors, 0 – 80Hz Small motors, 0 – 120 Hz; 50% peak force	Large motors, 0 – 80Hz Small motors, 0 – 120 Hz; 50% peak force Small motors, 0 – 160 Hz; 50% peak force

7.2.2 Offset VSP processing

The processing flow applied to the OVSP acquired with DAS and SOV sources consists of basically three main stages (Table 7.3). The first stage aims to deconvolve the data with source wavelet; the second stage performs wavefield separation to obtain the upgoing P-waves; the third stage performs migration of the upgoing P-waves.

When using conventional source that generate a sweep signal, usually the data acquired is correlated with the source wavelet to obtain a zero-phase broadband wavelet. Due to the unbalanced frequency spectrum of the orbital vibrators, where the force increases as frequency squared, if the source sweep is autocorrelated, the resulting frequency spectrum has amplitudes increasing with fourth power of the frequencies. This yields a wavelet with pronounced side lobes. To reduce this effect, the sweep signal is deconvolved (division in frequency domain) with the record, which compresses the amplitudes and reduces wavelet sidelobes (Daley and Cox, 2001). The deconvolution of acquired datasets and source sweeps is performed using a MATLAB script.

After deconvolution, the resulting datasets are loaded to RadExPro seismic processing software. For each sweep, the position of the centred mass in the source starts at a different position, which results in sweeps that are slightly out of phase. Therefore, each sweep had statics applied and then they were stacked in order to increase signal and reduce random noise. The stacking of sweeps increases the S/N. For the May test, SOV1 and SOV2 were stacked with 14 repeated sweeps in each direction of rotation. For the November test, DAS datasets with large motors were stacked with 10 repeated sweeps, with small motors of maximum sweep frequency of 120 Hz - 16 repeated sweeps were stacked, and for small motors of maximum sweep frequency of 160 Hz - 5 repeated sweeps were stacked. After stacking the sweeps, the geometry for each dataset was assigned where each trace was given a depth and geographical position. A band pass filter was applied to the data, passing the dominant frequency band of the respective sweep.

In the next step, wavefield separation was applied in the dataset using FK filter to suppress the downgoing wavefield. An extra pass of FK filter was applied in order to filter S- and PS- upgoing waves. The amplitudes were then corrected for spherical

divergence by multiplying the amplitudes by the time squared. The upgoing filtered P-waves were reduced to a 5 m spatial interval by stacking adjacent traces, and then they were NMO corrected using a one-dimensional velocity model, through the VSP-CDP-Transform. The NMO corrected dataset was then migrated by using Kirchhoff OVSP migration algorithm.

Table 7.3 OVSP processing flow.

Process	**Parameters**
Data Input	Data measured is the strain rate equivalent.
Deterministic source signature deconvolution	Deconvolution with source sweep. Added 0.1 white noise.
Source statics	Correct source delays.
Stack of multiple sweeps	Stack sweeps and average (mean).
Geometry assignment	Assign coordinates
Bandpass filtering	8-14-50-82 Hz for sweeps up to 80 Hz (8 -14-100-122 for sweeps up to 120 Hz; 8 -14-120-160 Hz for sweeps up to 160 Hz).
Wavefield separation (FK filter)	Select downgoing waves (positive wavenumbers).
S- and PS-waves attenuation	Separate using FK filter.
Amplitude correction	Multiplied by time. Two passes.
VSP-CDP-Transform OR Kirchhoff VSP migration	Depth from 0 to 2600, every 1 m. Preferred boundary slope equals to 0. Preferred slope range equals to 5.

7.2.2 Analysis of data acquired in May field trial

The use of DAS combined with SOV sources has an enormous potential in permanent reservoir monitoring applications as it offers reduced environmental and social impact, while imaging the development of the injected gas. However, it is

important to address issues, such as lack of higher frequencies and poor sensitivity that often hinder the broader use of the DAS method.

For this purpose, I analyse the data quality of the VSP acquired by DAS with both SOV sources deployed on site (Figure 7.7). To compare both DAS systems, a band pass filter was applied on all shots to select frequencies from 5 to 140 Hz (filter tapered from 5 to 10 Hz, and from 80 to 140Hz). Each display shows a stack of 14 repeated shots. Figure 7.7(a – d) shows the VSP data acquired for SOV1, at 630 m distance from the well. The VSP data acquired with the enhanced cable (a – b) presents less random noise when compared to the standard single-mode fibre (c – d), probably due to the stronger signal amplitude in relation to noise. The enhanced fibre is engineered to increase light backscatter, which results in stronger seismic amplitudes. The enhanced fibre presents a set of traces, at depth of approximately 1390 m that was damaged during the manufacturing process. The standard fibre was able to detect the same P-wave reflections presented on the enhanced fibre, though, with higher level of random noise. Additionally, for direction 1 and direction 2 of the source sweeps, the recorded reflections present slightly different signature (mostly seen on the recorded S-waves), which suggests directions are not repeatable.

During VSP-CDP-Transform (often referred to as ‘mapping’), the reflected energy is relocated to the position on the image which would correspond to the location of the reflection point in a 1D velocity model. However, unlike in migration, no summation over the travel time curves of diffracted waves happens at this stage. Figure 7.8 shows the results of application of VSP-CDP-Transform for each dataset. Both directions were stacked after the transform. The 2D line produced for each source is displayed side by side; the well location is where both lines meet. Note that the reflections on the 2D line for SOV1 match well with the reflections for the 2D line for SOV2, for both the enhanced fibre (Figure 7.8a), and the standard fibre (b). The standard fibre shows a higher level of random noise at the end of the record.

The results of the Kirchhoff migration are presented in Figure 7.9. The 2D lines show smooth reflection with minimum noise, due to the stacking effect of the migration algorithm. The lines recorded by the standard fibre (Figure 7.9b and d) match well with the reflections recorded by the enhanced cable (Figure 7.9a and c).

After VSP-CDP-Transform, each 2D line produced was converted form depth to time (Figure 7.10). The 2D line generated from SOV1 source shows a good match with a previously acquired crossline from the conventional surface geophone survey (Monitor 5). The match is more profoundly observed at approximately 500 ms, 600 ms, 1100, and 1200 ms, the last coinciding with the time relative to the injection interval. The 2D line, however, presents low frequency character, as a result of the source sweeps maximum frequency of 80 Hz. Although, the migrated 2D line presents good quality signal, low levels of noise, and good match with the conventional data, the line produced from a single SOV source has a narrow illumination pattern of up to approximately half a distance between the well and the source. This imposes a limitation on the application of using DAS/SOV for 3D plume monitoring, given a limited amount of possible sources and wells on site.

Figure 7.11 shows the 2D line for SOV1 acquired by the standard fibre after VSP to CDP transform. Note that, despite the high level of random noise present on the shot record for the standard fibre, the reflections also correlate well with the crossline from the conventional data. Reflections seen on the standard fibre are similar to the reflection seen on the enhanced fibre. However, it is possible to observe strong random noise away from the well at the end of the record, from 1500 ms. Nonetheless, the standard fibre is also able to image reflection from the injection interval.

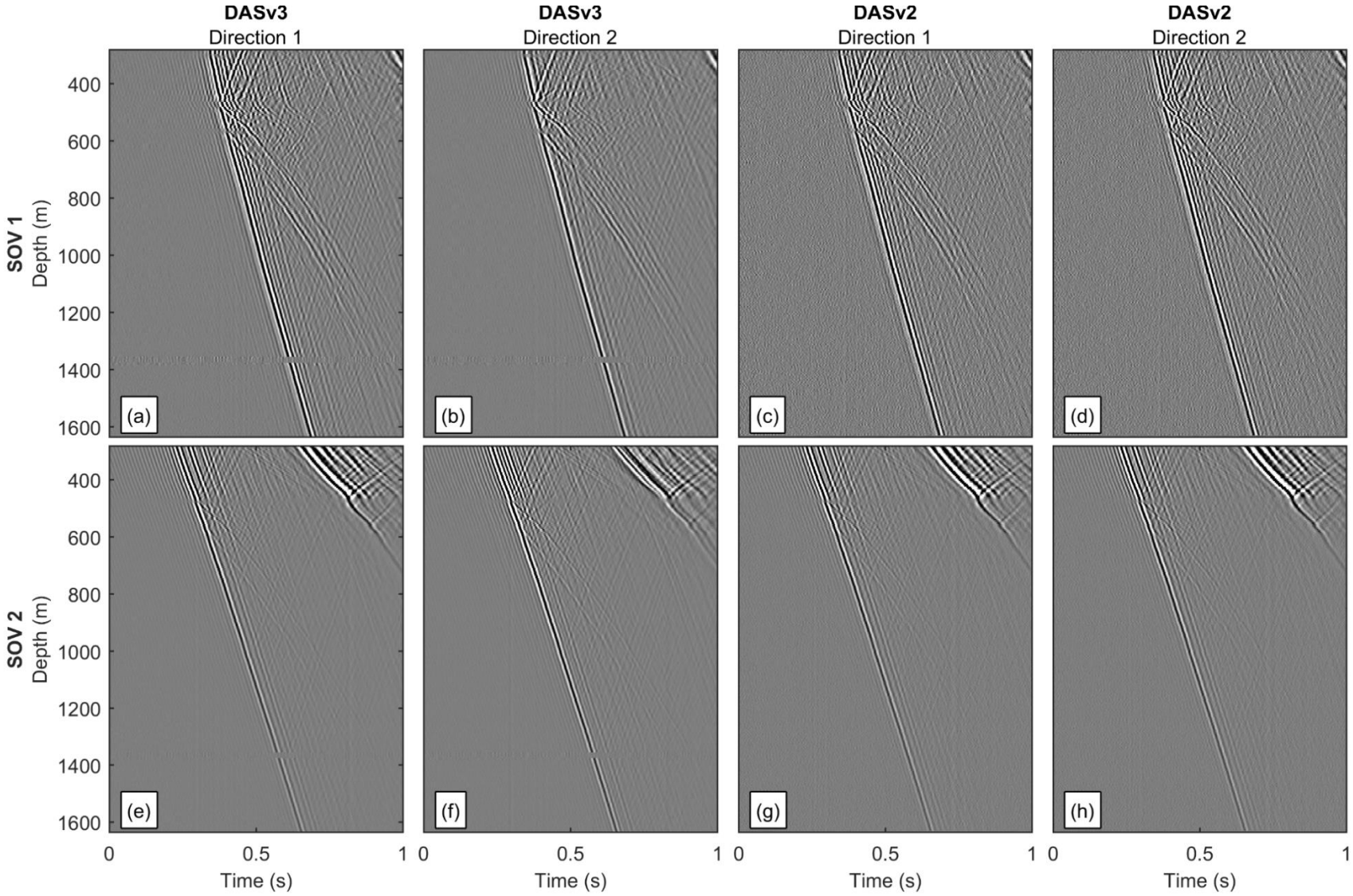

Figure 7.7 VSP records acquired for SOV 1 (a – d), and SOV 2 (e – h), stack of 14 sweeps.

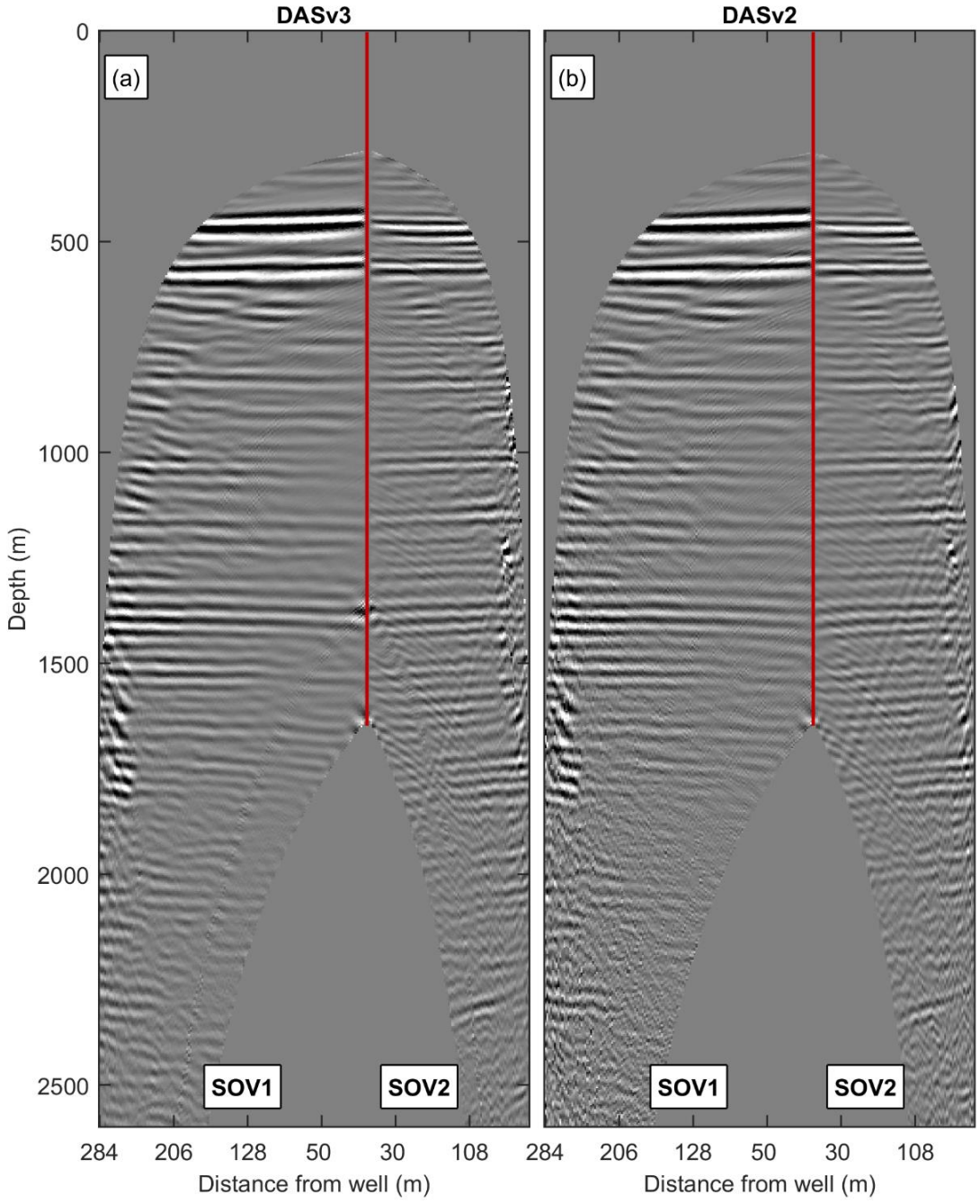

Figure 7.8 VSP-CDP-Transform for DASv3 (a) and DASv2 (b). The 2D line correspondent to SOV1 and SOV2 are displayed side by side. Well path displayed in red.

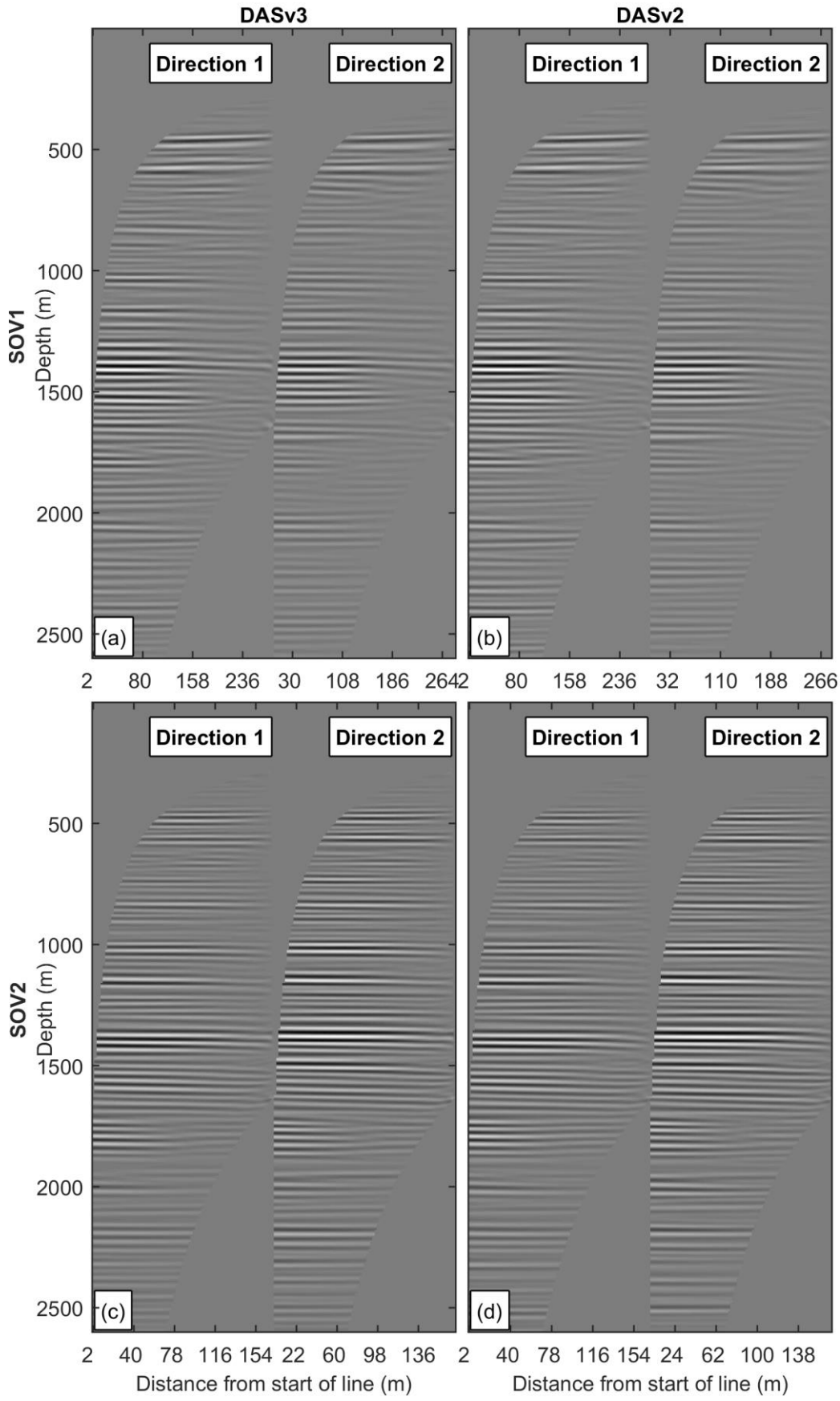

Figure 7.9 Migrated 2D lines for direction 1 and direction 2 for each test.

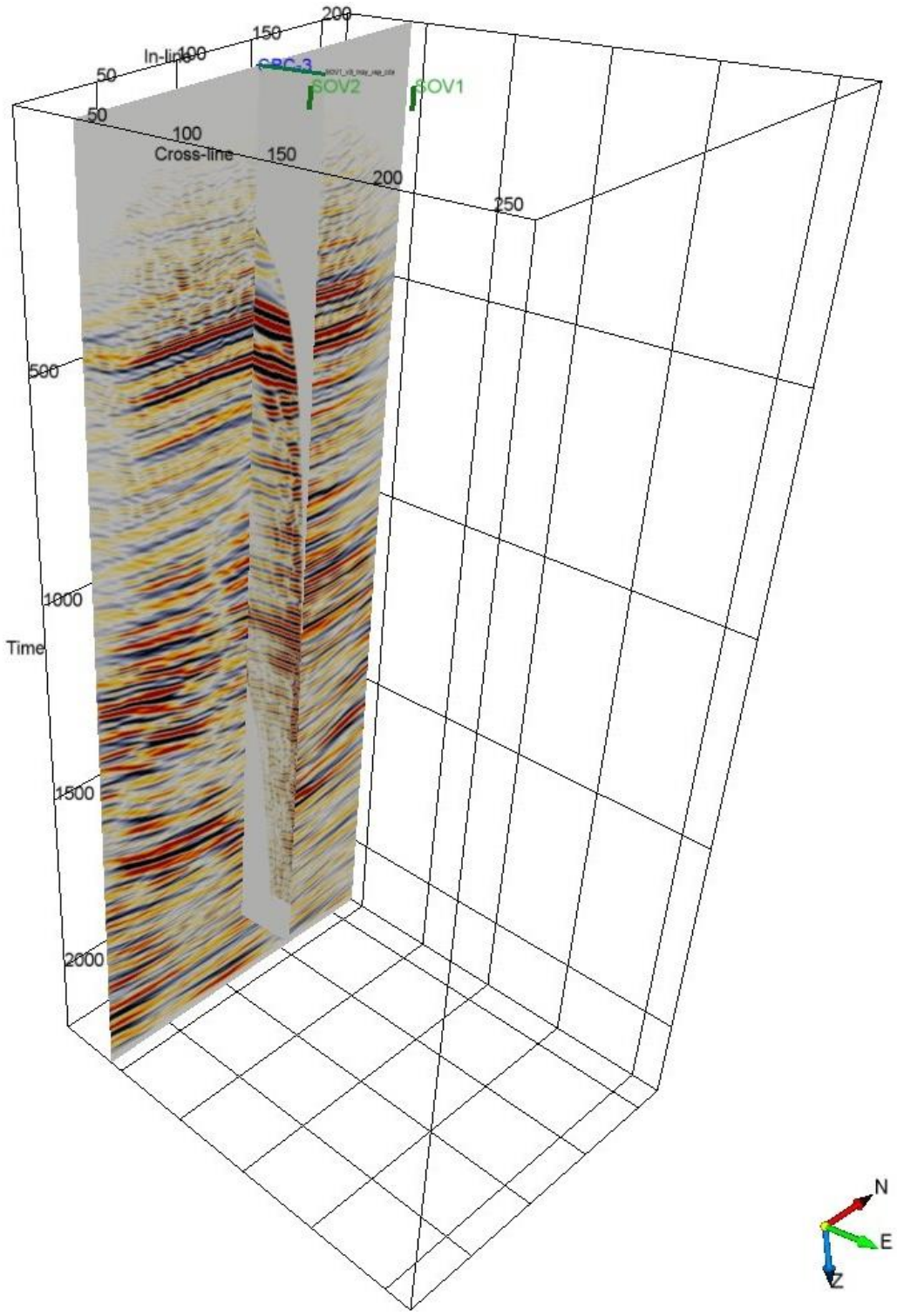

Figure 7.10 DAS/SOV 2D line acquired with the enhanced fibre (DASv3) after VSP-CDP-Transform (shorter line). The displayed crossline is migrated from the surface geophone Monitor 5 data.

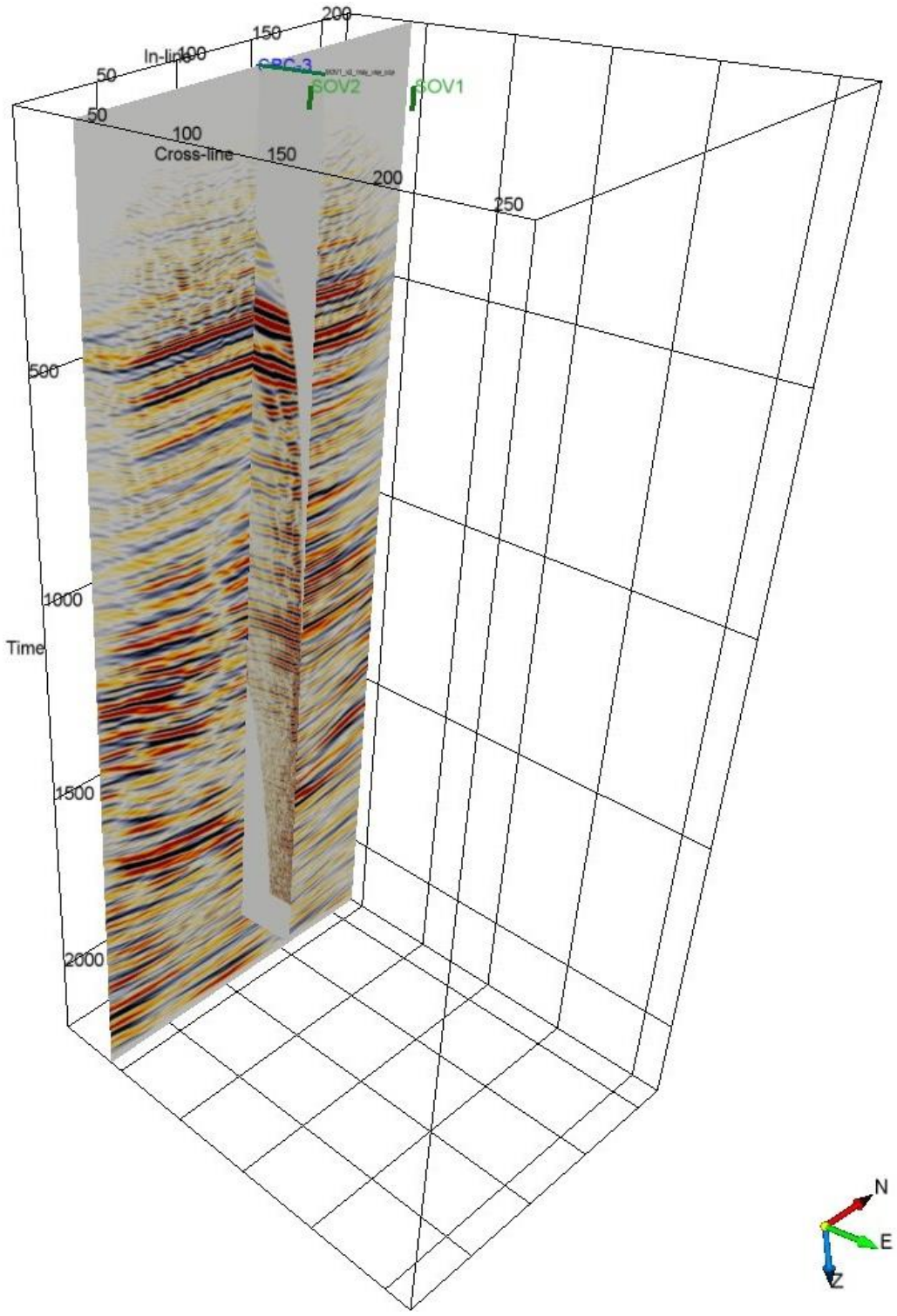

Figure 7.11 DAS/SOV 2D line acquired with the standard single-mode fibre (DASv2) after VSP-CDP-Transform (shorter line). The displayed crossline is migrated from the surface geophone Monitor 5 data.

7.2.3 Analysis of data acquired in November field trial

In order to find an optimal configuration for DAS and SOV surveys, a series of DAS VSP acquisitions were performed using the standard straight fibre-optic cable cemented behind the casing of the CRC-3 well. As the acoustic source signal, we use two permanently installed SOV sources, testing a range of sweep designs using large and small motors.

The force of the sweep on SOV sources is proportional to the frequency squared. This means that the force on the low frequencies of the sweep is much lower than the force at the high frequencies. To overcome this issue, the SOV sources were tested using a larger motor, which will consequently increase the force. However, on large motors, the SOV sweeps should only go up to approximately 80 Hz, as beyond this frequency the amount of force produced might become a safety hazard. To overcome the lack of high frequencies in the data, we tested sweeps using small motors, varying frequencies to up to 160 Hz.

DAS was able to acquire upgoing P-wave reflections and S-waves using all sweep designs (Figure 7.12). As expected, the large motors provide stronger signal with better defined reflections than the small motor. The quality of the datasets decreases significantly when using smaller motors,. However, DAS was still able to record P-wave reflections, even at a long distance from the source (Figure 7.12b). Although the large motors provide higher quality datasets due to the bigger strength of the forces, the higher frequency of the small motors increases considerably the resolution of the records.

The S/N was calculated by dividing the RMS amplitude of the record in a window around the first breaks with the RMS amplitude of a window of noise at the start of the record. The large motors provide the highest S/N, reaching approximately 20 dB at both locations. This is a promising result considering that geophones VSP acquired at a similar offset (600 m) using vibroseis sources show approximately 50 dB S/N (Correa et al., 2017a). Due to the weaker force, small motors provide lower S/N, by approximately 5 to 10 dB.

Each test was processed through the same seismic processing flow (Table 7.3). The VSP-CDP-Transform data for direction 1 and direction 2 were stacked to form a

single line. The sweep tests from 0 to 80 Hz (Figure 7.13a) record the P-wave reflections clearly, and both lines, for SOV1 and SOV2, match well. When the sweep frequency ranges from 0 to 120 Hz, DAS senses reflections up to approximately the target depth of 1500 m, however, due to the low power of the source, the dataset is noisy (Figure 7.13b). The test using sweep from 0 to 160 Hz was only acquired using SOV2, and, even at a near offset, the source power is not sufficient to image beyond 800 m.

The migrated line of the sweep tests up to 120 Hz (Figure 7.14b and d) shows better resolution than the sweep up to 80 Hz, as expected. Migrating the 120 Hz sweep test data improves the imaging range to 1600 m depth (Figure 7.14a and c). While the 160 Hz sweep tests data (Figure 7.14e) are able to detect reflections from target depth of 1500m, the reflections are influenced by noise content present in the raw data.

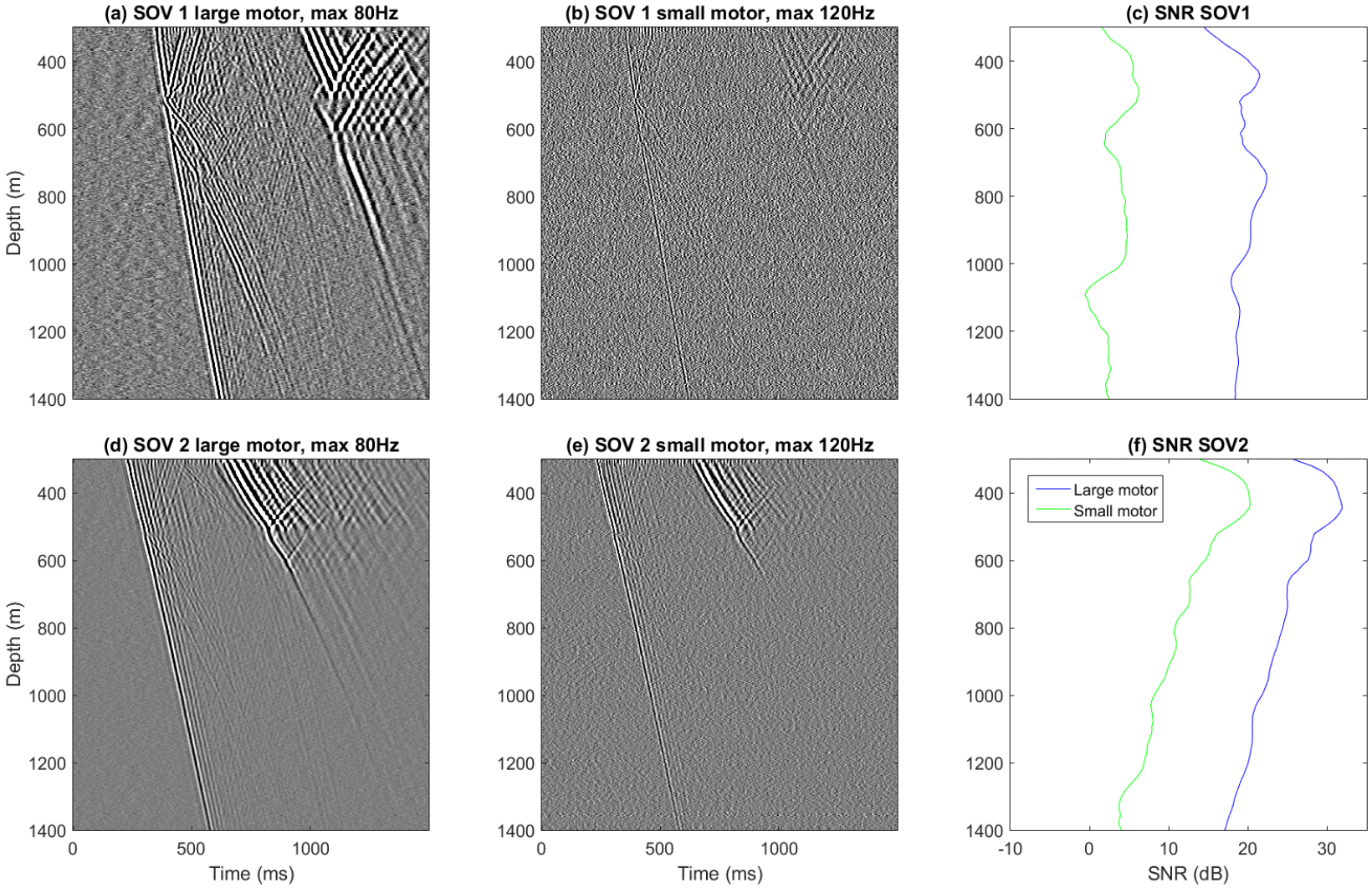

Figure 7.12 VSP acquired with DAS using large motor and small motors on SOV1 (a,b) and on SOV2 (d,e). S/N was calculated for DAS with SOV1 (c) and DAS with SOV2 (f).

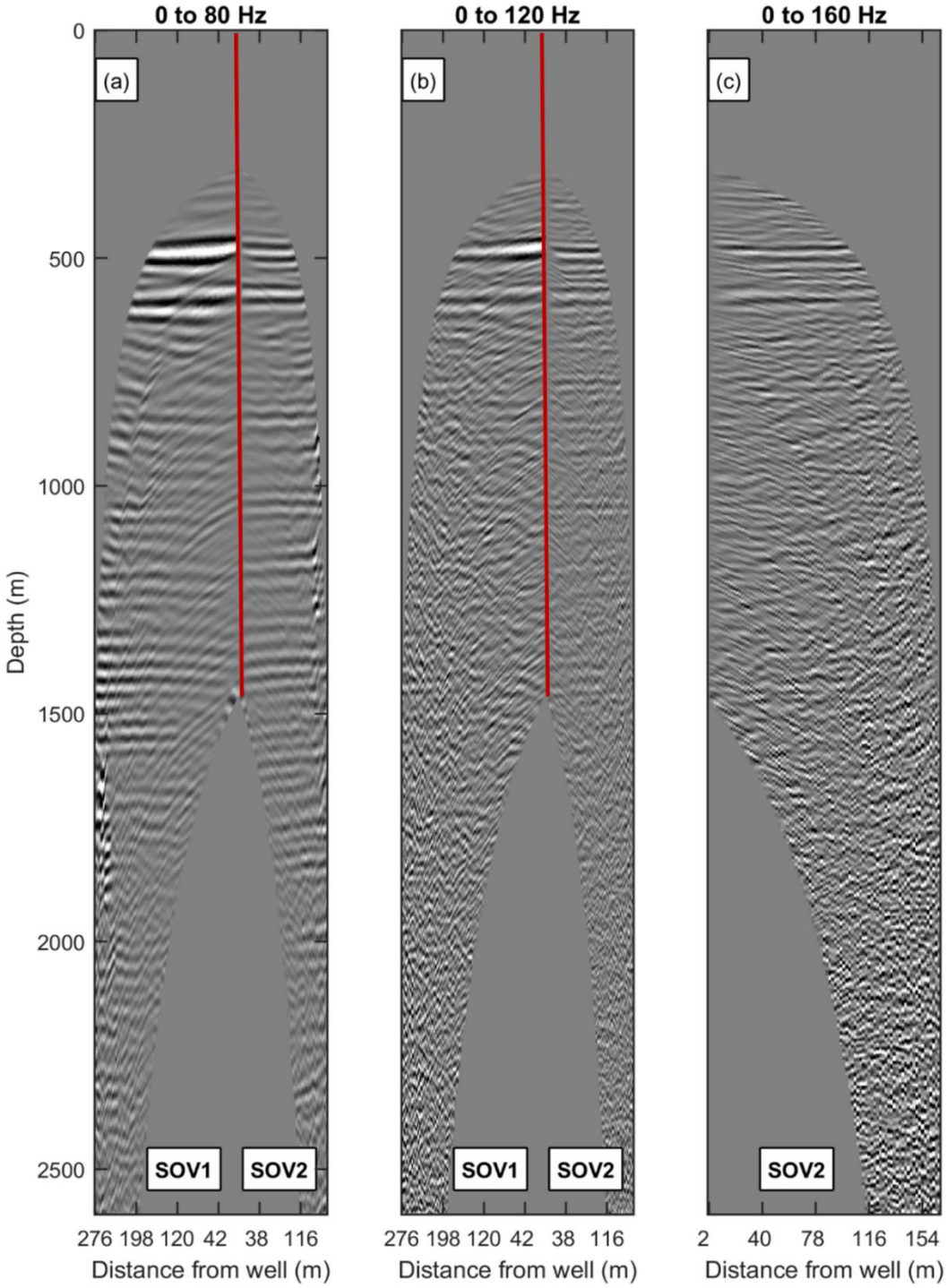

Figure 7.13 Results of VSP-CDP-Transform for test with sweeps from 0 to 80 Hz, large motors (a), from 0 to 120 Hz, small motors (b), and from 0 to 160 Hz, small motors (c). The 2D line corresponding to SOV1 and SOV2 are displayed side by side. Well path is displayed in red.

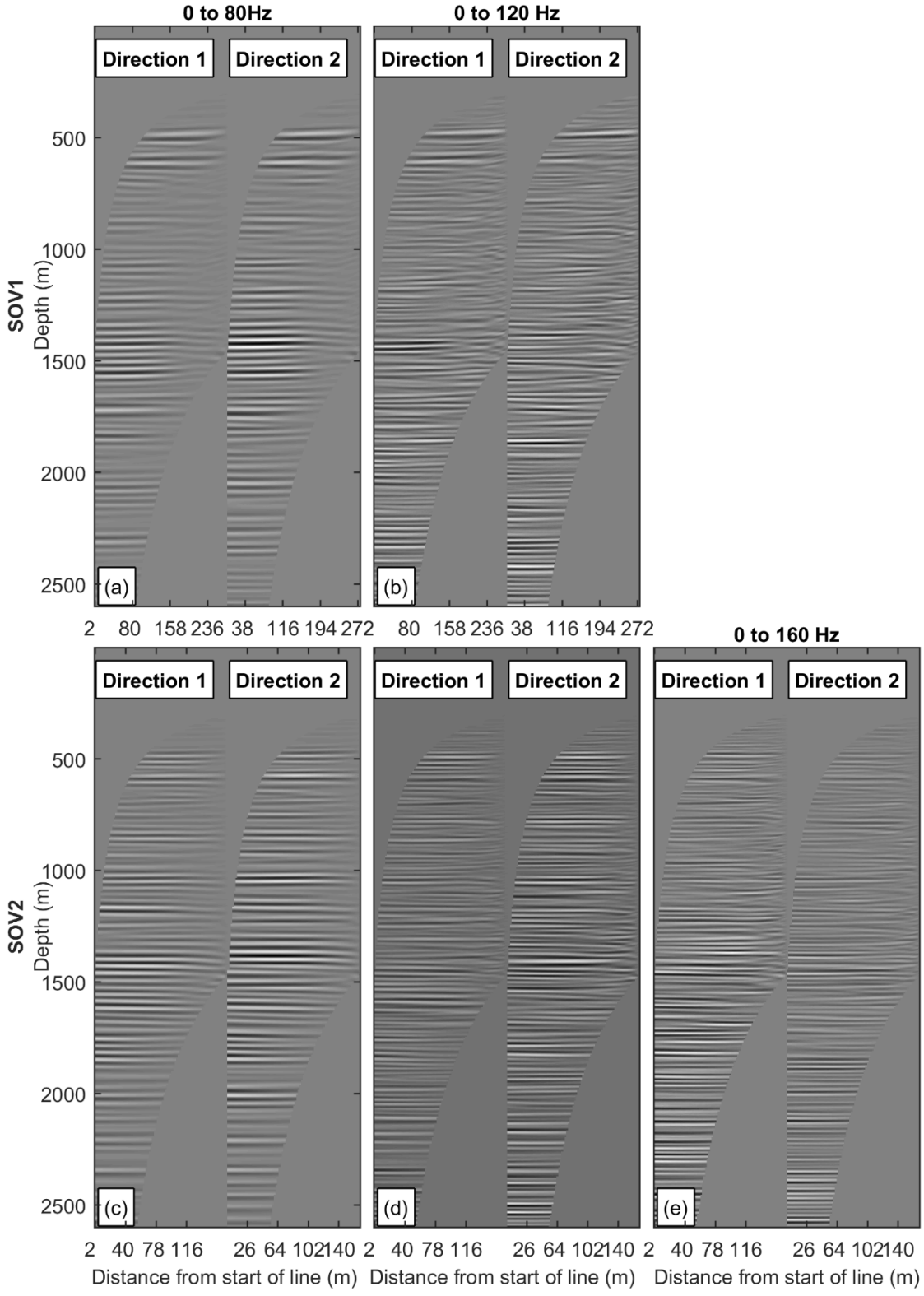

Figure 7.14 Migrated 2D lines for direction 1 and direction 2 for each test.

7.2.4 Conclusions

Restricted land accessibility, poor repeatability and long survey durations are common issues that limit permanent reservoir monitoring applications. I present an efficient alternative methodology for permanent reservoir monitoring using DAS and permanently installed sources SOV. The use of DAS in conjunction with SOV sources provides the possibility to acquire good quality time-lapse VSP surveys with almost no mobilisation effort. In order to test for an optimal DAS/SOV configuration, two VSP surveys were acquired using cemented fibre-optic cables at two offset location using SOV sources, at ~380 m (SOV2) and ~630 m (SOV1). The first field trial assessed the performance of DAS/SOV using a stand fibre-optic cable and an "enhanced" sensitivity cable. The second field trial aimed to test for optimal performance of the source by acquiring a range of sweeps with large and smaller motors, from maximum frequency of 80 to 160 Hz.

The results show that VSP data acquired with DAS using a cemented cable and SOVs yields high quality datasets, sufficient to image the injected gas plume. At both locations DAS was able to acquire upgoing P-wave reflections. DAS acquired with the enhanced fibre shows lower levels of random noise compare to the standard fibre. Nevertheless, the standard fibre was able to record the same P-wave reflections (while using larger motors). After migration, the 2D line acquired with the standard fibre presents similar quality as the 2D line acquired with the enhanced fibre due to the stacking performed through migration.

The large motors provide higher signal levels due to the higher source power than the small motors. Due to the higher frequency content, small motors provide better resolution. Both sweeps from up to 80 Hz and up to 120 Hz were able to record reflections from the target depth at 1500 m at the nearest offset (SOV2).

CHAPTER 8 3D VSP USING FIBRE OPTIC CABLE CEMENTED BEHIND THE CASING

In this chapter, I present the results from a 3D VSP survey acquired using a cemented single-mode fibre-optic cable, as part of Stage 3 of the Otway Project. I focus on the data processing and imaging of the 3D VSP data with the cemented DAS. I investigate the imaging limitations of the 3D VSP acquired with DAS by analysing the quality of DAS data in relation to offset and angle, as well as assess a migrated image line from the DAS data sets.

This work was published as an extended abstract in (Correa et al., 2018).

8.2 Data acquisition during the Monitor 5 survey at the Otway Project

The 3D VSP data was acquired in the CRC-3 well, simultaneously with the 3D surface seismic survey (buried geophone array) as part of the Monitor 5 acquisition. The CRC-3 well is instrumented with two fibre-optic cables, cemented behind the casing. One cable is deployed to the total depth of 1668 m. It has 3 single-mode cores, 2 multi-mode cores and one special high-sensitivity single-mode core. Pairs of cores are meant to be looped back at the bottom through the optical turnaround, however the turnaround was damaged during the installation. The second cable is deployed to 1450 m, just above the shallowest prospective perforation interval. This cable has 4 single-mode and 2 multi-mode fibre-optic cores. Corresponding pairs of fibres are connected at the bottom through a turnaround.

The 3D survey was acquired using two 26,000 lbs Inova vibroseis trucks. A vibroseis truck was generating a single linear 24 s sweep 6-150 Hz per source point position. Approximately 4800 shot points were acquired (Figure 8.1). As mentioned above, the 3D VSP survey in CRC-3 was acquired simultaneously with the fifth monitor survey. The fifth monitor survey is acquired in combination with the 3D surface seismic and 3D VSP survey in CRC-1 using an 8-level 3C geophone shuttle (1 geophone per level/per component) deployed at 760-865 m MD with 15 m receiver spacing.

In the CRC-3 well, two 3D VSPs were acquired using two interrogator units (from different manufacturers), connected to one single-mode fibre from each cable. Channel spacing on both interrogators was approximately 0.5 m. In addition to DAS, a single high-sensitivity (4 geophones per level per component) 3-component geophone shuttle was deployed at 775 m MD at the CRC-3 well. The purpose of this geophone tool was to provide a basis for comparison with single sensor tool used in this well in previous surveys, as well as acquiring high quality reference data for future interferometric analysis of DAS data.

In this chapter, I focus on the processing and imaging of the 3D VSP acquired with DAS in the CRC-3 well. A Silixa iDAS version 2 interrogator unit was used to acquire the strain data from a standard single-mode fibre in the CRC-3 well using the longer cable.

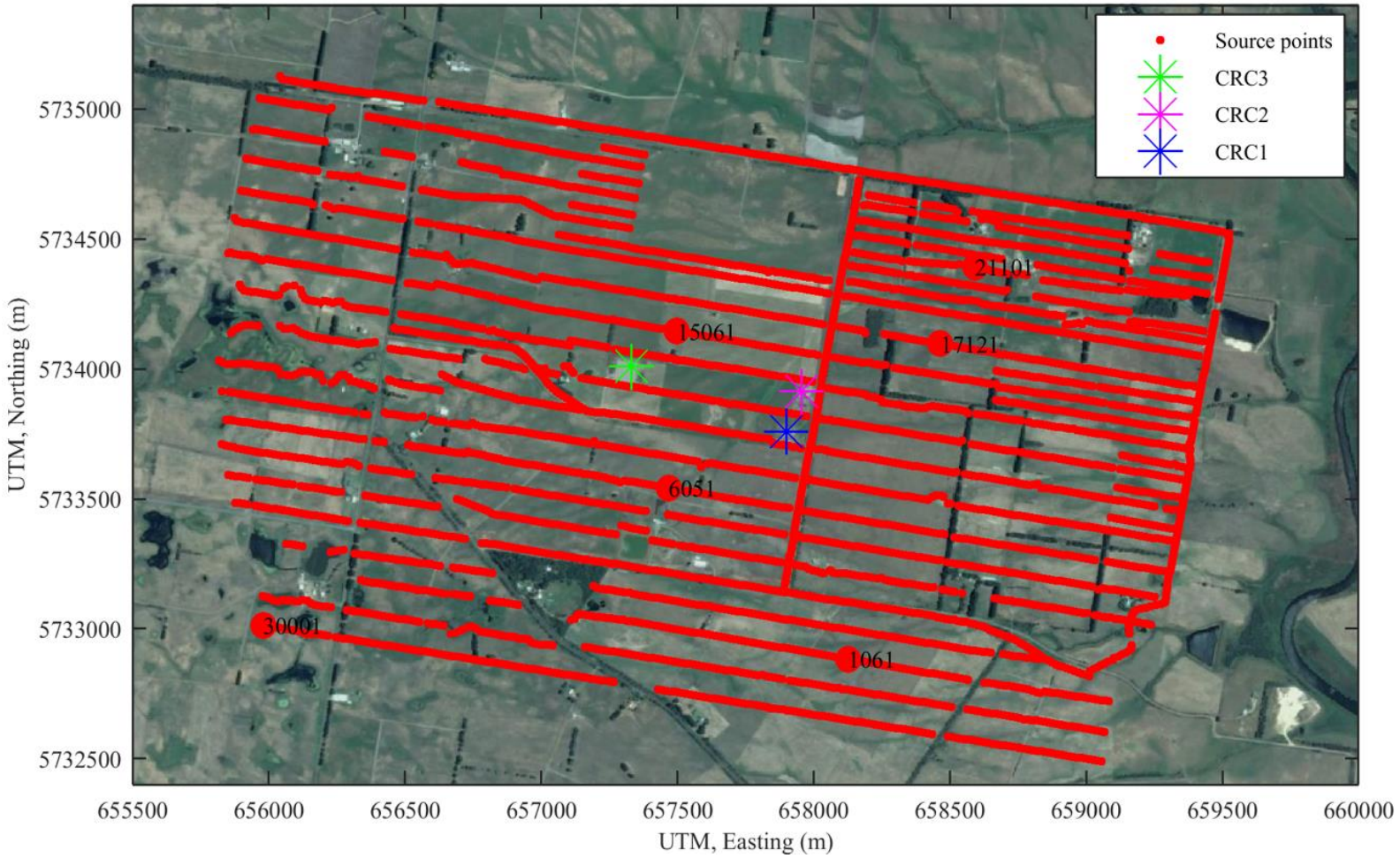

Figure 8.1 3D seismic survey geometry. Approximately, 4800 source points were acquired (red). Featured shots are displayed in Figure 8.2.

8.3 Data quality

Cemented fibres provide optimal coupling, thus higher S/N compared to other deployment types, such as cable on production tubing (Li et al., 2015). The 3D VSP acquired with a cemented fibre in the CRC-3 well shows clear P-wave reflection with low levels of noise (Figure 8.2). P-wave reflections can be seen throughout the well even for a far offset, above 1600 m. The datasets present strong background noise, which is observed also in near offsets. Most of these noise patterns can be characterized as random noise, as well as "striped noise" observed with infinite velocity (also known as common mode noise). Additional to P-wave reflections, DAS is able to record PS-waves in some instances, especially at 500 m depth, as well as S-waves at near offsets. Note that, for far offsets, the direct arrivals are almost non-existent due to the directivity pattern of DAS. Overall, single shots recorded by DAS VSP in the CRC-3 well are of satisfactory quality.

To quantify the level of signal and noise present in the dataset, I calculate the S/N from source lines 1 to 29, totalling approximately 3000 shots. The S/N for the VSP data was calculated by dividing the RMS amplitude of a 20 ms window around the first breaks with the RMS amplitude of a 100 ms window of noise at the beginning of the record. The calculated S/N is then binned in 1 degree segments of incidence angle and every 20 m distance from a shot to receiver. Figure 8.3a shows the calculated S/N for the cemented DAS with respect to an incidence angle and distance of a receiver from a shot position.

S/N tends to decrease with increasing angles of incidence and an offset, as expected. When offsets are larger than approximately 1000 m, S/N decreases to approximately 0 dB at the shallowest parts of the well (~ 70 ˚ angle of incidence). This occurs due to the directivity pattern of DAS. S/N of 0 dB or lower means that the signal level is equal or below the noise level. Such low S/N happens from angles of incidence above approximately 75^{o} and distances above of approximately 2000 m. The calculated S/N is derived from a single shot; this could be improved by stacking repeated sweeps, using a stronger source, or increasing the brightness of the light in an interrogator unit (IU).

Figure 8.3b shows the calculated S/N of a 3D VSP previously acquired with DAS on tubing in CRC-2. This dataset was acquired during the fourth monitor survey using the buried receiver array, which has a total length of approximately 20 km of fibre (see Chapter 6). The S/N for DAS in CRC-2 was calculated over the same lines and using the same binning as S/N for cemented DAS in CRC-3. When comparing the S/N for the cemented DAS and the tubing deployed DAS, it is noticeable that the cemented deployment provides better S/N, as expected. However, they both show a similar region where DAS records no signal (dark blue).

The difference between the S/N for the cemented and tubing deployment was also calculated (Figure 8.3c). The improvement given by the cemented fibres is roughly of 10 to 15 dB, on areas as DAS is able to record signal. The dark blue area shows where DAS was unable to record signal either for cemented or on tubing fibres. This means that the acquisition range of cemented DAS did not improve significantly in comparison with tubing deployment. Note that the length of the fibre in the tubing deployment is approximately 7 times longer than on the cemented, which decreases the laser repetition rate and possibly influences negatively on the S/N. Therefore, the difference in S/N between the cemented and tubing deployment could be decreased by comparing between similar fibre lengths.

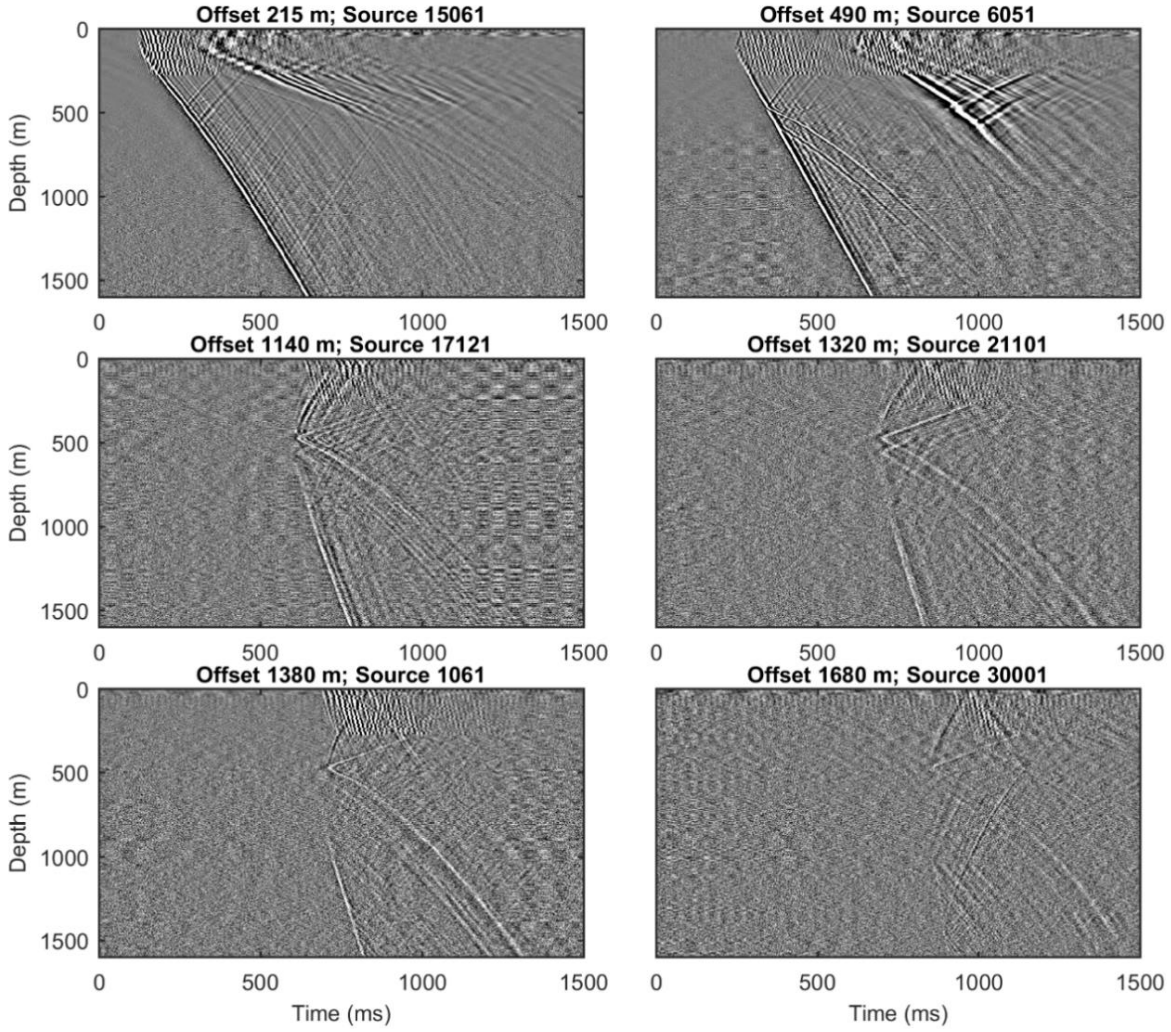

Figure 8.2 Raw shot examples acquired by DAS VSP (cemented fibre). Shots displayed have offsets varying from 215 m to 1680 m distances.

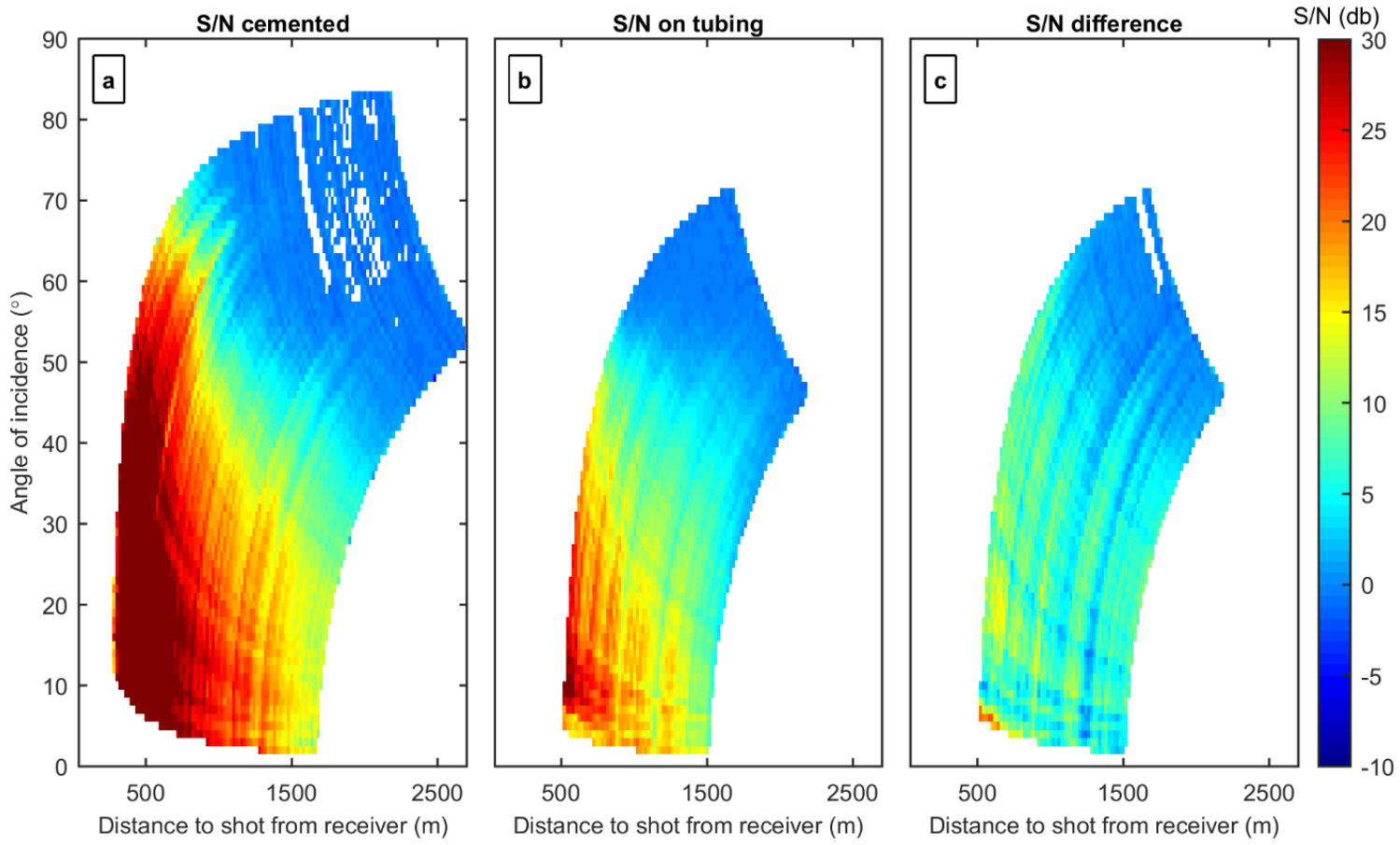

Figure 8.3 S/N calculated for cemented DAS (a), DAS on tubing (b), and the calculated difference between both (c).

8.4 Data processing

Following the same process as described in the previous chapters, the field data were acquired in strain rate and converted to strain by integrating in time. The strain response was correlated with the sweep and saved to SEG-Y format. To match source geometry, I use GPS time stamps available for each shot records and compare them across DAS and geophone surveys.

The correlated SEG-Y files were loaded into a seismic processing software (RadExPro), where depth was assigned to DAS traces. Assigning the receiver geometry to DAS traces is still a problematic step, as the trace positions recorded in the system are only relative to the fibre length (Ellmauthaler et al., 2016). To correctly assign depths to the same shot points for CRC-3, the May 2017 geophone survey was used where OVSPs were acquired for the entire well using geophones. I match the travel time curve from the geophone to DAS offset shots.

A simple noise attenuation flow was performed, where a band-pass filter from 8 to 150 Hz was applied. Additionally, a notch filter targeting a 25 Hz noise anomaly was also applied, followed by burst noise removal. To separate the upgoing wavefield, I use an FK filter. To decrease artefacts, AGC is applied prior to the FK filter and removed after.

After wavefield separation, the P-wave reflections are clearly visible on DAS data at offsets as far as 1680 m. Although 3D VSP was acquired with a single sweep per shot point, upgoing reflections are easily identified (Figure 8.4). Note that, at offset 1680 m, DAS was able to record a strong upgoing PP reflection from the target zone at 1500 m.

One of the advantages of acquiring VSP with DAS is the dense spatial sampling. However, the large amount of data can be difficult to manipulate and unnecessary at times. In order to decrease the amount of data and increase S/N, I stack the data in every 5 m depth. Additionally, I resample the data to 2 ms, also to reduce the size.

The upgoing wave went through additional processing to attenuate the PS-wave present in the data through FK filter. Also, the “striped noise”, commonly seen

on DAS, was removed through FK filter. I chose to mute the S-waves due to its complexity for the noise attenuation flow.

The upgoing P-wave processed data was migrated using VSP Kirchhoff migration. Due to the large volume of data, even after group stacking, the input was divided into ten subsections and migrated individually. Each subsection was grouped by randomly selected shots. Due to the high dependency of DAS amplitudes towards angles of incidence (Kuvshinov, 2016), we modify the migration operator to take into consideration the amplitude decay by dividing with cosine of the angle of incidence. A 7.5m x 7.5m grid was used for the migration, and 2 m depth step. The processes applied to the DAS data are described in Table 8.1. The migrated DAS VSP volume shows DAS was able to image reflections up to depths of over 2000 m, along almost 2 km of lateral distance (Figure 8.5).

DAS provides high quality VSP datasets suitable for imaging. Application of DAS technology is able to partially solve issues with the inefficient deployment of extensive receiver arrays. However, monitoring surveys are still associated with the application of large sources in dense geometries, which yields strong acquisition footprint. As part of this experiment, I test the efficiency of DAS when acquiring the data using smaller source efforts. For this, I migrate the data using 20%, 40%, 60%, and 80% of the total number of shot points. Comparison of a migrated image slice using different source efforts illustrates (Figure 8.6) that DAS is able to record reflections using source effort as little as 20 % of total sources. However, it is noticeable that reflections are clearer and stronger when using more sources, as expected. Though, little difference is observed at 60% and above of the total source effort.

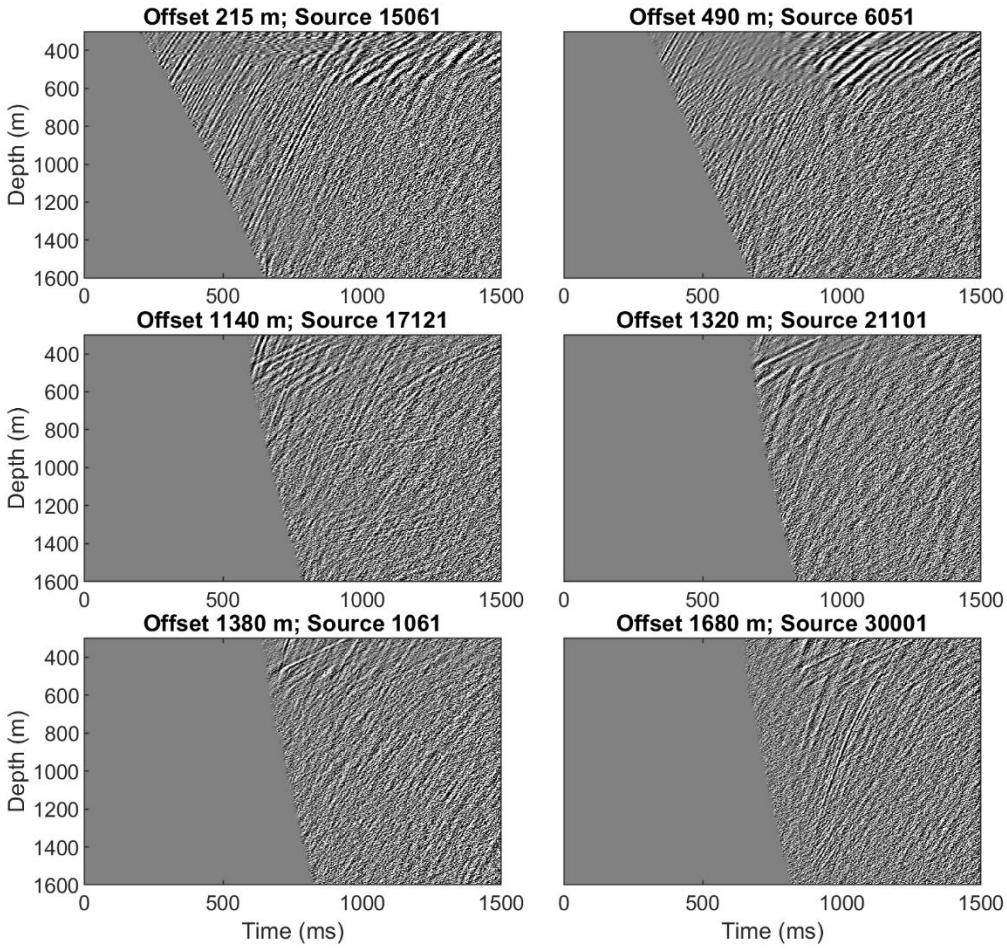

Figure 8.4 Upgoing P-waves after wavefield separation. Data is normalised trace by trace.

Table 8.1 VSP processing flow.

Procedure	**Parameter**
Data input	Native iDAS format
Geometry	Data matched to surface 3D seismic using DGPS time stamps, geometry information transferred from surface seismic data
Conversion from strain rate to strain	Integration in time
Correlation	Correlation with source sweep
First break picking	
Band pass filter	8 to 150 Hz (Ormsby bandpass filter)
Notch filter	24 to 28 Hz
Burst noise removal	
AGC	500 ms operator length
FK filter	Wavefield separation
Remove AGC	Removal of AGC 500 ms operator length
Amplitude correction	Time raised to power of 1
Group stacking	Stacking traces along 5 m depth intervals
Resample	2 ms
AGC	Wavefield separation
FK filter	Filtering PS-waves
FK filter	Filtering striped “infinite velocity” noise
Remove AGC	
Bottom mute	Mute S-waves
Top mute	Mute above first breaks
3D migration	Kirchhoff

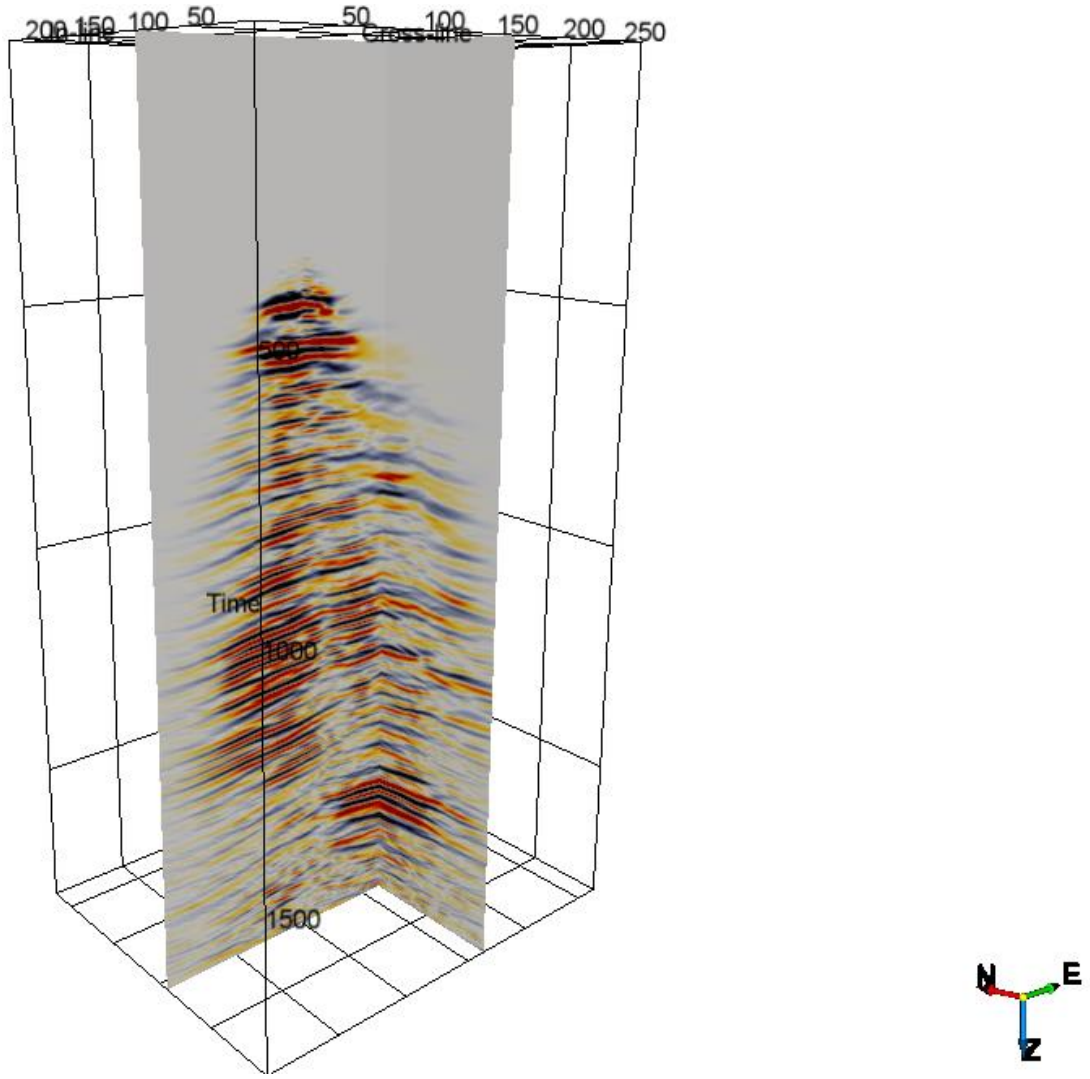

Figure 8.5 Migrated 3D DAS VSP cube, cemented cable.

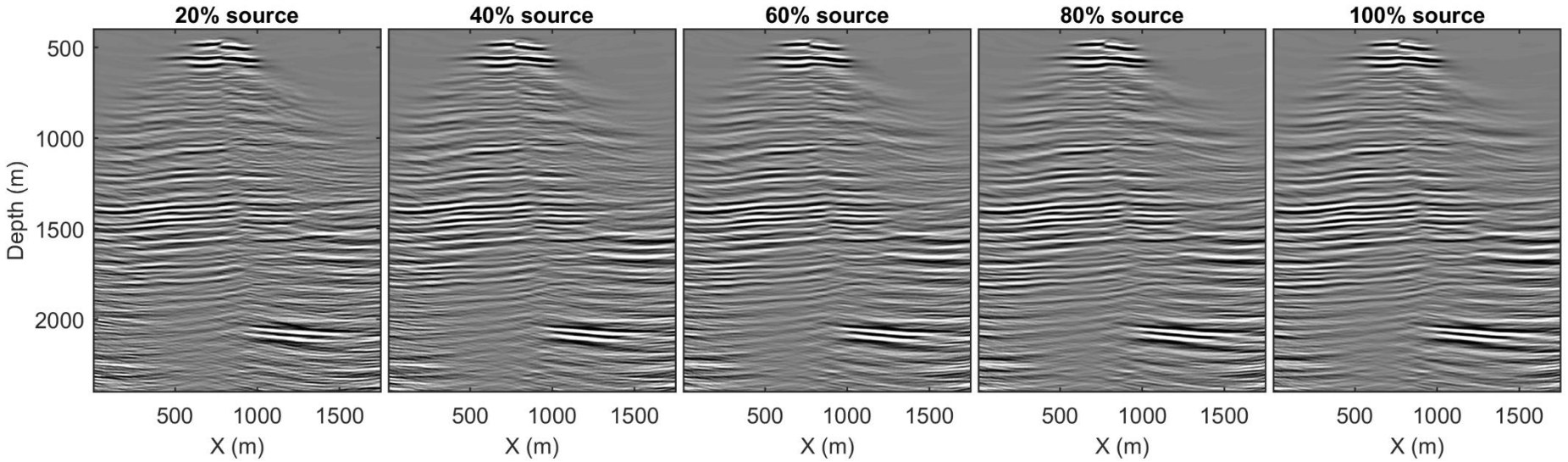

Figure 8.6 Inline 101 from migrated cube. Each display shows migrated inline using 20%, 40%, 60%, 80%, and 100% source effort.

8.5 Conclusions

The preliminary conclusions derived from the fast-track 3D VSP data analysis show that PP reflections from the target depth (~1500 m) for source point offsets up to ~1.7 km can be recorded, while using only a single sweep per shot point. PP reflections are clear for most shots through-out the well.

The direct P-wave, however, is weak for far offsets. This complicates certain processes, such as wavelet estimation for the application of deterministic deconvolution, as the direct waves are used for estimating the wavelet. Thus, an alternative method for source signature estimation in far offsets is needed. An option would be using a combination of DAS and 3C geophone VSP arrays designed for monitoring purposes (through, for instance, deployment of the hybrid cables). I chose not to apply deconvolution in this processing flow as it could damage the sharpness of the wavelet in far offsets.

The S/N analysis shows that DAS directivity is the major controlling factor for the signal levels, especially for shots from far offsets. This angle sensitivity limitation should be taken into consideration when acquiring 3D VSP with DAS. Also, it can be observed that by cementing the fibre, the acquisition range (in offset and incidence angle) does not increase significantly than when acquiring DAS on tubing deployment. However, S/N increases by approximately 10 to 15 dB where signal is acquired.

The overall data quality is sufficient to produce good migrated images for almost 2 km of inline at depth ~1500 m. The imaged cube contains reflections from the target depth of 1500 m. Additionally, acquiring repeated shots in far offsets could be an alternative to increase S/N and improve the imaging range.

Another important observation is that, while DAS (using single-mode fibre) sensitivity is clearly sufficient to image the subsurface using primary reflections for the given source effort, utilizing multiples for imaging might be challenging due to their weaker amplitudes. In this case, the use of special high sensitivity fibres or increasing the source energy on individual shot points could be applied.

Finally, reducing the number of shots to approximately 60% of the total number of vibration points seems to cause little effect on the overall seismic imaging. By

reducing the number of shot points, the cost of a survey and acquisition footprint can be decreased significantly.

CHAPTER 9 CONCLUSIONS AND FUTURE OUTLOOK

9.1 Discussion and conclusions

The objective of this thesis is to demonstrate the viability of DAS for cost-effective seismic imaging and time-lapse monitoring, and to determine the influence of fibre type, cable deployment and acquisition parameters on final data quality. To do this, I analysed the results of DAS applied to 3D surface seismic and downhole seismic in a variety of geometries (3D VSP, walk-away VSP and offset VSP). DAS VSP datasets were acquired with fibre-optic cables deployed along the well tubing, cemented behind the well casing, and loosely suspended inside the well. This thesis also includes analysis of the performance of different fibres (standard single-mode fibres and enhanced sensitivity fibres) and variety of cable designs (straight vs helically wound cables).

DAS offers many advantages over the use of conventional geophones. Though, often DAS data gets associated with lack of sensitivity and high noise levels. Furthermore, straight fibres present a narrower directivity pattern when compared to geophones. Another common issue with DAS acquisition is the lack of an accurate positioning/depth calibration method. The DAS data sets in this thesis have been acquired simultaneously with the geophone data, therefore, depth assignment was not an issue since the geophone data was used to calibrate the DAS data. Such issues usually hinder the broader application of DAS in the seismic industry.

Chapter 4 provides a comparison of VSP data acquired with DAS, geophones and hydrophones. These experiments were performed at the NGL site, a controlled purpose-built test environment. The experiments show that DAS data acquired with cemented cable has similar S/N to geophone data, at all offsets. Due to the dense spatial sampling, DAS properly samples incident PP reflections, as opposed to the aliased geophone records. DAS data typically exhibits greater attenuation of high frequencies than geophones and hydrophones due to effects of the gauge length.

The comparison between DAS data and other known sensors, like geophones, is important to establish a benchmark of data quality. However, such comparisons often

end up creating a perception of DAS as of some sort of geophone equivalent with slightly higher noise level and poor sensitivity. Distributed acoustic sensing gives a principally different measurement compared to sensors like geophones and hydrophones. To fully benefit from the DAS method, we must understand the principles of DAS measurements and the main parameters involved in its acquisition.

Although in this thesis I did not test each parameter individually, we can conclude that pulse repetition frequency (PRF), gauge length and pulse lengths are the some of the most important parameters which can affect the DAS data quality. Gauge and pulse lengths are linked to the wavelength of the seismic waves which can be recorded using the fibre. On one hand, they limit the spatial (and temporal) frequency range of the seismic waves which can be recorded. On the other – they can be used to optimise the sensitivity to the specific components of the wavefield.

The PRF (which is controlled by the cable length and properties of the hardware) parameter is especially important in DAS acquisition. This parameter controls how fast the laser pulses are emitted from the IU along the fibre. Each laser pulse is recorded at its return to the IU. This means that the higher is the PRF, the higher the sampling frequency will be. A faster sampling of the backscattered light means that the IU can better sample the phase, and thus discriminate more accurately the phase change. The manifestation of better sampled phase means that the recorded data presents less phase noise, and thus, higher S/N. Therefore, when acquiring DAS data, one should select the highest possible PRF in the IU parameters. It is important to take the total cable length into account while designing the survey. As it is shown in this thesis, having excessive cable length could significantly affect the data quality by limiting the maximum possible PRF (see Chapter 6).

Using engineered fibres decreases the level of random noise in DAS data. Engineered fibres are purposely built to increase backscattering of the laser pulses. Chapter 7 showed a comparison with data acquired by an engineered/enhanced sensitivity fibre and single-mode fibre. A series of offset VSPs were acquired at the Otway site, with offset positions varying from 50 m to 1.8 km. VSP data were acquired using both 3C geophones and DAS cables cemented behind the casing, using the standard single-mode fibre and enhanced backscatter fibre. In these experiments, we saw that the engineered fibres provide higher S/N ratio than standard fibres by

decreasing the noise floor. S/N for the single mode fibre decreases significantly at far offsets compared to the enhanced sensitivity fibre. The use of engineered fibre increased S/N of the DAS data by approximately 15 dB. However, such fibres are currently significantly more expensive than conventional fibres.

The cost of a seismic survey is driven by the cost of the equipment and the crew, the number of source points, and the duration of the survey. Decreasing the source effort can reduce significantly survey costs and its impact on land. It is clear that we can acquire quality seismic data while using conventional single-mode fibres by doing a vertical stack of repeated shots. Though, it is important to note that using engineered fibres can reduce the required source effort needed for single-mode fibre to achieve similar data quality and, thus, reducing the overall cost of the survey.

For instance, to get the same benefit in S/N as shown by engineered fibres (~15 dB), source effort would have to be increased by ~32 times ($20 \log \sqrt{32}$). Therefore, to get the same data quality as engineered fibres, 32 repeated shots recorded by the DAS data would have to be stacked. The cost-benefit of choosing to increase source effort or choosing to use engineered fibres will depend on each survey.

In this thesis, I also compare DAS data recorded with various cable deployments. Chapter 5 presents 3D surface seismic data acquired with the permanent installation of fibre on the surface at Otway. Chapter 6 demonstrates the results of a 3D VSP survey acquired using a standard fibre-optic cable deployed on the production tubing. Chapter 8 shows a 3D VSP acquired with cemented fibres.

Analysis of the DAS data acquired on cables deployed in shallow trenches near the surface (Chapter 5) shows it mostly recorded S-waves and ground roll due to the inherent directionality pattern seen on DAS method. After processing the data, we can see that DAS was able to record some P reflections, particularly from shallow interfaces. Random noise decreases significantly after migration due to its stacking characteristic. From analysing the DAS migrated data, we see that the fibre was only sensitive to waves up to 50° incident angle. Significant improvements in cable design are required in order for surface DAS to be viable alternative to geophones, such as helical winding and improved sensitivity.

The on tubing 3D DAS VSP was acquired simultaneously with the 3D surface DAS (Chapter 6). Our aim was to determine whether the DAS data from fibre deployed on tubing has sufficient S/N to image the injection interval of a gas plume. DAS recorded on tubing shows low levels of signal and P-wave reflections are barely detectable on the shot records. The low data quality is mostly attributed to the long cable length (~20 km) and poor selection of parameters during acquisition (e.g. small PRF). The S/N shows that signal levels are equal to noise levels (0 dB) for incident waves above 55˚ at 900 m distance, and for incident wave of 45˚ at distances of 1500 m. This clearly indicates that the angle sensitivity of DAS needs to be taken into consideration when planning DAS VSP surveys. Furthermore, S/N of DAS data acquired on tubing could be increased by using engineered fibres or increasing source effort.

The 3D DAS VSP dataset acquired with a fibre cable cemented behind the casing shows by far the best data quality. PP reflections from the target depth (~1500 m) were recorded for source point offsets up to ~1.7 km, while using only a single sweep per shot point. It can be observed that, by cementing the fibre, the acquisition range (in offset and incidence angle) does not increase significantly compared to on tubing cable deployment. The difference in S/N between cemented DAS and on tubing DAS was of about 15 dB.

Stage 2C of the Otway Project focussed on the technology itself, not on imaging the injection. Each DAS dataset recorded throughout the surveys (surface DAS and 3D VSP on tubing DAS) were acquired using different parameters. In some monitoring surveys, the IU box was changed. This contributed to poor repeatability of data. For this reason, analysis of the time-lapse response to the injection using DAS were not conducted.

In the next Stage of the Otway Project (Stage 3), we hope to develop an on-demand seismic monitoring technique, while decreasing acquisition impact and footprint on land to its minimum. For this, we have tested the use of permanently installed SOV sources coupled with permanently installed DAS. The second section of Chapter 7 shows the experiments at the Otway Project with DAS/SOV configuration. In order to test for an optimal DAS/SOV configuration, two VSP surveys were acquired using cemented fibre-optic cables at two offset location using SOV sources. The first field

trial assessed the performance of DAS/SOV using a standard fibre-optic cable and an engineered/enhanced sensitivity cable. The second field trial aimed to test for optimal performance of the source by acquiring a range of sweeps with large and smaller motors, from maximum frequency of 80 to 160 Hz. The results show that VSP data acquired with DAS using a cemented cable and SOVs yields high quality datasets, sufficient to image the injected gas plume. The large motors provide higher signal levels due to the higher source power than the small motors. The use of SOV sources and engineered fibres provide the best data quality. However, as the SOV sources work based on centrifugal forces, the low frequencies had low power. Monitoring during the Stage 3 is still an on-going work, therefore, no time-lapse response was shown in this thesis.

During Stage 3, we plan to automate data acquisition and processing. We plan to automatically acquire data on site every day and produce an image of the development of the plume regularly. For this, one of the objectives is to apply full waveform inversion (FWI) to the VSP data. The use of DAS data for this objective is a disadvantage, as traditional FWI algorithms are purposely built for particle velocity or pressure. A work-around would be converting DAS data to particle velocity. Chapter 7 proposes a filter that converts DAS data to geophone equivalent. After conversion, DAS signature becomes very close to the geophone signature, correcting for polarity differences of the upgoing and downgoing fields. Such conversion is necessary when using DAS in applications that require particle velocity response, such as in Full Waveform Inversion.

Lessons learned

From my experiences with the different DAS data sets analysed, the following lessons can be taken from this thesis:

- At this present state, DAS can produce a similar, or even higher, quality dataset when compared to conventional geophones for the acquisition of VSP data;
- There are various approaches which could further improve the sensitivity of DAS and address the narrow directivity pattern issue, these include helically wound cables and enhanced sensitivity fibres;

- DAS can easily image the injection interval at Otway when acquired in VSP configuration. Therefore, DAS technology will be the primary seismic receiver for the next stage of the project;
- Fibre length influences significantly the signal-to-noise ratio of the data through the limitations on PRF. The shorter the fibre length, the higher the pulse repetition rate can be set during acquisition;
- The angle sensitivity of DAS must be considered when planning surveys. For the case of surface seismic, the azimuth range between the shot point and DAS trace should also be considered as the azimuth range relates to the range of incidence angles;
- Permanent surface orbital vibrators can be used together with DAS to create a permanent on-demand seismic array to continuously image the injected CO_2; decreasing land impact and acquisition footprint, while increasing survey efficiency.

9.2 Future outlook

DAS is a rapidly evolving technology. It has experienced significant improvements in fibre optic cable design, cable deployments and interrogator units, and future developments are likely to lead to further improvement in signal to noise ratio and sensitivity. The results from this thesis show the potential of DAS for seismic imaging and reservoir monitoring. I believe that, in the future, most wells will be instrumented with fibre-optic cable for DAS to enable on-demand continuous monitoring of the reservoir. Furthermore, DAS presents itself as a versatile method. It can acquire low and high frequencies, while the deployment and acquisition are relatively easy. I believe DAS method has a lot to offer to the seismic industry and to other non-seismic applications, such as road and pipeline monitoring.

The Oil & Gas industry is experiencing an increasing need for imaging deeper and thinner structures. This means there is an increasing need for broad frequency data acquisition. The gauge length and PRF in a DAS acquisition box are the major controllers of the frequency range and S/N of the DAS data. One of the greatest advantages about DAS is the ability to change PRF. By increasing the PRF, we can increase S/N in the data, as well as increasing the high frequency limit to far beyond

seismic frequency range, meaning it can adapt to any survey objective. No other seismic sensor has such ability.

Additionally, variable gauge length acquisition is another huge advantage of DAS sensors, as it can increase the range of detectable seismic velocities. However, few IU manufactures at this stage allow for variable gauge lengths during data acquisition. Ideally, the IU would interrogate using multiple different gauge lengths. Therefore, in the future, we expect to see more developments in interrogator units, where there would be the possibility of acquiring DAS simultaneously from multiple fibres attached to a single unit, each fibre acquiring data with a different gauge length. Another approach would be selecting different gauge lengths to be applied at a post processing stage in IU. Also, I expect that, as technology gets better, hardware will also improve. With this, I believe the system noise present on DAS interrogator will only decrease.

To this date, most IU manufactures still treat DAS as a black box. The exact method for interrogating the signal, as well as post processing flow applied to the DAS data are sometimes unknown to the end user. The DAS IU construction method and processing algorithms are proprietary and sometimes are kept secretive. Processes are applied with the objective to reduce the noise floor and increase S/N; such processes can be applied in the IU box or in-house. Depending on the processing applied to the data, this can harm useful information. For example, if a long spatial filter is applied with the objective to average out random noise, this could end up harming the resolution of the data. Therefore, it is essential that the geophysicist knows what kind of processing has been applied to the DAS data prior to its delivery. Ideally, IU manufactures should consider delivering DAS data in raw, or almost raw state. With this, the geophysicist can apply their own in-house processing flow, tailored to a particular survey objective. Having the signal processing knowledge of the geophysicist can also allow the development of processes particularly aimed at DAS data.

Furthermore, the contemporaneous society is experiencing an increase of environmental awareness. In this context, seismic acquisition still produces a considerable amount of land impact. During land seismic acquisition, heavy vibroseis sources a deployed. At times, the sources are vibrating in intervals as little as 3 m.

Moreover, sources can vibrate multiple times at the same point. This can translate to high land impact, especially if acquiring on soft ground. When vibroseis sources are not used, the other common option is the use of dynamite. In both cases, the source effort produces a huge amount of land impact. The constant deployment and retrieval of seismic receivers is an additional cause of land impact. Thus, we must develop ways to reduce land impact and acquisition footprint during seismic surveys.

At the Otway Project, we plan to use primarily DAS to monitor the CO_2 injection. The monitoring plan during Stage 3 of the project is to use 4D DAS VSP acquired with conventional vibrators, as well as DAS offset VSP with multiple SOV sources. The SOV sources offer the advantage of being accessible remotely, as well as reducing land impact. In Stage 3, we plan to automate data acquisition and processing. With this, VSP seismic data will be acquired everyday using DAS in-well and SOV sources. The data acquired would then be processed automatically using previously tested processing flows. As a result, we will have an image of the reservoir being produced every day. Additionally, we plan to reduce the vibroseis land impact by reducing the amount of vibration points. The combination of DAS sensors and SOV sources with automated acquisition and automated processing makes the Otway Project stand out from other current PRM projects worldwide.

The advantages offered by DAS extend to other applications beyond seismic monitoring, such as road and pipeline monitoring. DAS can record low frequencies, which means that imaging applications, such as FWI, would be ideal with DAS method (though, a conversion of strain to particle velocity should be considered as most FWI algorithms are built based in particle velocity). Also, depending on the acquisition setting, such as gauge length and PRF, DAS can record a wide range of seismic velocities, making the method suitable for deep earth imaging and near surface imaging.

The development of DAS for surface seismic are currently relatively slow. DAS does not produce surface seismic data of sufficiently high quality for deep imaging due to its directivity pattern. However, the seismic industry is recently tending to prefer less invasive seismic imaging techniques, such as VSP imaging. With VSP configuration, the land and environmental impact associated with receiver deployment can be decreased. Therefore, I believe DAS will remain a method for primarily VSP

acquisition. Though, developments in cable design, such as the HWC fibre and the enhanced sensitivity fibre, can aid on the surface seismic acquisition. Moreover, recent experiments show that DAS has a lot of potential for near surface imaging.

REFERENCES

Al Adawi, R., G. Rocco, S. Al Busaidi, A. Al Maamari, S. Al Ghafri, D. Kiyashchenko, J. Lopez, and W. and Zwaan, M. Berlang. 2013. "Seismic Reservoir Monitoring of a Thermal EOR Redevelopment; Thick Heavy oil Field in Oman." *SPE Middle East Oil and Gas Show and Conference, SPE, Extended Abstracts.* doi:10.2118/164353-MS.

Allen, S. J. 1980. "Seismic method." *Geophysics*, 1619-33.

Arts, R., O. Eiken, A. Chadwick, P. Zweigel, L. Van der Meer, and B. Zinszner. 2004. "Monitoring of CO2 injected at Sleipner using time-lapse seismic data." *Energy, Elsevier* 29 (9): 1383-1392.

Atkin, R. J.; Fox, N. 1980. *An introduction to the theory of elasticity.* Dover Publications.

Bacci, V. O., S. O'Brien, J. Frank, and M. Anderson. 2017. "Using a walk-away DAS time-lapse VSP for CO2 plume monitoring at the Quest CCS Project." *CSEG Recorder* 42 (3): 18–21.

Bakku, S. K. 2015. "Fracture Characterization from Seismic Measurements in a Borehole." Massachusetts Institute of Technology.

Bakku, S., P. Wills, M. Fehler, J. Mestayer, A. Mateeva, and J. Lopez. 2014a. "Vertical Seismic Profiling Using Distributed Acoustic Sensing in a Hydrofrac Treatment Well." *84th Annual International Meeting, SEG, Extended Abstracts.* 5024-5028.

Bakku, Sudhish, Peter Wills, and Michael Fehler. 2014b. "Monitoring Hydraulic Fracturing Using Distributed Acoustic Sensing in a Treatment Well." *84th Annual International Meeting, SEG, Extended Abstracts.* 5003-5008.

Bakulin, A., P. Golikov, R. Smith, K. Erickson, I. Silvestrov, and M. Al-Ali. 2017. "Smart DAS upholes for simultaneous land near-surface characterization and subsurface imaging." *The Leading Edge* 36 (12): 1001-1008.

Barberan, C., C. Allanic, D. Avila, J. Hy-Billiot, A. Hartog, B. Frignet, and G.P. Lees. 2012. “Multi-offset Seismic Acquisition Using Optical Fiber Behind Tubing.” *74th Conference and Exhibition, EAGE, Extended Abstracts.* Y003.

Barnoski, M. K., and S. M. Jensen. 1976. “Fiber waveguides: a novel technique for investigating attenuation characteristics.” *Applied Optics* 15 (9): 2112.

Beck, B., P. Cunha, M. Ketzer, H. Machado, P. S. Rocha, Fernando Zancan, A. S. Almeida, and D. Z. Pinheiro. 2011. “The current status of CCS development in Brazil.” *Energy Procedia* 4: 6148-6151.

Berraki, M., S. Buizard, J. Ramirez, R.M. Elde, S.S. Roy, and D. and Synnevåg, J.F Eckert. 2017. “Grane PRM - From acquisition to interpretation in record time.” *79th Conference and Exhibition, EAGE, Extended Abstract.*

Biondi, B., E. Martin, S. Cole, M. Karrenbach, and N. Lindsey. 2017. “Earthquakes analysis using data recorded by the Stanford DAS Array.” *87th Annual International Meeting, SEG, Extended Abstracts.* 2752-2756.

Bona, A., T. Dean, J. Correa, R. Pevzner, K.V. Tertyshnikov, and L. Van Zaanen. 2017. “Amplitude and Phase Response of DAS Receivers.” *79th Conference and Exhibition, EAGE, Extended Abstracts.*

Bostick, F. X. 2000. “Field experimental results of three-component fiber-optic seismic sensors.” *70th Annual International Meeting, SEG, Extended Abstract.* 21-24.

Bourne, S., S. Crouch, and M. Smith. 2014. “A risk-based framework for measurement, monitoring and verification of the Quest CCS Project, Alberta, Canada.” *International Journal of Greenhouse Gas Control* 26: 109-126.

Brown, R. J., R. R. Stewart, and D. C. Lawton. 2002. “A proposed polarity standard for multicomponent seismic data.” *Geophysics* 67 (4): 1028-1037.

Chapman, Wm. L., G. L. Brown, and D. W. Fair. 1981. “The Vibroseis system - A high-frequency tool.” *Geophysics* 46 (12): 1657-1666.

CO2CRC. n.d. *The Cooperative Research Centre for Greenhouse Gas Technologies.* http://www.co2crc.com.au/.

Cole, S., M. Karrenbach, D. Kahn, J. Rich, K. Silver, and D. Langton. 2018. “Source Parameter Estimation from DAS Microseismic Data.” *88th Annual International Meeting, SEG, Extended Abstracts.* 4928-4932.

Correa, J C, T. Dean, L. Van Zaanen, K.V. Tertyshnikov, R. Pevzner, and A. Bona. 2017b. “A Comparison of DAS and Geophones for VSP Acquisition At a Dedicated Field Laboratory .” *79th Conference and Exhibition, EAGE, Extended Abstracts.* Tu P7 16.

Correa, J., A. Egorov, K. Tertyshnikov, A. Bona, R. Pevzner, T. Dean, B. Freifeld, and S. Marshall. 2017a. “Analysis of signal to noise and directivity characteristics of DAS VSP at near and far offsets — A CO2CRC Otway Project data example.” *The Leading Edge* 36 (12): 994a1-994a7.

Correa, J., L. Van Zaanen, K. Tertyshnikov, T. Dean, R. Pevzner, and A. Bona. 2017d. “DAS Versus Geophones : a Quantitative Comparison of a VSP Survey at a Dedicated Field Laboratory.” *4th Borehole Geophysics Workshop, EAGE, Extended Abstracts.* BGP10.

Correa, J., Pevzner, R., B. Freifeld, M. Robertson, T. Daley, T. Wodd, S. Dou, K. Tertyshnikov, S. Yavuz, S. Glubokovskikh, and A. Bona. 2019. “Continuous downhole seismic monitoring using surface orbital vibrators and distributed acoustic sensing at the Otway Project.” *AGU Books* Submitted for publication.

Correa, J., R. Pevzner, A. Bona, K. Tertyshnikov, B. Freifeld, M. Robertson, and T. Daley. 2019. “3D VSP acquired with DAS on tubing installation: a case study from the CO2CRC Otway Project.” *Interpretation* 7 (1): Accepted.

Correa, J., R. Pevzner, S. Popik, K. Tertyshnikov, A. Bona, and B. Freifeld. 2018. “Application of 3D VSP acquired with DAS and 3C geophones for site characterization and monitoring program design: preliminary results from Stage 3 of the CO2CRC Otway project.” *88th Annual International Meeting, SEG, Extended Abstracts.* 4933-37.

Correa, J., T. Dean, L. Van Zaanen, K. Tertyshnikov, R. Pevzner, and A. Bona. 2018. “a Comparison of a Conventional Borehole Tool and Distributed Acoustic Sensing At a Dedicated Field.” *AEGC Extended Abstracts 2018: First Australasian Exploration Geoscience Conference.* 1-3.

Correa, J.C., B.M. Freifeld, M. Robertson, R. Pevzner, A. Bona, D. Popik, S. Yavuz, et al. 2017c. “Distributed acoustic sensing applied to 4D seismic - Preliminary results from the CO2CRC Otway site field trials.” *79th Conference and Exhibition, EAGE, Extended Abstracts.* Tu A1 15.

Cotton, J., and E. and Meunier J. Forgues. 2013. “Continuous land seismic reservoir monitoring of thermal EOR in the Netherlands.” *75th Conference and Exhibition, EAGE, Extended Abstracts.* TU 08 03.

Cox, B, P Wills, Denis Kiyashchenko, J Mestayer, J Lopez, Stephen Bourne, R Lupton, et al. 2012. “Distributed Acoustic Sensing for Geophysical Measurement, Monitoring and Verification.” *CSEG Recorder* (February): 7-12.

Dakin, J. P., and C. Lamb. 1990. Distributed fibre optic sensor system. US Patent GB2222247A.

Daley, T. M., and D. Cox. 2001. “Orbital vibrator seismic source for simultaneous P- and S-wave crosswell acquisition.” *Geophysics* 66 (5): 1471-1480.

Daley, T. M., B. M. Freifeld, J. Ajo-Franklin, S. Dou, R. Pevzner, V. Shulakova, S. Kashikar, et al. 2013. “Field testing of fiber-optic distributed acoustic sensing (DAS) for subsurface seismic monitoring.” *The Leading Edge* 32 (6): 699-706.

Daley, T. M., D. E. Miller, K. Dodds, P. Cook, and B. M. Freifeld. 2016. “Field testing of modular borehole monitoring with simultaneous distributed acoustic sensing and geophone vertical seismic profiles at Citronelle, Alabama.” *Geophysical Prospecting* 64 (5): 1318-1334.

Daley, T. M., L. R. Myer, J. E. Peterson, E. L. Majer, and G. M. Hoversten. 2008. “Time-lapse crosswell seismic and VSP monitoring of injected CO2in a brine aquifer.” *Environmental Geology* 54 (8): 1657-1665.

Dean, M., and O. Tucker. 2017. “A risk-based framework for Measurement, Monitoring and Verification (MMV) of the Goldeneye storage complex for the Peterhead CCS project, UK.” *International Journal of Greenhouse Gas Control* 61: 1-15.

Dean, T., A. Hartog, T. Cuny, and F. Englich. 2016. “The Effects of Pulse Width on Fibre-optic Distributed Vibration Sensing Data.” *78th Conference and Exhibition, EAGE, Extended Abstracts.* P407.

Dean, T., T. Cuny, A. Constantinou, P. Dickenson, C. Smith, and E. Hamouche. 2016. “Depth calibration of fibre-optic distributed vibration sensing measurements.” *First Break* 36 (June): 29-34.

Dean, T., T. Cuny, and A. H. Hartog. 2017. “The effect of gauge length on axially incident P-waves measured using fibre optic distributed vibration sensing.” *Geophysical Prospecting* 65 (1): 184-193.

Delvaux, J., L. Nicoletis, G. Noual, and J.F. Dutzer. 1987. “Acquisition Techniques in Cross-Hole Seismic Surveys.” *SPE Conference Paper* 413-419.

Didraga, C. 2015. “DAS VSP Recorded Simultaneously in Cemented and Tubing Installed Fiber Optic Cables.” *77th Conference and Exhibition, EAGE, Extended Abstracts.* Tu N118 14.

Dodds, K., T. Daley, B. Freifeld, M. Urosevic, A. Kepic, and S. Sharma. 2009. “Developing a monitoring and verification plan with referenceto the Australian Otway CO2 pilot project.” *The Leading Edge* 28 (7): 812-818.

Dou, S., J. Ajo-Franklin, T. Daley, M. Robertson, T. Wood, B. Freifeld, R. Pevzner, et al. 2016. “Surface orbital vibrator (SOV) and fiber-optic DAS: Field demonstration of economical, continuous-land seismic time-lapse monitoring from the Australian CO 2 CRC Otway site.” *86th Annual International Meeting, SEG, Extended Abstracts.* 5552-5556.

Dou, S., N. Lindsey, A. M. Wagner, T. M. Daley, B. Freifeld, M. Robertson, J. Peterson, C. Ulrich, E. R. Martin, and J. B. Ajo-Franklin. 2017. “Distributed Acoustic Sensing for Seismic Monitoring of the Near Surface: A Traffic-Noise Interferometry Case Study.” *Scientific Reports* 7 (1).

Egorov, A., R. Pevzner, A. Bóna, S. Glubokovskikh, V. Puzyrev, K. Tertyshnikov, and B. Gurevich. 2017. “Time-lapse full waveform inversion of vertical seismic profile data: Workflow and application to the CO2CRC Otway project.” *Geophysical Research Letters* 44 (14): 7211-7218.

Ellmauthaler, A., D. A. Barfoot, M. E. Willis, X. Wu, C. Erdemir, O. Barrios, D. Quinn, and S. Shaw. 2016. "Depth calibration for DAS VSP – Lessons learned from two field trials." *86th Annual International Meeting, SEG, Extended Abstracts* 632-636.

Farhadiroushan, M. 2018. "Seismic and Microseismic Detection Using a Wide Dynamic-Range Distributed an Engineered Fiber Optic Acoustic Sensor." *80th Conference and Exposition, EAGE, Extended Abstracts.* 11-13.

Farhadiroushan, M., T. R. Parker, and S. V. Shatalin. 2010. Method and apparatus for optical sensing. Patent WO2010/136810A2.

Flett, M., J. Brantjes, R. Gurton, J. McKenna, T. Tankersley, and M. Trupp. 2009. "Subsurface development of CO2 disposal for the Gorgon Project." *Energy Procedia*, 3031-38.

Freifeld, B. M., R. Pevzner, S. Dou, J. Correa, T. M. Daley, M. Robertson, K. Tertyshnikov, et al. 2016. "The CO2CRC Otway Project deployment of a Distributed Acoustic Sensing network coupled with permanent rotary sources." *78th Conference and Exhibition, EAGE, Extended Abstracts.* 2-6.

Freifeld, B.M., T.M. Daley, S.D. Hovorka, J. Henninges, J. Underschultz, and S. Sharm. 2009. "Recent advances in well-based monitoring of CO2 sequestration." *Energy Procedia* 1: 2277-2284.

Fürre, A. K., O. Eiken, H. Alnes, J. N. Vevatne, and A. F. Kiær. 2017. "20 Years of Monitoring CO2-injection at Sleipner." *Energy Procedia* 114: 3916-3926.

Galarraga, M. A., and Wang K. and Farmer H. G. 2015. "First results of 4D monitoring from the deepwater BC-10 life of field seismic (LoFS), Brasil." *85th Annual International Meeting, SEG, Extended Abstracts.*

Galperin, E. I., and P. Kennett. 1985. *Vertical seismic profiling and its exploration potential.* D. Reidel Publishing Company.

GCCSI. n.d. *Large-scale CCS projects.* https://www.globalccsinstitute.com/projects/large-scale-ccs-projects.

GCCSI. 2017. "The Global Status of CCS." Global CCS Institute, Australia.

GCCSI. 2018. “The Global Status of CCS.” Global CCS Institute, Australia.

Gollakota, S., and S. McDonald. 2014. “Commercial-scale CCS Project in Decatur, Illinois – Construction Status and Operational Plans for Demonstration.” *Energy Procedia* 63: 5986-5993.

Götz, J., S. Lüth, J. Henninges, and T. Reinsch. 2018. “Vertical seismic profiling using a daisy-chained deployment of fibre-optic cables in four wells simultaneously – Case study at the Ketzin carbon dioxide storage site.” *Geophysical Prospecting* 66 (6): 1201-1214.

Greenwood, A., C. J. Dupuis, M. Urosevic, and A. Kepic. 2012. “Hydrophone VSP surveys in hard rock.” *Geophysics* 77 (5): WC223-WC234.

Gulati, J. S., R. R. Stewart, and B. H. Hoffe. 2001. “Vertical hydrophone cable acquisition and imaging on land.” *Geophysics* 66 (4): 1190-1194.

Gurevich, B., R. Pevzner, M. Urosevic, A. Kepic, V. Shulakova, and E. Caspari. 2014. “2D and 3D seismic investigations for Stage 1 and 2C.” In *Geologically storing carbon: learning from the Otway Project experience*, by B. Gurevich, R. Pevzner, M. Urosevic, A. Kepic, V. Shulakova and E. Caspari, 155-196.

Hance, T., T. Jiang, G. Zhan, E. Kjos, R. Geetan, and S. and Thomas, I. Soulas. 2016. “Learnings from distributed acoustic sensing data processing for seismic applications - a case study from the north sea.” *78th Conference and Exhibition, EAGE, Extended Abstracts.* Th STZ2 04.

Hardage, B. A. 1981. “An examination of tube wave noise in vertical seismic profiling data.” *Geophysics* 46 (6): 892-903.

—. 2000. *Vertical seismic profiling : principles.* Oxford: Elsevier Science Ltd.

Harris, K., D. White, and C. Samson. 2017. “Imaging the Aquistore reservoir after 36 kilotonnes of CO 2 injection using distributed acoustic sensing.” *Geophysics* 82 (6): M81-M96.

Hartog, A. H. 1983. “A Distributed Temperature Sensor Based on Liquid-Core Optical Fibers.” *Journal of Lightwave Technology* 1 (3): 498-509.

—. 2017. *An Introduction to Distributed Optical Fibre Sensors.* CRC Press (Taylor and Francis).

Hartog, A. H., and K. Kader. 2012. Distributed fiber optic sensor system with improved linearity. US Patent US2012/0067118A1.

Hartog, A., B. Frignet, D. Mackie, and M. Clark. 2014. "Vertical seismic optical profiling on wireline logging cable." *Geophysical Prospecting* 62 (4): 693-701.

Hartog, A., O.I. Kotov, and L.B. Liokumovich. 2013. "The Optics of Distributed Vibration Sensing." *2nd Workshop on Permanent Reservoir Monitoring 2013 – Current and Future Trends, EAGE, Extended Abstracts.*

Hatton, L., M. H. Worthington, and J. Makin. 1986. *Seismic Data Processing.* Oxford: Blackwell Scientific Ltd.

Hornby, B. E. 2006. "VSP : Beyond time-to-depth." *The Leading Edge* 25 (4): 446-452.

Hornman, J. C. 2017. "Field trial of seismic recording using distributed acoustic sensing with broadside sensitive fibre-optic cables." *Geophysical Prospecting* 65 (1): 35-46.

Hornman, J. C., A. Mateeva, and J. H. H. M. and Lopez, J. L. Potters. 2015. "New concepts for lowering the cost of frequent seismic reservoir monitoring onshore." *85th Annual International Meeting, SEG, Extended Abstracts.*

Hornman, K., B. Kuvshinov, P. Zwartjes, and A. Franzen. 2013. "Field Trial of a Broadside-sensitive Distributed Acoustic Sensing Cable for Surface Seismic." *75th Conference and Exhibition, EAGE, Extended Abstracts.* 10-13.

Hovorka, S. D., T. A. Meckel, and R. H. Treviño. 2013. "Monitoring a large-volume injection at Cranfield, Mississippi-Project design and recommendations." *International Journal of Greenhouse Gas Control* 18: 345-360.

IPCC. 2005. *IPCC Special Report on Carbon Dioxide Capture and Storage.* Cambridge : Cambridge University.

Jenkins, C. 2014. “Monitoring and verifications.” In *Geologically storing carbon: learning from the Otway Project experience*, by C. Jenkins, 141-153.

Jenkins, C. R., P. J. Cook, J. Ennis-King, J. Undershultz, C. Boreham, T. Dance, P. de Caritat, et al. 2012. “Safe storage and effective monitoring of CO2 in depleted gas fields.” *Proceedings of the National Academy of Sciences* 109 (2): E35-E41.

Jenkins, C., S. Marshall, T. Dance, J. Ennis-King, S. Glubokovskikh, B. Gurevich, T. La Force, et al. 2017. “Validating Subsurface Monitoring as an Alternative Option to Surface M&V - The CO2CRC's Otway Stage 3 Injection.” *Energy Procedia* 114: 3374-3384.

Jervis, M., and A. and Smith, R. Bakulin. 2018. “Making time-lapse seismic work in a complex desert environment for CO2 EOR monitoring — Design and acquisition.” *The Leading Edge* 37 (8): 598-606.

Johannessen, K., B. K. Drakeley, and M. Farhadiroushan. 2012. “Distributed Acoustic Sensing - A New Way of Listening to Your Well/Reservoir.” *SPE Intelligent Energy International.* 149602-MS.

Johnston, D. 2013. *Practical Applications of Time-lapse Seismic Data.*

Juškaitis, R., A. M. Mamedov, V. T. Potapov, and S. V. Shatalin. 1994. “Interferometry with Rayleigh backscattering in a single-mode optical fiber.” *Optics letters*, 225-27.

Kersey, A. D. 2011. “Distributed and Multiplexed Fiber Optic Sensors.” In *Fiber Optic Sensors: An Introduction for Engineers and Scientists: Second Edition,* by A. D. Kersey, 277-314.

Knott, C. G. 1899. “Reflexion and refraction of elastic waves, with seismological applications.” *The London, Edinburgh, and Dublin Philosophical Magazine and Journal of Science,* 64-97.

Kragh, E., and P. Christie. 2002. “Seismic repeatability, normalized rms, and predictability.” *The Leading Edge* 21 (7): 640-647.

Krassay, A. A., D. L. Cathro, and D. J. Ryan. 2004. “A regional tectonostratigraphic framework for the Otway Basin.” *Eastern Australasian Basins Symposium II* 97-116.

Krohn, C. E., and S. T. Chen. 1992. “Comparison of downhole geophones and hydrophones.” *Geophysics* 57 (6): 841-847.

Kuvshinov, B. N. 2016. “Interaction of helically wound fibre-optic cables with plane seismic waves.” *Geophysical Prospecting* 64 (3): 671-688.

La Follett, J. R., P. Wills, J. L. Lopez, and J. K. and Van Lokven, M. Przybysz-Jarnut. 2015. “Continuous seismic reservoir monitoring at Peace River: Initial results and interpretation.” *85th Annual International Meeting, SEG, Extended Abstracts.*

Lamb, C., and J. P. Dakin. 1990. Distributed fibre optic sensor system.

LBNL. n.d. *Fibre deployment at Otway, iDAS unit 024.* LBNL, Berkeley.

Li, M., H. Wang, and G. Tao. 2015. “Current and Future Applications of Distributed Acoustic Sensing as a New Reservoir Geophysics Tool.” *The Open Petroleum Engineering Journal* 8 (1): 272-281.

Lindsey, N. J., E. R. Martin, D. S. Dreger, B. Freifeld, S. Cole, S. R. James, B. L. Biondi, and J. B. Ajo-Franklin. 2017. “Fiber-Optic Network Observations of Earthquake Wavefields.” *Geophysical Research Letters* 44 (23): 11,792-11,799.

Lopez, J. L., B. E. Cox, and P. J. and Wang, K. Hatchell. 2017. “Technology Options for Low-Cost On-Demand Seismic Monitoring in Deepwater Brazil.” *15th International Congress of the Brazilian Geophysical Society.*

Lowrie, W. 1997. *Fundamentals of geophysics.* Cambridge University Press.

Lumley, D. E. 2001. “Time-lapse seismic reservoir monitoring.” *Geophysics* 66 (1): 50-53.

Mallet, R. 1851. “Second report on the facts of earthquake phenomena.” *BAAS*, 272-320.

—. 1848. “On the dynamics of earthquakes; being an attempt to reduce their observed phenomena to the known laws of wave motion in solids and fluids.” *Royal Irish Academy*, 50-106.

Martens, S., A. Liebscher, F. Möller, J. Henninges, T. Kempka, S. Lüth, B. Norden, et al. 2013. “CO2storage at the Ketzin pilot site, Germany: Fourth year of injection, monitoring, modelling and verification.” *Energy Procedia* 37: 6434-6443.

Martin, E. R., C. M. Castillo, S. Cole, P. S. Sawasdee, S. Yuan, R. Clapp, M. Karrenbach, and B. L. Biondi. 2017. “Seismic monitoring leveraging existing telecom infrastructure at the SDASA: Active, passive, and ambient-noise analysis.” *The Leading Edge* 36 (12): 1025-1031.

Marzetta, T. L., M. Orton, and A. Krampe. 1988. “A hydrophone vertical seismic profiling experiment.” *Geophysics* 53 (Ii): 1437-1444.

Mateeva, A., J. Lopez, D. Chalenski, M. Tatanova, P. Zwartjes, Z. Yang, S. Bakku, K. de Vos, and H. Potters. 2017. “4D DAS VSP as a tool for frequent seismic monitoring in deep water.” *The Leading Edge* 36 (12): 995-1000.

Mateeva, A., J. Lopez, H. Potters, J. Mestayer, B. Cox, D. Kiyashchenko, P. Wills, et al. 2014. “Distributed acoustic sensing for reservoir monitoring with vertical seismic profiling.” *Geophysical Prospecting* 62 (4): 679-692.

Mateeva, A., J. Mestayer, Z. Yang, J. Lopez, P. Wills, J. Roy, and T. Bown. 2013. “Dual-Well 3D VSP in deepwater made possible by DAS.” *83rd Annual International Meeting, SEG, Extended Abstracts* 5062-5066.

McDonald, S. 2018. “Intelligent Monitoring Systems and Advanced Well Integrity and Mitigation.” *Carbon Storage and Oil and Natural Gas Technologies Review Meeting.*

Mestayer, J., B. Cox, P. Wills, D. Kiyashchenko, J. Lopez, M. Costello, S. Bourne, et al. 2011. “Field trials of distributed acoustic sensing for geophysical monitoring.” *81st Annual International Meeting, SEG, Extended Abstracts.* 4253-4257.

Metz, B., O. Davidson, H. de Coninck, M. Loos, and L. Meyer. 2005. “IPCC Special Report on Carbon Dioxide Capture and Storage.” Working Group III of the Intergovernmental Panel on Climate Change.

Miller, D. E., T. M. Daley, D. White, B. M. Freifeld, M. Robertson, J. Cocker, and M. Craven. 2016. “Simultaneous acquisition of distributed acoustic sensing VSP with multi-mode and single-mode fiber optic cables and 3-component geophones at the Aquistore CO2 storage site.” *CSEG Recorder.*

Miller, D., T. Parker, S. Kashikar, M. Todorov, and T. Bostick. 2012. “Vertical Seismic Profiling Using a Fibre-optic Cable as a Distributed Acoustic Sensor.” *74th Conference and Exhibition, EAGE, Extended Abstracts.* Y004.

Milligan, P. A., J. W. Rector, and R. W. Bainer. 1997. “Hydrophone VSP imaging at a shallow site.” *Geophysics* 62 (3): 842-852.

Nur, A.M., C. Tosaya, and D. V. Thanh. 1984. “Seismic monitoring of thermal enhanced oil processes.” *54th Annual International Meeting, SEG, Extended Abstracts.* 337-340.

Oristaglio, M. L. 1985. “A guide to current uses of vertical seismic profiles.” *Geophysics* 50 (12): 2473.

Parker, T., and S. V. Shatalin. 2014. “Distributed Acoustic Sensing-A New Tool for Seismic Applications.” *First Break* 32 (2): 61-69.

Partridge, A. D. 2001. “Revised Stratigraphy of the Sherbrook Group, Otway Basin.” In *Eastern Australian Basin Symposium*, by A. D. Partridge, 455-464.

Personick, S. D. 1977. “Photon Probe - an Optical-Fiber Time-Domain Reflectometer.” *Bell Syst Tech J* 56 (3): 355-366.

Pevzner, R., K. Tertyshnikov, and A. Bona. 2018. “Feasibility of Passive Vertical Seismic Profiling Using Distributed Acoustic Sensing for Monitoring Applications.” *80th Conference and Exhibition, EAGE, Extended Abstracts.* Th F 16.

Pevzner, R., K. Tertyshnikov, V. Shulakova, M. Urosevic, A. Kepic, B. Gurevich, and R. Singh. 2015. “Design and deployment of a buried geophone array for CO2

geosequestration monitoring: CO2CRC Otway Project, Stage 2C." *85th Annual International Meeting, SEG, Extended Abstracts.*

Pevzner, R., M. Urosevic, D. Popik, K. Tertyshnikov, J. Correa, A. Kepic, S. Glubokovskikh, et al. 2017. "Seismic monitoring of CO2 geosequestration: Preliminary results from Stage 2C of the CO2CRC Otway Project one year post injection." *87th Annual International Meeting, SEG, Extended Abstracts.* 5895-5900.

Pevzner, R., M. Urosevic, D. Popik, V. Shulakova, K. Tertyshnikov, E. Caspari, J. Correa, et al. 2017. "4D surface seismic tracks small supercritical CO2injection into the subsurface: CO2CRC Otway Project." *International Journal of Greenhouse Gas Control* 63: 150-157.

Popik, D., V. Shulakova, K. Tertyshnikov, S. Ziramov, M. Urosevic, and R. Pevzner. 2018. "Time-lapse surface seismic processing for Stage 2C of CO2CRC Otway Project." *ASEG Conference, Extended Abstracts.* 1-6 .

Posey, R., G. A. Johnson, and S. T. Vohra. 2000. "Strain sensing based on coherent Rayleigh scattering in an optical fibre." *Electronics Letters*, 1-2.

R. Pevzner, B. Gurevich, K. Tertyshnikov, A. Pirogova, S. Glubokovskikh. 2018. "Repeat logging using distributed acoustic sensors and earthquakes." *Reservoir Geoscience Conference, EAGE.*

Rockwater Pty Ltd. 2016. "Yarragadee aquifer geophysical instrument calibration bore – completion report."

Schmidt, A. 1888. "Ein Beitrag zur Dynamik der Erdbeben." *Jahrenshefte des Vercins fur Vaterlandische Naturkunde in Wurttenberg*, 248-70.

Shatalin, S. V., V. N. Treschikov, and A. J. Rogers. 1998. "Interferometric optical time-domain reflectometry for distributed optical-fiber sensing." *Applied Optics* 37 (24): 5600.

Sherriff, R. E., and L. P. Geldart. 1995. *Exploration Seismology.* Cambridge University Press.

Shulakova, V., R. Pevzner, C. J. Dupuis, M. Urosevic, K. Tertyshnikov, D. E. Lumley, and B. Gurevich. 2015. "Burying receivers for improved time-lapse seismic

repeatability: CO2CRC Otway field experiment." *Geophysical Prospecting* 63 (1): 55-69.

Stalker, L., and S. Whittaker. 2017. "South West Hub CCS Project: Evolution of Storage Site Characterization through Targeted Research and its Impact on Uncertainty Reduction." *Energy Procedia*, 5981-93.

Telford, W. M., L. P. Geldart, and R. E. Sheriff. 1990. *Applied Geophysics.* Cambridge University Press.

Tertyshnikov, K., H. AlNasser, R. Pevzner, M. Urosevic, and A. Greenwood. 2018. "3D VSP for Monitoring of the Injection of Small Quantities of CO2 – CO2CRC Otway Case Study." *80th Conference and Exhibition, EAGE, Extended Abstracts.* Th F 13.

Udd, E., and W. B. Spillman Jr. 2011. *Fiber Optic Sensors: An Introduction for Engineers and Scientists.* John Wiley & Sons, Inc.

Urosevic, M., R. Pevzner, A. Kepic, P. Wisman, V. Shulakova, and S. Sharma. 2010. "Time-lapse seismic monitoring of CO2 injection into a depleted gas resevoir - Naylor Field, Australia." *The Leading Edge* 29 (2): 164-169.

Van Gestel, J-P, J. H. Kommedal, O. I. Barkved, I. Mundal, and R. and Best, K. D. Bakke. 2008. "Continuous seismic surveillance of Valhall Field." *The Leading Edge* 27 (12): 1616-1621.

Van Zaanen, L., A. Bona, J. Correa, K. Tertyshnikov, T. Dean, and R. Pevzner. 2017. "A comparison of borehole seismic receivers." *87th Annual International Meeting, SEG, Extended Abstracts.* 5974-78.

Verliac, M., V. Lesnikov, and C. Euriat. 2015. "The Rousse-1 DAS VSP experiment – Observations and comparisons from various optical acquisition systems." *85th Annual International Meeting, SEG, Extended Abstracts.* 5534-5538.

Virieux, J., and S. Operto. 2009. "An overview of full-waveform inversion in exploration geophysics." *Geophysics* 74 (6): WCC1-WCC26.

Weatherby, B. B. 1940. "History and development of seismic prospecting." *Geophysics*, 215-30.

Webster, P., J. Wall, C. Perkins, and M. Molenaar. 2013. “Micro-Seismic Detection using Distributed Acoustic Sensing.” *83rd Annual International Meeting, SEG, Extended Abstracts.* 1-4.

Wiechert, E., and K. Zoeppritz. 1907. “Uber Erdbebenwellen.” *Nachrichten von der Koniglichen Gesellschaft der Wissenschaft,* 415-549.

Willis, M. E., D. Barfoot, A. Ellmauthaler, X. Wu, O. Barrios, C. Erdemir, S. Shaw, and D. Quinn. 2016. “Quantitative quality of distributed acoustic sensing vertical seismic profile data.” *The Leading Edge* 35 (7): 605-609.

Winbow, G. A. 1991. “Seismic sources in open and cased boreholes.” *Geophysics* 56 (7): 1040-1050.

Yavuz, S., B. M. Freifeld, R. Pevzner, K. Tertyshnikov, A. Dzunic, S. Ziramov, V. Shulakova, et al. 2016. “Subsurface imaging using buried DAS and geophone arrays - preliminary results from CO2CRC Otway Project.” *78th Conference and Exhibition, EAGE, Extended Abstracts.* Th SBT4 04.

Zeng, X., C. Lancelle, C. Thurber, D. Fratta, H. Wang, N. Lord, A. Chalari, and A. Clarke. 2017. “Properties of noise cross-correlation functions obtained from a distributed acoustic sensing array at Garner Valley, California.” *Bulletin of the Seismological Society of America* 107 (2): 603-610.

Zhan, G., and Kommedal J. and Nahm J. 2015. “VSP field trials of distributed acoustic sensing in Trinidad and Gulf of Mexico.” *85th Annual International Meeting, SEG, Extended Abstracts.*

Zhang, Q., R. R. Stewart, and Z. Sun. 1996. “3D-VSP survey design and data analysis.” *66rd Annual International Meeting, SEG, Extended Abstracts.* 190 - 193.

Zimmerman, L. J., and S. T. Chen. 1993. “Comparison of vertical seismic profiling techniques.” *Geophysics* 58 (1): 134-140.

APPENDIX A: ATTRIBUTION OF AUTHORSHIP

1- Paper "Correa, J., A. Egorov, K. Tertyshnikov, A. Bona, R. Pevzner, T. Dean, B. Freifeld, and S. Marshall. 2017. Analysis of signal to noise and directivity characteristics of DAS VSP at near and far offsets — A CO2CRC Otway Project data example. *The Leading Edge* 36 (12): 994a1-994a7."

Authors	Conception and design	Acquisition of data	Data processing	Data analysis	Paper writing	Paper review
Julia Correa		x	x	x	x	
I acknowledge that these represent my contribution to the above research output Sign: Julia de Jesus Moreira Correa						
Anton Egorov			x	x	x	
I acknowledge that these represent my contribution to the above research output Sign:						
Konstantin Tertyshnikov		x			x	
I acknowledge that these represent my contribution to the above research output Sign:						
Andrej Bona						x
I acknowledge that these represent my contribution to the above research output Sign:						
Roman Pevzner	x		x			x
I acknowledge that these represent my contribution to the above research output Sign:						
Tim Dean						x
I acknowledge that these represent my contribution to the above research output Sign:						
Barry Freifeld	x					x
I acknowledge that these represent my contribution to the above research output Sign:						
Steve Marshall	x					x
I acknowledge that these represent my contribution to the above research output Sign:						

2- Paper "Correa, J., R. Pevzner, A. Bona, K. Tertyshnikov, B. Freifeld, M. Robertson, T. Daley. 2019. 3D VSP acquired with DAS on tubing installation: a case study from the CO2CRC Otway Project. Accepted to *Interpretation* 7(1). DOI: 10.1190/int-2018-0086.1"

Authors	Conception and design	Acquisition of data	Data processing	Data analysis	Paper writing	Paper review
Julia Correa		x	x	x	x	
I acknowledge that these represent my contribution to the above research output Sign: Julia de Jesus Correa						
Roman Pevzner	x	x	x			x
I acknowledge that these represent my contribution to the above research output Sign:						
Andrej Bona						x
I acknowledge that these represent my contribution to the above research output Sign:						
Konstantin Tertyshnikov		x				x
I acknowledge that these represent my contribution to the above research output Sign:						
Barry Freifeld	x					x
I acknowledge that these represent my contribution to the above research output Sign:						
Michelle Robertson	x	x				
I acknowledge that these represent my contribution to the above research output Sign:						
Thomas Daley	x					
I acknowledge that these represent my contribution to the above research output Sign:						

3- Paper "Correa, J., R. Pevzner, B. Freifeld, M. Robertson, T. Daley, T.Wodd, S. Dou, K. Tertyshnikov, S. Yavuz, S. Glubokovskikh, A. Bona. Continuous Downhole Seismic Monitoring Using Surface Orbital Vibrators and Distributed Acoustic Sensing at the Otway Project – Field Trial for Optimum Configuration. Submitted as a chapter to *AGU Books*".

Authors	Conception and design	Acquisition of data	Data processing	Data analysis	Paper writing	Paper review
Julia Correa		x	x	x	x	
I acknowledge that these represent my contribution to the above research output Sign: Julia de Jesus Hoo. Pinn						
Roman Pevzner	x	x	x			x
I acknowledge that these represent my contribution to the above research output Sign:						
Barry Freifeld	x	x				x
I acknowledge that these represent my contribution to the above research output Sign:						
Michelle Robertson	x					
I acknowledge that these represent my contribution to the above research output Sign:						
Thomas Daley	x					
I acknowledge that these represent my contribution to the above research output Sign:						
Todd Wood	x					
I acknowledge that these represent my contribution to the above research output Sign:						
Shan Dou	x					
I acknowledge that these represent my contribution to the above research output Sign: Shan Dou						
Konstantin Tertyshnikov		x				
I acknowledge that these represent my contribution to the above research output Sign:						
Sinem Yavuz		x				x
I acknowledge that these represent my contribution to the above research output Sign:						
Stanislav Glubokovskikh						x
I acknowledge that these represent my contribution to the above research output Sign:						
Andrej Bona						x
I acknowledge that these represent my contribution to the above research output Sign:						

APPENDIX B: COPYRIGHT PERMISSION

This thesis utilises previously published material under the following papers:

Correa, J., A. Egorov, K. Tertyshnikov, A. Bona, R. Pevzner, T. Dean, B. Freifeld, and S. Marshall. 2017. Analysis of signal to noise and directivity characteristics of DAS VSP at near and far offsets — A CO2CRC Otway Project data example. *The Leading Edge* 36 (12): 994a1-994a7. DOI: 10.1190/tle36120994a1.1"

Correa, J., R. Pevzner, A. Bona, K. Tertyshnikov, B. Freifeld, M. Robertson, T. Daley. 2019. 3D VSP acquired with DAS on tubing installation: a case study from the CO2CRC Otway Project. Accepted to *Interpretation* 7(1). DOI: 10.1190/int-2018-0086.1

To this date (December 2018), as per the SEG policy on publishing, authors have open-access permission to reuse their papers published with SEG in a thesis or dissertation. This applies to both The Leading Edge and Interpretation journals. The policy states:

"Authors may reuse all or part of their papers published with SEG in a thesis or dissertation that authors write and are required to submit to satisfy criteria of degree-granting institutions."

For more details on SEG policies and permissions, please refer to https://seg.org/Publications/Policies-and-Permissions/Open-Access-Policy.